Stream geochemistry and water flow paths in alpine headwater catchments: the influence of shrub encroachment and soil cover

Inauguraldissertation
zur
Erlangung der Würde eines Doktors der Philosophie

vorgelegt der
Philosophisch-Naturwissenschaftlichen Fakultät
der Universität Basel

von
Matthias Heidulf Müller
aus Kiel, Deutschland

Basel, 2014

Genehmigt von der Philosophisch-Naturwissenschaftlichen Fakultät
auf Antrag von

Prof. Dr. Christine Alewell
Fakultätsverantwortliche und Dissertationsleiterin

Prof. Dr. Jan Seibert
Korreferent

Basel, den 18.2.2014

Prof. Dr. Jörg Schibler
Dekan

Namensnennung-Keine kommerzielle Nutzung-Keine Bearbeitung 3.0 Schweiz
(CC BY-NC-ND 3.0 CH)

Sie dürfen: **Teilen** — den Inhalt kopieren, verbreiten und zugänglich machen

Unter den folgenden Bedingungen:

Namensnennung — Sie müssen den Namen des Autors/Rechteinhabers in der von ihm festgelegten Weise nennen.

Keine kommerzielle Nutzung — Sie dürfen diesen Inhalt nicht für kommerzielle Zwecke nutzen.

Keine Bearbeitung erlaubt — Sie dürfen diesen Inhalt nicht bearbeiten, abwandeln oder in anderer Weise verändern.

Wobei gilt:

- **Verzichtserklärung —** Jede der vorgenannten Bedingungen kann **aufgehoben** werden, sofern Sie die ausdrückliche Einwilligung des Rechteinhabers dazu erhalten.
- **Public Domain (gemeinfreie oder nicht-schützbare Inhalte) —** Soweit das Werk, der Inhalt oder irgendein Teil davon zur Public Domain der jeweiligen Rechtsordnung gehört, wird dieser Status von der Lizenz in keiner Weise berührt.
- **Sonstige Rechte —** Die Lizenz hat keinerlei Einfluss auf die folgenden Rechte:
    - Die Rechte, die jedermann wegen der Schranken des Urheberrechts oder aufgrund gesetzlicher Erlaubnisse zustehen (in einigen Ländern als grundsätzliche Doktrin des **fair use** bekannt);
    - Die **Persönlichkeitsrechte** des Urhebers;
    - Rechte anderer Personen, entweder am Lizenzgegenstand selber oder bezüglich seiner Verwendung, zum Beispiel für **Werbung** oder Privatsphärenschutz.
- **Hinweis —** Bei jeder Nutzung oder Verbreitung müssen Sie anderen alle Lizenzbedingungen mitteilen, die für diesen Inhalt gelten. Am einfachsten ist es, an entsprechender Stelle einen Link auf diese Seite einzubinden.

Quelle: http://creativecommons.org/licenses/by-nc-nd/3.0/ch/ Datum: 12.11.2013

Table of Contents

Summary

Headwater catchments in mountainous regions provide freshwater for lowland areas and therefore play an important role for water quality in downstream areas and the ecological integrity of downstream rivers.

Various external and internal factors such as atmospheric inputs and catchment characteristics, e.g. soil and vegetation cover, influence stream water geochemistry. In the Swiss Alps, shrubs (e.g. *Alnus viridis subsp. viridis*, *Sorbus aucuparia*, *Calluna vulgaris*, *Salix appendiculata*, *Rhododendron ferrugineum*) are encroaching into formerly open habitats and the effects of the latter on the catchment and hillslope scale hydrology and stream water geochemistry have not been investigated so far. The shrub encroachment might affect soil hydrological properties, which in turn could influence runoff generation. Moreover, alder species (*Alnus spp*.) are known to affect chemical soil properties (e.g. total organic carbon or nitrogen content or soil pH) and can therefore alter the export of nutrients via stream water.

Therefore, the hydrological and geochemical behavior of four alpine headwater sub catchments, which differ in vegetation and soil cover characteristics, were investigated. The aim was to gain information on water flow paths and export of nutrients during base flow, rainfall and snowmelt conditions at the micro catchment scale. Subsurface water flow paths at the hillslope scale were also investigated.

First, the influence of vegetation cover on mean transit times of water (MTT) was assessed. The MTT of water in a catchment provides important information about storage, flow paths, sources of water and thus also about retention and release of solutes in a catchment. MTTs between 70 to 102 weeks were calculated via time series of water stable isotopes using a convolution integral method. The high temporal variation of the stable isotope signals in precipitation was strongly dampened in stream base flow samples. This pointed to deeper flow paths and mixing of waters of different ages at the catchments' outlets, which was supported by additional geochemical stream water data (e.g. Ca and Si). The study with four sub catchments suggests that MTTs are neither related to topographic indices nor vegetation cover. Water balance calculations and the geochemical data suggest that the major part of the quickly infiltrating precipitation likely percolates through fractured and partially karstified deeper rock zones. This process increases the control of bedrock flow paths on MTT.

In a next step, the water pathways at two steep hillslopes were tracked, since they strongly affect runoff generation processes and therefore control water geochemistry on the short term scale. Soil water stable isotope profiles, which offer a time-integrating overview of subsurface hydrological processes, were used. Furthermore, an advection-dispersion model was applied to simulate the $\delta^{18}O$ profiles. The variability of $\delta^{18}O$ values with depth within each profile and a comparison of the simulated and measured profiles revealed that vertical downward subsurface flow plays an important role, even at high slope angles.

Lateral subsurface flow was also observed in deeper soil layers (approx. 0.3 to 0.9 m depth) and at sites near a small stream. Physical soil data further supported the fast percolation of water towards deeper soil layers, from where it can subsequently recharge to the fractured bedrock, which led to the aforementioned strong dampening of stable isotope signals in base flow stream water.

Finally, the study focused on the hydrological and geochemical processes on the short term scale, i.e. a rainfall event in the growing season and a spring snowmelt period. The hydrological and geochemical differences in the sub catchments were assessed. Stream water was sampled at hourly intervals during the rainfall event and on a daily basis during the snowmelt period. Stream geochemistry was strongly influenced by the land cover, i.e. soil and shrub cover. Riparian wetland soils were flushed by a high proportion of event water (up to 70 %), which increased dissolved organic carbon export during the rainfall event and the snowmelt period. A slight increase in nitrate export during the rainfall event was likely due to the encroachment of green alder shrubs.

In conclusion, the bedrock geology and geochemistry was mainly controlling stream water geochemistry on the hydrological long term scale, i.e. during base flow conditions. The soil properties in the investigated valley allow vertical downward flow of water within soil profiles even at steep slopes, and facilitate recharge of water to deeper zones and subsequently to the bedrock. The differences in vegetation and soil cover characteristics were most notably observed on the hydrological short term scale, when stream water geochemistry was highly variable. The connection of the shallow soil layers, which act as a "reservoir" for biogeochemical reactions, with the streams is mostly activated during rainfall and snowmelt events. Since duration of snow cover will be shortened and rainfall events during the growing season will become more frequent and intense due to climatic changes, the importance of vegetation and soil characteristics for the export of nutrients might still increase in the future.

1 Introduction

1.1 Framework of the thesis

This PhD thesis was part of the interdisciplinary SNF project "The ecological and socio-economic consequences of land transformation in alpine regions: an interdisciplinary assessment and valuation of current changes in the Urseren Valley, key region in the Swiss central Alps (*ValUrsern*)." The main aim of the project was to assess the status and current change of vegetation cover, plant diversity, soil characteristics, and their combined effects on the water balance at different spatial and temporal scales in the headwater catchments of the Urseren Valley in the Swiss Alps (ValUrsern, 2012). In total, five groups were involved in the project. The group of Plant Ecology (Prof. C. Körner, Departement of Environmental Sciences, University of Basel, Switzerland) investigated the current status of vegetation cover, altitudinal gradients of evapotranspiration, and water balances in dependence of vegetation types and structures. The group of Hydrology (Prof. R. Weingartner, Institute of Geography, University of Bern, Switzerland) assessed water balances and discharges at the catchment scale (micro- to mesoscale) and surface runoff at the plot and hillslope scale by field measurements and modeling tools. The group of Environmental Economics (Prof. F. Krysiak, Faculty of Business and Economics, University of Basel, Switzerland) investigated the economic implications of current and future land use changes. The socio-historical development of the Urseren Valley was assessed by the group of General Modern History (Prof. M. Schaffner, Department of History, University of Basel, Switzerland), which collaborated as an associated group in the project. This thesis was conducted within the group of Environmental Geosciences (Prof. C. Alewell, Department of Environmental Sciences, University of Basel, Switzerland). Its main aim was to collect hydrological and geochemical information of the investigated micro catchments, to track hydrological flow paths on the plot and hillslope scale and to assess physical and chemical soil and stream water data in order to evaluate their dependence on vegetation and land cover.

1.2 Hydrological importance of headwater catchments

On the global scale, headwater catchments in mountainous regions contribute disproportionally more water to total runoff in the adjacent lowlands than can be expected on the basis of the headwater catchments' sizes (Viviroli et al., 2011; Weingartner et al., 2007). This disproportional contribution of headwater catchments strengthens their importance in providing freshwater for lowland areas, where it is e.g. used for irrigation or sustains production of drinking water (Viviroli et al., 2011; Weingartner et al., 2007). According to Viviroli et al. (2003), about 50 % of the world's population rely on water resources from mountainous regions. Headwater catchments in mountainous regions are subjected to changing environmental conditions and land use practices (IPCC, 2007; Lambin and Geist, 2008). The environmental changes include for example increases in

frequency and intensity of torrential rainfall events and reduced duration of winter snow cover. Land use changes comprise for example deforestation, afforestation, extensification or intensification of agricultural use at different locations worldwide (Lambin and Geist, 2008). These environmental and land use changes are likely to affect the hydrology in headwater catchments and adjacent lowlands (e.g. Lambin and Geist, 2008). Besides quantitative considerations, water quality of headwaters (e.g. stream water geochemistry) also strongly influences the water quality in downstream areas (Alexander et al., 2007) and the ecological integrity of downstream rivers (Bishop et al., 2008; Freeman et al., 2007). Knowledge about hydrological and geochemical functioning of headwater catchments is therefore crucial to deduce management strategies in order to maintain ecosystem services of headwaters and their adjacent lowlands.

1.3 Headwater catchment hydrology and stream geochemistry

The hydrological regime of headwater catchments in mountainous areas is mainly characterized by temporal storage of precipitation in the systems as snow or ice, which is released to the streams during the melt periods (Buttle, 1998). Meteorological and climatological factors therefore regulate timing of water flow and its chemistry in these environments (Rodhe, 1998). Besides the atmospheric inputs which control water chemistry (Gibbs, 1970), intrinsic catchment characteristics also strongly affect stream water chemistry. These characteristics include geology and mineralogy of rocks (Drever, 1982), chemical soil characteristics (Billett and Cresser, 1992), topography, which in turn influences hydrological response (McGuire et al., 2005), land use (e.g. agricultural use) (Hill, 1978) and land/vegetation cover (Andersson and Nyberg, 2009).

On a secondary level, these factors determine the transit time of water within the different compartments in a catchment. The water transit time, as a combined catchment characteristic, is a crucial factor that influences stream water geochemistry, since most (bio)geochemical reactions are kinetically controlled (Bethke, 2008). It can be used to estimate flow paths and sources of water and solutes in a catchment (McDonnell et al., 2010; McGuire et al., 2005). Large differences in solute concentrations can be observed on the long and the short term scale, i.e. during base flow and storm flow or snowmelt conditions (e.g. Kendall et al., 1999; Neff et al., 2012). Furthermore, the water transit time is important to assess the vulnerability of a system to anthropogenic inputs or land use changes (McGuire and McDonnell, 2006).

Flow paths through the hillslopes and runoff generation processes also strongly affect water geochemistry on the short term scale (e.g. Weiler and McDonnell, 2006). Pre-event water (i.e. groundwater or soil water) with relatively higher solute concentrations compared to event water (i.e. rainwater or snowmelt) can be transported to the streams due to rising groundwater tables (e.g. Hornberger et al., 1994). On the other hand, preferential flow paths due to plant roots (Jarvis, 2007) can lead to fast arrival of geochemically weakly buffered event water in streams (Bachmair and Weiler, 2011). This emphasizes that flow paths and

runoff generation processes are strongly influenced by the vegetation cover and soil properties (Bachmair and Weiler, 2011).

Hence, investigations on different spatial scales (i.e. catchment and hillslope scale) and temporal scales (i.e. base flow *versus* storm flow or snowmelt) are required to describe the hydrological and geochemical processes of headwater catchments.

1.4 Hydrological importance of headwaters in the Swiss Alps

Due to higher precipitation and lower evaporation rates at high altitudes, Swiss alpine headwater catchments contribute disproportionally more water to total runoff in downstream areas in relation to the headwater catchments' surface area (Weingartner et al., 2007). This emphasizes the hydrological importance of headwater catchments of the Swiss Alps. The current changing environmental conditions and land use practices increased sediment loads in streams (Asselman et al., 2003), but hydrological regimes might also be altered. This subsequently can affect spatial and temporal patterns of stream water geochemistry in alpine headwater catchments.

In the Swiss Alps, an intensified agricultural use of easily accessible areas and a simultaneous abandonment of remote areas is widely observed (BFS, 2005). These changing agricultural practices induce an encroachment of e.g. *Alnus viridis subsp. viridis* (green alder), *Sorbus aucuparia* (mountain-ash), *Calluna vulgaris* (common heather), *Salix appendiculata*, and *Rhododendron ferrugineum* (rusty-leaved alpenrose) into formerly open areas in the Swiss Alps (Kägi, 1973; Küttel, 1990; Wettstein, 1999). The shrub encroachment might affect the hydrological and geochemical functioning of headwater catchments during base or event flow (storm events or snowmelt) in these areas. The water balance might be affected through higher soil hydraulic conductivities of soils under green alder stands compared to grassland sites (Alaoui et al., 2013) and altered evapotranspiration patterns in the catchments (ValUrsern, 2012). The geochemistry of the systems, especially the nitrogen dynamics, can be affected through the symbiotic relationship between the green alder roots and the nitrogen-fixing bacterium *Frankia alni* (Benecke, 1970; Pawlowski and Newton, 2008). Alder species (*Alnus spp.*) can increase nitrogen (N) and carbon (C) concentrations in soils (e.g. Mitchell and Ruess, 2009) and have been shown to increase nitrate concentrations in soil water under green alder stands (*Alnus viridis subsp. viridis*) in the Urseren Valley in the Swiss Central Alps (Bühlmann, 2011). As a consequence, stream geochemistry (C and N) might be affected. Changes on the short term scale (storm events or snowmelt) might be enhanced through changed precipitation patterns due to climatic changes, i.e. changes in snowmelt dynamics and increased intensity of summer rainfall events (IPCC, 2007). Therefore, not only timing and amount of high flow runoff can be altered, but also nutrient export patterns might be changed.

According to Burt et al. (2010), small catchments are especially suitable to investigate the link between hydrology and (bio)geochemistry, because of the usually high variability of catchment characteristics on the spatial scale, e.g. land use or vegetation cover. We

therefore investigated contrasting alpine micro catchments (< 1 km^2) in order to depict the influence of vegetation cover changes on their hydrological and geochemical behavior.

1.5 Aims and outline of the study

The thesis is divided into three main parts (chapters 2, 3 and 4), which provide insights into the hydrological and geochemical functioning from the long term to the short term scale (base flow *versus* event flow) and from the plot scale to the micro catchment scale.

First, the importance of vegetation, topography and flow paths for water transit times of base flow in alpine headwater catchments was assessed (chapter 2). The shrub encroachment can increase saturated hydraulic conductivity of soils (Alaoui et al., 2013). Therefore, it was hypothesized that higher infiltration rates of water into the unsaturated zone and subsequent recharge to groundwater in the bedrock will result in longer mean water transit times. Mean water transit times were calculated via stable water isotopes using a convolution integral method (e.g. McGuire and McDonnell, 2006).

In a second step, soil water flow and transport processes at two steep subalpine hillslopes were investigated, in order to depict water flow paths at the hillslope scale (chapter 3). The knowledge of water pathways at the hillslope scale is important to assess nutrient transport in the unsaturated zone (Bachmair and Weiler, 2011). Profiles of soil water $\delta^{18}O$ values at two steep hillslopes were measured in order to infer information on water pathways. Additionally, the measured time-integrating soil water $\delta^{18}O$ profiles were compared to simulated $\delta^{18}O$ values using a numerical advection-dispersion model. $\delta^{2}H$ values were also measured and are given in the appendix 1 (chapter 6).

Finally, the thesis focuses on the influence of invading shrubs and wetland soils on the export of nutrients during a summer storm event and a snowmelt period (chapter 4). Geochemical tracers were used to infer information on runoff generation mechanisms and water flow paths. It was hypothesized that the encroachment of green alder shrubs increases concentrations of nitrate in stream water during high flow periods of rainfall and snowmelt events. The water during these high flow periods most likely flushes riparian wetlands and the areas where green alder shrubs grow. It was therefore also hypothesized that the flushing of riparian wetlands subsequently increases the export of dissolved organic carbon from the catchments.

Additional hydrological soil data from plot scale measurements are presented in the appendix 3 (chapter 8), which will give further insights into the hydrological functioning of the investigated soils.

The results of this study will give an integrated picture of the water flow paths at different spatial and temporal scales in contrasting alpine headwater catchments.

2 Importance of vegetation, topography and flow paths for water transit times of base flow in alpine headwater catchments

Mueller, M. H.[1], Weingartner, R.[2,3], and Alewell, C.[1]

[1]Environmental Geosciences, University of Basel, Bernoullistrasse 30, 4056 Basel, Switzerland

[2]Institute of Geography, University of Bern, Hallerstrasse 12, 3012 Bern, Switzerland

[3]Oeschger Centre for Climate Change Research, University of Bern, Zähringerstrasse 25, 3012 Bern, Switzerland

This chapter is published in:

Hydrology and Earth System Sciences, 17, 1661-1679, 10.5194/hess-17-1661-2013, 2013

2.1 Abstract

The mean transit time (MTT) of water in a catchment gives information about storage, flow paths, sources of water and thus also about retention and release of solutes in a catchment. To our knowledge there are only a few catchment studies on the influence of vegetation cover changes on base flow MTTs. The main changes in vegetation cover in the Swiss Alps are massive shrub encroachment and forest expansion into formerly open habitats. Four small and relatively steep headwater catchments in the Swiss Alps (Urseren Valley) were investigated to relate different vegetation cover to water transit times.

Time series of water stable isotopes were used to calculate MTTs. The high temporal variation of the stable isotope signals in precipitation was strongly dampened in stream base flow samples. MTTs of the four catchments were 70 to 102 weeks. The strong dampening of the stable isotope input signal, as well as stream water geochemistry point to deeper flow paths and mixing of waters of different ages at the catchments' outlets. MTTs were neither related to topographic indices nor vegetation cover. The major part of the quickly infiltrating precipitation likely percolates through fractured and partially karstified deeper rock zones, which increases the control of bedrock flow paths on MTT. Snow accumulation and the timing of its melt play an important role for stable isotope dynamics during spring and early summer.

We conclude that in mountainous headwater catchments with relatively shallow soil layers, the hydrogeological and geochemical patterns (i.e. geochemistry, porosity and hydraulic conductivity of rocks) and snow dynamics influence storage, mixing and release of water in a stronger way than vegetation cover or topography do.

2.2 Introduction

The time of water traveling through a catchment gives information about storage, flow paths, sources of water and thus also about retention and release of solutes in a catchment (McDonnell et al., 2010; McGuire et al., 2005). The mean transit time (MTT) of water can be defined as the mean time that elapses from the input of water to a system until the output of that water (Eriksson, 1971; McDonnell et al., 2010). It can be calculated via stable isotopes of the water molecule (McGuire and McDonnell, 2006). The stable isotope signals in precipitation are influenced by air temperature, varying storm trajectories, precipitation amounts and relative air humidity (e.g. Ingraham, 1998). In regions with seasonally varying air temperatures, the stable isotope signature in precipitation also varies seasonally (Dansgaard, 1964). This variability can also be observed in stream flow samples, but often is delayed and/or dampened, depending on the MTT and transport properties within the aquifer (McGuire and McDonnell, 2006).

Water storage and flow in the bedrock (e.g. Asano and Uchida, 2012; Gabrielli et al., 2012), landscape structure and topography (e.g. McGlynn et al., 2003; McGuire et al., 2005; Rodgers et al., 2005; Soulsby and Tetzlaff, 2008) play an important role as controlling factors on water transit times, but their influence can vary in different environments. Gabrielli et al. (2012) found that tortuous flow paths through the deeper fractured bedrock of a headwater catchment in the H.J. Andrews Experimental Forest, USA, can lead to longer estimates of MTT of stream flow. In small mountainous catchments with shallow soil layers underlain by fractured granites in Japan, Asano and Uchida (2012) found that MTT of base flow was positively related to the contributing flow path depth. Their conclusion was based on dissolved silica concentrations in stream flow which could be used as a tracer to identify flow path depth. Soulsby and Tetzlaff (2008) analyzed a large catchment in Scotland and found that MTT correlates negatively with the percentage of soils which rapidly generate storm runoff and (counter-intuitively) positively with mean catchment slope. The more freely draining soils, which can be found at steeper slopes in formerly glaciated landscapes, facilitate recharge to groundwater and subsequent mixing of pre-event and event waters, which therefore leads to longer MTT estimates. McGuire et al. (2005), on the other hand, found flow path gradient to the stream network to be negatively correlated to MTT of stream flow in small catchments of the H.J.A. Experimental Forest. In the studies of McGuire et al. (2005), Soulsby and Tetzlaff (2008) and Tetzlaff et al. (2011), the authors found that catchment area does not seem to influence MTT, whereas, e.g. Dewalle et al. (1997), found a positive correlation between the two parameters in three small forested catchments in the Appalachian Mountain, USA, which indicates that catchment surface characteristics partially control MTT.

To our knowledge there are several studies on the influence of land use/vegetation cover on the reaction of the catchments during storm events (e.g. Bariac et al., 1995; Buytaert et

al., 2004; Monteith et al., 2006; Roa-Garcia and Weiler, 2010; Wenjie et al., 2011), but only a few catchment studies on the influence of vegetation cover on stream base flow MTTs (e.g. Roa-Garcia and Weiler, 2010). Wenjie et al. (2011) investigated the impact of land use on runoff generation processes in a small tropical seasonal rain forest catchment and a small artificial rubber plantation catchment. Soil compaction through land use changes resulted in higher amounts of infiltration-excess overland flow and subsequent higher fractions of event water in runoff. Monteith et al. (2006) studied hydrographs and groundwater transit times in a small harvested and a small undisturbed hardwood forest in Ontario, Canada. They found that mean groundwater transit time was not influenced by land use, at least not during a snowmelt period. Buytaert et al. (2004) investigated two small catchments in the Ecuadorian Andes under different land use (extensive grazing versus intensive grazing, cultivation and drainage). They found a substantially faster response of discharge to precipitation in the cultivated catchment compared to the extensively use catchment. Bariac et al. (1995) compared the runoff generation of small deforested and forested catchments in the north of French Guiana. Retention of precipitation was higher in the forested catchment, which the authors ascribe to soil porosity. Roa-Garcia and Weiler (2010) investigated three small catchments in the Columbian Andes with thick soil layers. Catchments differed in percentage of forest, grassland and wetlands. The authors found higher rates of stream discharge during precipitation events in the catchment with a higher percentage of grazed grassland, which is explained by compaction of soils. On the long time scale they found differences in the MTTs, which they ascribe to the difference in vegetation cover/land use, notably the occurrence of wetlands and forests which increased MTTs due to an increased water holding capacity (Roa-Garcia, 2009).

Darling and Bath (1988) measured more negative $\delta^{18}O$ values in the percolate of a lysimeter compared to soil water samples of drill cores from the same depth. These two methods involve two distinct pools of soil water, i.e. fast and slowly moving water. Therefore, different flow patterns in the unsaturated zone can influence timing and stable isotope characteristics of soil water recharging to deeper bedrock zones. In a lysimeter, study Stumpp et al. (2009a) found that water flow was faster and MTT was shorter when the lysimeter surface was covered with maize compared to the periods when it was covered with canola or wheat. They concluded that soil hydraulic properties were changed by vegetation cover changes. Distinct root growth of different crops can partially explain their results. The influence of roots on water infiltration into and flow within the soil was suggested by Beven and Germann (1982). Several studies confirmed the importance of root induced preferential flow (Bundt et al., 2001) and especially the influence of different land use (i.e. vegetation types) on preferential flow (Bachmair et al., 2009; Jinhua et al., 2010).

The main changes in vegetation cover in the Swiss Alps are massive shrub (mainly *Alnus viridis* and also *Sorbus aucuparia*; see also section 2.3.1) encroachment and forest expansion into formerly open habitats (Tasser et al., 2005; Wettstein, 1999). In the Urseren Valley the shrub cover increased by 32 % between 1965 and 1994 (Wettstein, 1999) and

again by 24 % between 1994 to 2004 (van den Bergh et al., unpublished data, 2013). Since shrub encroachment can increase saturated hydraulic conductivity of soils (Alaoui et al., 2013), we hypothesize that higher infiltration rates of water into the unsaturated zone and subsequent recharge to groundwater in the bedrock will result in longer MTTs.

In four alpine micro catchments we modeled the MTT under base flow conditions using stable water isotopes. Our sampling approach enabled us to estimate the influence of vegetation cover as well as topography on MTT under the same geological and climatological conditions. Furthermore, we evaluate additional geochemical data, which also allows us to estimate the contribution of groundwater to base flow runoff and its influence on MTT.

2.3 Material and Methods

2.3.1 Study site

The Urseren Valley (Figure 2.1) has a U-shaped profile and is characterized by rugged terrain. Elevation ranges from 1400 to 3200 m a.s.l. The whole catchment covers an area of 191 km^2 and is drained to the north-east by the Reuss River. The southern mountain ridge is built by the gneiss massif of the Gotthard system whereas the northern mountains are part of the granite massif and the pre-existing basement of the Aar system (Labhart, 1977). The two massifs are separated by intermediate vertically dipping layers along a geological fault line which corresponds to the valley axis. These layers consist of Permocarbonic and Mesozoic sediments and they comprise sandstones, rauhwackes, dolomites, dark clay-marls and limestones. Throughout the formation of the Alps the material was metamorphosed to schist (Ambuehl, 1929). Due to erosion of these soft layers a depression developed (Kägi, 1973). The soluble limestones and also gypsum rich rocks, which are prone to karst formation, underlie the outcropping rocks or are incorporated as lenses in the granites and gneisses (Ambuehl, 1929; Buxtorf, 1912; Labhart, 1977; Winterhalter, 1930). The most abundant outcropping bedrock material is a white mica-rich gneiss. This was confirmed by the detection of phyllosilicates (muscovite/illite) in the soil by X-ray diffraction (Schaub et al., 2009).

Podsols, Podzocambisols and Cambisols are the dominant soil types in the valley (Meusburger and Alewell, 2008). At higher elevations and on steep valley slopes, Leptosols are common. At the valley bottom and lower slopes, predominantly clayey gleyic Cambisols, Histosols, Fluvisols and Gleysols developed (Meusburger and Alewell, 2008).

The valley is characterized by a high mountain climate with a mean air temperature of 3.1°C (1901 to 1961). Mean annual rainfall at the climate station in Andermatt (1442 m a.s.l.) of MeteoSwiss is about 1400 mm. The valley is snow covered for 5 to 6 months (from November to April) with maximum snow height in March (Angehrn, 1996). Runoff is usually dominated by snowmelt in May and June.

Vegetation shows strong anthropogenic influences due to pasturing for centuries (Kägi, 1973). An invasion of shrubs mainly by *Alnus viridis*, *Calluna vulgaris*, *Salix appendiculata*, *Sorbus aucuparia* and *Rhododendron ferrugineum* was identified, particularly on the north-facing slopes (Kägi, 1973; Küttel, 1990; Wettstein, 1999). The south-facing slopes are dominated by dwarf-shrub communities of *Rhododendron ferrugineum* and *Juniperus sibirica* (Kägi, 1973; Küttel, 1990) and diverse herbs and grass species. Wettstein (1999) estimated that approximately one third of shrubs (mainly consisting of *Alnus viridis* and *Sorbus aucuparia*) have invaded since 1965. For more detailed information about the Urseren Valley, the reader is referred to Meusburger and Alewell (2008).

Four micro catchments located on north-east and north-west facing slopes in the Urseren Valley (Table 2.1 and Figure 2.1) were chosen with regard to their differing percentage of shrub cover. The steep micro catchments are smaller than 1 km^2 and shrub vegetation covers a range from 13.8 to 82.2 %. The Chämleten micro catchment also includes several wetland sites which presumably play an important role for the hydrology in this micro catchment. From field observations we can assume that mean discharge during the snow covered period is at the lower end of the discharge range given in Table 2.1. In all micro catchments small springs could be indentified as the starting point of the streams permanently discharging water (also observed in winter months) (Figure 2.1).

Table 2.1: Characteristics of micro catchments (vegetation data from van den Bergh et al. (2011) and Fercher (2013), modified; discharge data from Lagger (2012) and Schmidt (2012)).

	Chämleten	Wallenboden	Bonegg	Laubgädem
projected area (km^2)	0.01981	0.56431	0.34302	0.02981
shrub cover (mainly *Alnus viridis* and *Sorbus aucuparia*) (%)	82.2	13.8	38.5	14.5
vegetation cover (%)	100.0	78.9	95.9	100.0
elevation range (m a.s.l.)	1669 – 1810	1501 – 2354	1551 – 2492	1721 – 1915
mean elevation (m a.s.l.)	1740	2082	2026	1836
slope range (°)	4 .0 – 55.7	0.6 – 60.5	0.5 – 73.1	0.3 – 49.3
mean catchment slope (°)	24	20	28	20
aspect	NE	NNW	NW	NE
range of discharge (L s^{-1})	0.09 – 36.02	0.46 – 44.03	2.00 – 93.54	0.10 – 14.61
mean discharge (L s^{-1}) (summer 2010 and 2011)	1.08	2.42	6.3	2.91

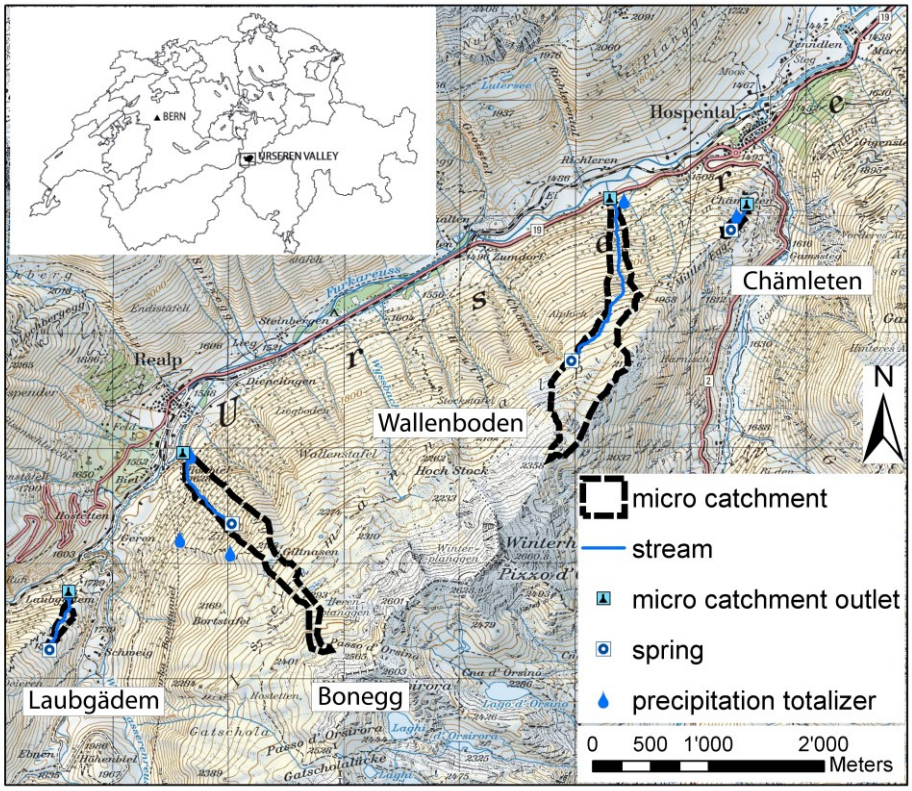

Figure 2.1: Location of the micro catchments in the Urseren Valley. Micro catchment limits from van den Bergh et al. (2011) and Fercher (2013), modified. Geodata reproduced by permission of swisstopo (BA12066).

2.3.2 Sampling and Analysis

2.3.2.1 Precipitation, discharge and stable water isotopes

Precipitation was continuously measured with a Davis Vantage pro2 weather station at the MeteoSwiss station Andermatt by the Swiss Federal Office of Meteorology and Climatology (MeteoSwiss, 2013). Discharge was measured with pressure transducers (PDCR1830, Campbell Scientific) and a radar sensor (Vegapuls61, VEGA). Discharge data availability was restricted to summer months because streams and installed weirs were completely snow covered and/or frozen during winter. We sampled precipitation and stream base flow biweekly for stable isotope analysis from March 2010 to May 2012. Precipitation was sampled near the catchment outlets with a 0.02 m^2 totalizer and a buried and covered 5 L bottle to protect the water from evaporation. Precipitation amount was determined and a subsample was transferred in a 250 ml poly ethylene (PE) bottle. In summer 2010, we installed three precipitation samplers at an elevation gradient ranging from 1600 to 2100 m a.s.l. in the Bonegg micro catchment to determine a possible elevation gradient in stable isotope values of precipitation.

Stream water was also sampled by hand with 250 ml PE bottles, which were filled completely. Samples were taken at base flow conditions defined as the "baseline" of the hydrograph when discharge was not increased by the influence of precipitation events. When a storm event coincided with a planned sampling day, we adapted our strategy and sampled one day in advance or after the originally fixed day. This is justified since storm flow peaks decreased back to pre-event conditions very fast within a few hours after the precipitation event, which was confirmed by discharge measurements. During five weeks from April to May 2012, we also sampled stream water in the Wallenboden and Bonegg micro catchments on a daily basis (except during high avalanche risk) to capture snowmelt runoff. Snow was sampled during the winter period as bulk samples with a plastic tube of 2 m length and a diameter of 3.5 cm. Each complete bulk snow sample was transferred into a 2 L PE bottle. After melting of the snow, we took a subsample for stable isotope analysis. Snow water equivalent was calculated from the known snow volume and snow density. Monthly samples were taken near the micro catchments' outlets. In March 2010, 2011 and 2012, shortly before the onset of snowmelt, we sampled snow spatially distributed over several kilometers along the valley slopes from 1500 to 2700 m a.s.l., depending on weather conditions and avalanche situation. A few snow samples on shadowed spots were also taken at the end of April 2011 when substantial snowmelt in most parts of the catchments had already happened. The bulk snow samples were used for MTT modeling (see below). For a discussion of fractionation of stable isotopes in snow samples, see also section 2.4.2.2.

Stable isotopes were measured with a Thermo Finnigan GasBench II connected to a DELTAplus XP continuous flow mass spectrometer (CF-IRMS, DELTAplus XP, Thermo, Bremen, Germany) and a liquid water isotope analyzer (Los Gatos Research, Inc. (LGR), Mountain View, USA). Results are reported as $\delta^{18}O$ or $\delta^{2}H$ in ‰ vs. the V-SMOW standard. Precisions are 0.05 ‰ for $\delta^{18}O$ and 1 ‰ for $\delta^{2}H$ with the IRMS and 0.1 ‰ for $\delta^{18}O$ and 0.3 ‰ for $\delta^{2}H$ with the LGR instrument, respectively. Samples were calibrated to known standards (V-SMOW, SLAP and GISP).

2.3.2.2 Additional geochemical parameters

In addition to the use of stable isotopes as a time orientated tracer, we also measured various geochemical parameters which served as geogenic tracers. Total dissolved alkali and earth alkali metals (Ca, Mg, K, Na) and silicon (Si) were measured by Inductively Coupled Plasma Optical Emission Spectrometry (ICP-OES, Spectro Genesis, Spectro Analytical Instruments, Germany). These elements can be found in aqueous solutions due to weathering of minerals and can be an indicator of the type of rocks which are weathered (Stumm and Morgan, 1996). Major anions were measured by ion chromatography (761 Compact IC, Metrohm, Switzerland). Sulfate in stream water can be an indicator for weathering of gypsum bearing rocks (Stumm & Morgan 1996). PH was measured continuously during the summer periods with a CS525 ISFET pH Probe (Campbell

Scientific, UK) and on a monthly basis during winter with a portable pH 340i probe (WTW, Weilheim, Germany).

All stream water samples for geochemical parameter determination were taken by hand in the field, filtered with 0.45 µm filters (Rotilabo-filter, PVDF, Roth, Switzerland), cooled during transport to the laboratory and kept frozen at -20°C until analysis.

2.3.3 Mean water transit time modeling

We determined MTTs from biweekly stable isotope data of precipitation and stream base flow ($\delta^{18}O$ of H_2O). The stable isotope data of precipitation were corrected for the elevation gradient (see results) using the difference between elevation of catchment base and mean catchment elevation. Stable isotope values of monthly winter samples were stepwise interpolated. We used the modeling procedure suggested, e.g. by Maloszewski and Zuber (1982; 2002) and their provided software FlowPC. From a known isotope input signal (precipitation samples) and the measured output signal in the four streams (base flow samples), MTTs can be modeled by solving a convolution integral which relates input and output stable isotope signals with water transit times:

$$\delta^{18}O_{out}(t) = \int_0^\infty \delta^{18}O_{in}(t-\tau)g(\tau)d\tau \,, \quad (1)$$

where $\delta^{18}O_{out}$ is the output signal, $\delta^{18}O_{in}$ is the input function, $g(\tau)$ the system response function and τ is the transit time.

The use of a MTT, which we calculate via this approach, is subject to some assumptions which are not always met in nature. For example, steady state of flow, linear tracer input-output relations and an equal distribution of precipitation over the entire catchment are assumed (Turner and Barnes, 1998). Recent studies have shown that transit time distributions are not time-invariant, which reflects the variability of climate, precipitation and hydrological conditions (e.g. Botter et al., 2011; Heidbuechel et al., 2012; McGuire et al., 2007). On the other hand, the hydrological response of a catchment is also subject to quasi-stationary characteristics as, for example, topography and structure of the subsurface (Hrachowitz et al., 2010). Despite the above mentioned assumptions, the MTTs are useful to inter-compare the behavior of catchments (McDonnell et al., 2010; Soulsby et al., 2010) and our aim is to compare four small catchments under the same boundary conditions (climate, geology, geomorphology and considered time span).

The use of a lumped parameter model offers the advantage that it only requires few parameters and is useful in catchments where information on hydraulic properties of underlying material is scarce (Maloszewski and Zuber, 1982; 2002). Furthermore, the provided software does not require extensive hydrological or meteorological data. Especially discharge data were not available for the winter periods in our micro catchments.

Therefore, more complex models, which take output flow into account (e.g. Rodhe et al., 1996), could not be applied in our study.

The system response function g(τ) describes the transit time distribution in the aquifer and hence implicitly includes hydraulic properties of the aquifer. We tested all the different system response functions g(τ) implemented in the software: the exponential, the exponential-piston-flow, the dispersion, the piston-flow and the linear model. The exponential model, which can be regarded as a special case of the gamma distribution model (e.g. Amin and Campana, 1996; Kirchner et al., 2000), is mathematically equivalent to a well-mixed reservoir. However, mixing only occurs at the system outlet (Maloszewski and Zuber, 1982; 2002). There is no exchange of tracer along the flow lines in the aquifer. The dispersion model, on the other hand, allows mixing of tracer within the aquifer itself. Using the exponential model would imply that there exists water with very short and water with very long transit times which only mix at the outlet. More detailed information about the flow models can be found in Maloszewski and Zuber (1982).

The stable isotope input function for the MTT modeling has to be weighted with the precipitation amount and recharge factor α (also called infiltration coefficient in the cited literature) (Grabczak et al., 1984; Maloszewski and Zuber, 1982; 2002):

$$\textbf{(2)} \quad \delta^{18}O_{in}(t_i) = \frac{N \cdot \alpha_i \cdot P_i}{\sum_{i=1}^{N} \alpha_i \cdot P_i} \cdot (\delta^{18}O_i - \delta G) + \delta G$$

N is the number of single sampling events, P_i and $\delta^{18}O$ are precipitation rates and its isotope values and δG is the mean value of δ^{18}O of the local groundwater originating from recent precipitation. Recharge factors are often difficult to estimate and even unknown (Grabczak et al., 1984; Maloszewski and Zuber, 2002). They can, for example, be estimated as a ratio of summer recharge to winter recharge from stable isotope data (Grabczak et al., 1984) (equation 3) or calculated from the water balance (Stumpp et al., 2009b) (equation 4).

$$\textbf{(3)} \quad \alpha = \frac{(\overline{\delta P_W} - \delta G) \cdot \sum_i (P_i)_W}{(\delta G - \overline{\delta P_S}) \cdot \sum_i (P_i)_S} \qquad \textbf{(4)} \quad \alpha_i = \frac{P_i - ET_{a,i}}{P_i}$$

$\overline{\delta P_W}$ and $\overline{\delta P_S}$ are the long-term weighted mean values of δ^{18}O for the winter and summer precipitation (P), respectively and $ET_{a,i}$ is the actual evapotranspiration.

Since in our case the volume weighted mean stable isotope signal in precipitation for the whole observation period equals the mean of base flow stream samples, we conclude that summer and winter precipitation equally contribute to the stable isotope signal in stream base flow. Therefore, the recharge factor calculated according to Grabczak et al. (1984) as a ratio of summer recharge to winter recharge is equal to 1. This would not represent the real situation since snow accumulates from November to March and recharge during winter

would only occur when short warm periods induce snowmelt. The isotope signal from this winter precipitation will substantially recharge and contribute to the base flow signal only during the spring snowmelt and early summer. We therefore made a simplification and estimated the recharge factors for the snow accumulation period to be 0.01. This low value is justified because only small amounts of meltwater were measured in several snow lysimeter studies during accumulation period (e.g. Gurtz et al., 2003).

Snowmelt was introduced into the model via the weighting procedure by recharge factors (set to 1) and precipitation amounts which accumulated during the winter season. From field observation and data from MeteoSwiss (2013), we know that snowmelt occurs from the end of March until the beginning of May. Accumulated snow during winter was therefore released during snowmelt within six weeks in our model. At the lower part of our micro catchments, snow had melted at the beginning of April whereas snow in the upper regions lasted a few weeks longer. The recharge factor during the summer period was calculated similar to Stumpp et al. (2009b) by correcting measured precipitation for evapotranspiration and direct flow (which was calculated from the hydrographs according to Wittenberg (1999) by the Institute of Geography, Group of Hydrology, University of Bern).

To account for uncertainty in model input parameters – including $\delta^{18}O$ values of precipitation, precipitation volume and recharge factor α – we conducted an uncertainty analysis with different parameter sets A to E (Table 2.2). The simplest parameter set A includes raw $\delta^{18}O$ values of precipitation and the more complex sets C to E are generated as described above, considering snow dynamics. With these different sets we can estimate a range of most plausible MTTs.

The stable isotope values of stream water are calculated via equation **(1)** by choosing a system response function and a MTT. Calibration of the model is carried out by a trial-and-error procedure comparing the modeled stable isotope values of stream water with the measured values via the σ–value, as defined by Maloszewski and Zuber (2002):

$$\sigma = \frac{\sqrt{\sum_{i=1}^{n} \left(c_{mi} - c_i\right)^2}}{n} \qquad \textbf{(5)}$$

c_{mi} = measured stable isotope value at time i

c_i = modeled stable isotope value at time i

n = number of measurements

This value can be used to compare model results for different parameter sets. The trial-and-error procedure aims to minimize the σ–values. We also report the model efficiency (E) according to Nash and Sutcliffe (1970) for the best fits according to the values of σ. Further description of the uncertainty and sensitivity analysis can be found in section 2.4.2.1.

Table 2.2: Description of the different model input parameter sets.

	Description of input parameters
set A	raw $\delta^{18}O$ values of precipitation, not weighted by precipitation volume or recharge, i.e. all precipitation enters the system and no snow accumulation occurs
set B	$\delta^{18}O$ values of precipitation, weighted by precipitation volume; recharge factor $\alpha = 1$, i.e. all precipitation enters the system, no snow accumulation occurs
set C	$\delta^{18}O$ values of precipitation weighted by precipitation volume and recharge into the system as described in section 2.3.3: recharge factors $\alpha_{winter} = 0.01$, $\alpha_{snowmelt} = \alpha_{summer} = 1$; snow accumulates during winter and is released during snowmelt; precipitation volume corrected for evapotranspiration and direct runoff; $\delta^{18}O$ values corrected for mean catchment elevation
set D	similar to set C, but snowmelt water of the first input interval is reduced by 2 ‰ (estimated value according to Taylor et al. (2001)), which increases the influence of the snowmelt on stream water stable isotope signals
set E	similar to set C, but recharge factor α during winter is set to 0.1, which increases influence of inputs on stream water stable isotope signals during the winter season

2.3.4 Vegetation cover, topographic and hydrogeological analysis

Vegetation cover and catchment topography were assessed by van den Bergh et al. (2011) and by Fercher (2013) by a combination of satellite images and field observation, and modified after additional field observations. Vegetated and bare lands were classified using maximum likelihood classification and a number of training samples on a composite spot image from the summer of 2004/2005. A map of vegetated and non-vegetated land was thus created. The remaining vegetation cover classes were manually drawn from Swissimage orthophotos (van den Bergh et al., 2011). The uncertainty of catchment area and shrub cover is about 5 to 10 %. Further topographic and hydrogeological analysis was performed with a digital elevation model with a cell size of 2 x 2 m below 2000 m a.s.l. and 25 x 25 m above 2000 m a.s.l. We used the geographic information system (GIS) software ArcGIS (ESRI) version 10 and its included hydrology tools.

To relate MTT to topographic features of the micro catchments, we determined ranges and means of the following parameters: slope, elevation, flow length, topographic wetness index, stream length and drainage density. Flow length was calculated as the downslope distance from each cell to the catchment outlet along the flow path. Topographic wetness index was computed as

$$\text{TWI} = \ln \frac{A}{\tan \beta}, \quad (6)$$

where A is the upslope area per unit contour length and β is the local slope (Beven and Kirkby, 1979). For stream length we determined two values. We defined length of base flow stream as the length of the perennial streams. Length of event flow streams additionally

includes ephemeral streams, which are presumably activated during rainfall events. Drainage densities were computed for both length parameters by dividing stream length by micro catchment area.

For further hydrogeological analysis we calculated the mean mobile catchment storage as

(7) $V_{H_2O} = Q_{mean} \cdot MTT$,

where Q_{mean} is the mean discharge. We then used the mean mobile catchment storage and an estimated volume of rocks (V_{rocks}) to calculate a mean porosity n_{mean} for the whole catchment as

(8) $n_{mean} = \frac{V_{H_2O}}{V_{rocks}}$.

The volume of rocks was determined with the ArcHydro tool "terrain morphology" (version 2.0 for ArcGIS 10).

From the topographic data we also estimated the flow path length x to calculate the tracer velocity (v) as

(9) $v = \frac{x}{MTT} \cdot n_{mean}$.

These data were subsequently used to calculate the hydraulic conductivity (K) with Darcy's law:

(10) $K = \frac{v}{\frac{\Delta h}{L}}$,

where $\frac{\Delta h}{L}$ is the hydraulic gradient (e.g. Zuber, 1986).

2.4 Results and Discussion

2.4.1 Stable water isotopes in precipitation and runoff

Decrease of $\delta^{18}O$ in liquid precipitation along an elevation gradient was 0.15 ‰ per 100 m elevation increase. This is only slightly lower than the measured decrease for locations on the Swiss plateau and in the western Alps by Siegenthaler and Oeschger (1980) (0.26 ‰ per 100 m) and in general in good agreement with other values from the Austrian Alps (Ambach et al., 1968, 0.2 ‰ per 100 m). We could not detect a clear elevation gradient in $\delta^{18}O$ for bulk snow samples with elevation during winter (Figure 2.2). At our sites the elevation gradient of stable isotopes is most probably caused by Rayleigh processes during the orographic uplift of air masses during storm events. Also, Rayleigh fractionation during precipitation coming from clouds at the same altitude can lead to the elevation gradient (Gat, 1996). The direction of the elevation gradient then depends on the storm trajectories.

In winter the elevation gradient was not clearly pronounced and it was even reversed for some of our samples near Wallenboden and Chämleten in March 2010. These slopes can be on the lee side of a storm during winter, which can lead to the reversed elevation gradient of stable isotopes (Friedman and Smith, 1970; Moran et al., 2007).

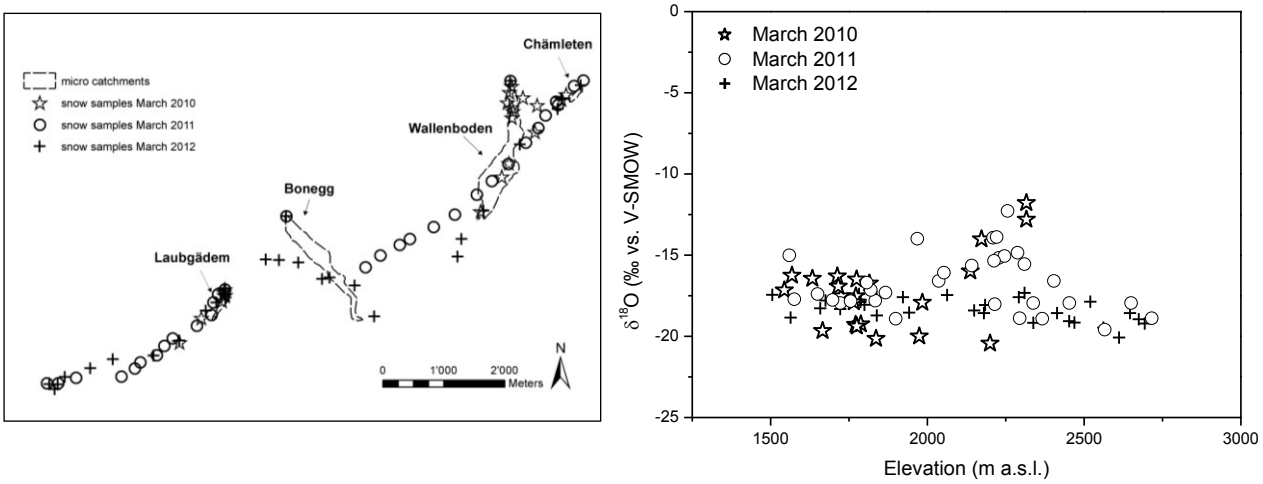

Figure 2.2: Location of snow sampling at the end of the winter (left) and stable isotopes values of snow (right).

Stream water and especially precipitation samples cover a wide range of $\delta^{18}O$ and $\delta^{2}H$ values (Figure 2.3). The local meteoric water line (LMWL) matches the global meteoric water line (GMWL) (Craig, 1961). The GMWL gives the relation between $\delta^{2}H$ and $\delta^{18}O$ in meteoric waters (including, e.g. precipitation, groundwater and water from streams or lakes) on a global scale which have not undergone excessive evaporation. Our stream water samples are between the minimum and maximum values of our measured precipitation samples (Figure 2.3). Therefore, stream water most likely represents a mixture of local precipitation from different dates. Since stream water samples plot close to the LMWL, we can presume that evaporation or other processes which would move the stream samples away from the LWML are negligible (Clark and Fritz, 1997).

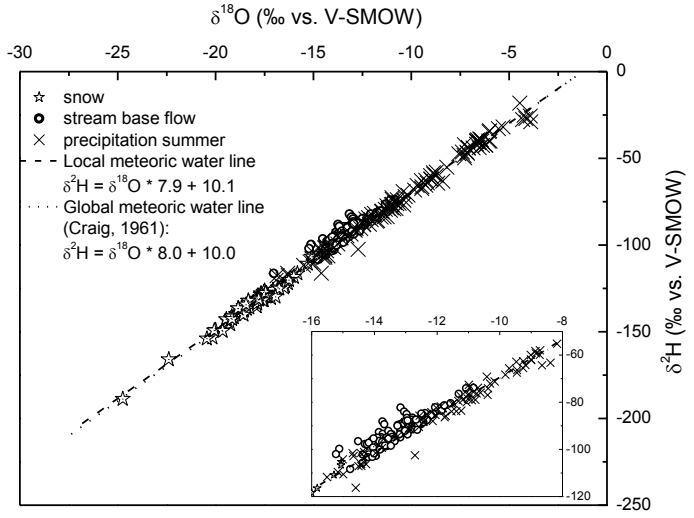

Figure 2.3: $\delta^{18}O$ vs. $\delta^{2}H$ (of H_2O) in precipitation and stream water base flow.

As expected, the stable isotope signal ($\delta^{18}O$) of precipitation strongly varied between seasons and ranged from -2.5 ‰ during summer storms to -25 ‰ (V-SMOW) for fresh snow samples (Figure 2.3 and Figure 2.4). The $\delta^{18}O$ values of the four micro catchments followed a rather parallel pattern even though they are distributed along the valley within a distance of about 8 km (Figure 2.1). The $\delta^{18}O$ values of precipitation samples (both summer precipitation as well as bulk snow samples in winter) slightly decrease from the Chämleten to the Laubgädem micro catchment. This east-west trend could be attributed to an air temperature trend with decreasing temperature from east to west along the valley (note that the difference of mean $\delta^{18}O$ values of precipitation is statistically not significant) or to the rainout effect for storms traveling from east to west. The east-west trend of $\delta^{18}O$ is more pronounced and consistent throughout the year in the base flow samples (Figure 2.4 and Table 2.3). The difference of mean base flow samples between the Chämleten and Laubgädem micro catchments is about 1 ‰ ($p < 0.01$). In addition to the slight east-west trend of $\delta^{18}O$ of precipitation, this could also point to a stronger influence of isotopically lighter winter precipitation from higher elevations at 2760 m a.s.l. above the Laubgädem micro catchment surface area.

The parallel pattern in the precipitation samples was only interrupted at the beginning of the winter in 2010 when first freshly fallen snow of this winter period was sampled. The high variation could be due to non-equilibrium processes during the formation of solid precipitation (Gat, 1996) combined with spatially highly variable meteorological conditions in this complex terrain.

The strong seasonal variability of $\delta^{18}O$ values in precipitation could hardly be detected in our biweekly base flow samples due to a strong dampening of isotope input signals. The isotope signal of precipitation was, however, reflected in the stream water during snowmelt (Figure 2.4). The strong attenuation of the input signal implies that only small fractions of the precipitation leave the basin via surface runoff in short time periods (Herrmann and

Stichler, 1980). Precipitation from different events and seasons can therefore mix when this water reaches the catchments' outlets.

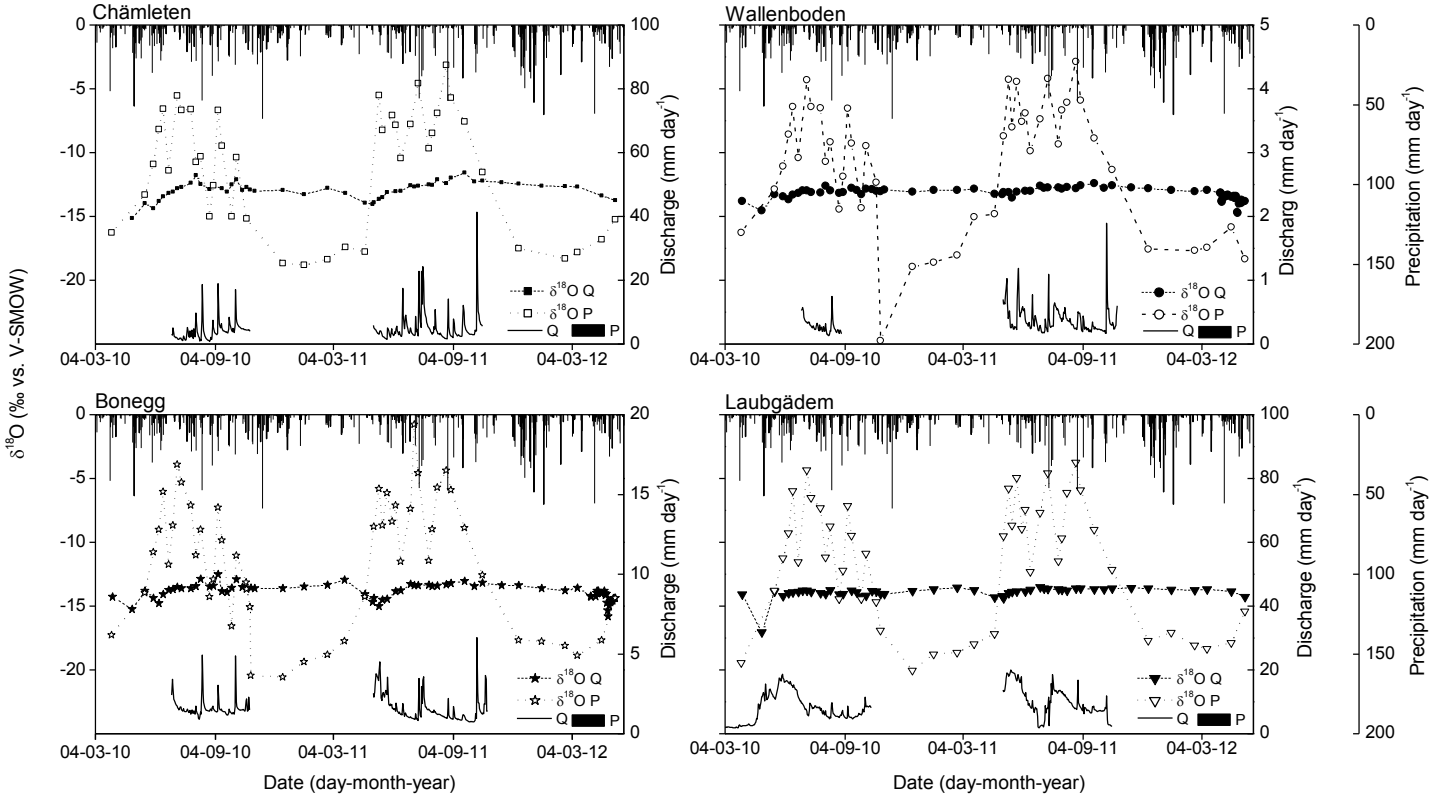

Figure 2.4: Stable isotopes ($\delta^{18}O$ of H_2O) of precipitation (P, open symbols) and stream water (Q, filled symbols) in the four micro catchments, discharge data (bottom of each plot; note the different scales), and precipitation data from the MeteoSwiss station Andermatt at the top of each plot (MeteoSwiss, 2013; scale on the rightmost side applies to all four plots).

Variability of $\delta^{18}O$ of stream water was most pronounced in the Chämleten micro catchment with $\delta^{18}O$ values of -15 ‰ in winter and up to -11.5 ‰ in summer. $\delta^{18}O$ of stream water varied very little in the other micro catchments. Especially the Laubgädem micro catchment exhibits an extremely dampened isotope signal, with the exception of 29 April 2010 when discharge was highly increased due to high snowmelt inputs. These very sharp snowmelt peaks were not detected for our biweekly samples in spring 2011 and 2012. Snowmelt in 2010 occurred later than in 2011, but in a shorter time period. Therefore, the isotope signal of the snow was transferred to the stream quicker and produced a sharp peak in 2010. In 2011, there was only half of the snow amount (snow depth was around 50 cm at the onset of snowmelt) and snowmelt took place earlier. We therefore might have missed the sharp peak in 2011. From the more detailed sampling during the snowmelt in the Wallenboden and Bonegg micro catchments in 2012 (Figure 2.4) we know that these sharp peaks appear within a few days only, which are easily missed by the 14 day sampling interval (Bucher, 2013). On 28 April 2012, the stream water in the Bonegg micro catchment

had a $\delta^{18}O$ value of -15.8 ‰, which was not captured with the 14 day sampling approach (data not included in MTT model evaluation, but shown in Figure 2.4).

In contrast to the snowmelt period, all $\delta^{18}O$ values of stream water were extremely stable during the winter period (Figure 2.4). $\delta^{18}O$ values of stream water reflect the approximate weighted mean $\delta^{18}O$ of previous winter and summer precipitation. Hence, the isotope signal of snow is only reflected in the streams during snowmelt. During the winter 2010/11 there was an increase in $\delta^{18}O$ of base flow samples especially in the micro catchments Bonegg and Laubgädem. This was not the case in the next winter of 2011/12. This could be explained by the higher precipitation amounts in summer 2010, which then discharged during the winter 2010/11. In summer 2011 there were 160 mm less precipitation than in 2010, which corresponds to a decrease of about 25 % of summer precipitation.

In 2011 we also measured stable isotopes of the Reuss River (Figure 2.5). Our sampling point was the outlet of a 132 km^2 subcatchment of the Urseren Valley that drains north and south-facing slopes (note that the whole Urseren catchment has an area of 191 km^2). Because the sampling point integrates a much larger area than our micro catchments, we can qualitatively compare hydrological characteristics of different scales. The data series for the larger Reuss subcatchment only covers the summer period in 2011 and we consider this time span too short for quantitative modeling of MTT. But from the similar stream water stable isotope pattern of the micro catchments and the Reuss subcatchment, we can conclude that water storage and flow in the fractured bedrock also plays an important role at the larger catchment scale. Also, the comparable pattern of stream water stable isotopes suggests that MTT in the Reuss subcatchment is presumably equal to or even longer than in the micro catchments.

We also determined $\delta^{18}O$ values of subsurface/overland flow which we collected in a wetland soil site in the Chämleten micro catchment during or shortly after precipitation events (Figure 2.5). They are more positive than the respective stream water samples (taken at base flow conditions). This indicates the influence of quickly discharging precipitation, which has not traveled through deeper zones, in subsurface/overland flow and a smaller influence of pre-event groundwater.

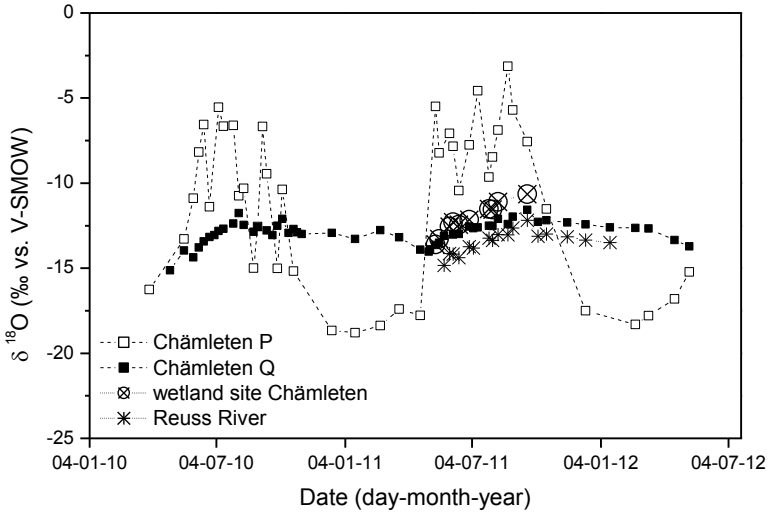

Figure 2.5: Stable isotopes ($\delta^{18}O$ of H_2O) of subsurface/overland flow in a Chämleten wetland site and the Reuss River. Stable isotope signals of precipitation (P, open symbols) and stream water base flow (Q, filled symbols) of the Chämleten micro catchment are shown for comparison.

2.4.2 Mean water transit time modeling

2.4.2.1 Mean water transit times

We first will introduce some aspects of sensitivity and uncertainty of the used modeling approach and then give the results of MTT modeling.

The sensitivity analysis with different flow models revealed that model parameters could be identified unambiguously (data not shown). The piston flow and the linear model gave unrealistic stream water stable isotope values (compared to the measured ones) and high values of σ. The exponential model gave overall the best fits and also performed better than the exponential-piston-flow model and the dispersion model. With an apparent dispersion parameter (P_D = reciprocal of the Péclet number) of 0.5 to 0.8 we also obtained good fits for the dispersion model, and the dispersion and the exponential distributions are quite similar with these chosen P_D values, but reproduction of the measured values was always better using the exponential model. Moreover, due to the hydrogeological situation we preferred the exponential model because a good mixing of all the waters within these steep aquifers is highly unlikely.

The uncertainty analysis with different model input parameter sets (Table 2.2) revealed that a minimum value of σ for each parameter set could be identified (Figure 2.6). For reasons of clarity we will only show the results of the uncertainty analysis for the exponential model. In general, the measured data were reproduced well for all catchments. MTTs range from 64 to 108 weeks (Figure 2.6 and Figure 2.7). The model efficiency (E) is quite low (Figure 2.7; except for Chämleten), which can be explained by the low variance of measured stream water stable isotope values. The measured values are often close to their mean. For the Chämleten and the Bonegg micro catchment, the minimum of the σ-value of

all five sets cluster around a quite narrow range of MTTs of 64 to 85 weeks, respectively (Figure 2.6). The discrepancy of the minimum σ–value between sets A+B and C+D+E increases in the order Chämleten – Bonegg – Wallenboden – Laubgädem (Figure 2.6). Nevertheless, even the very rough input sets A and B (raw $\delta^{18}O$ values of precipitation and volume weighted $\delta^{18}O$ values of precipitation, respectively) gave similar MTTs compared to the more complex parameter sets C to E. Moreover, even the strong dampening of the stable isotope input signal (-25 to -5 ‰) to the narrow range of -15 to -12 ‰ in stream water was quite well reproduced by the rough parameter sets A and B, except for the Laubgädem micro catchment (Figure 2.7). From the uncertainty analysis with the five different model input parameter sets we roughly estimate the uncertainty of our modeling approach to be about 10 to 15 weeks. Calculated average MTT of the more complex parameters sets C to E are 70 to 102 weeks (Table 2.3). The parameter sets C to E gave similar output of stable isotope values compared among each other (Figure 2.7). In general, the difference between these three parameter sets can be observed in the modeled data of autumn/winter of 2011. During that time period there is an overestimation of the measured stable isotope values of base flow in the Wallenboden, Bonegg and Laubgädem catchments, which is the lowest for parameter sets D and E. In fact, there are slightly more positive $\delta^{18}O$ values in summer precipitation samples from 2011 compared to 2010, which is also reflected in the slightly more positive base flow $\delta^{18}O$ values in all four micro catchments (Figure 2.4 and Figure 2.7). But this effect was more pronounced in the modeled than in the measured data. The overestimation by the modeled data in autumn/winter 2011 could be either due to heavy rains in July 2011 that produce a steplike increase in modeled autumn/winter values, or that the increase in the measured data is small because the subsurface reservoir is refilled after the relatively dry periods in spring and summer 2011. Afterwards this water discharges to the streams. Therefore, Chämleten must have a smaller storage reservoir since its reaction to precipitation input is more pronounced. Comparison of parameter sets C to E suggest that the overestimation could also be due to the underestimation of the snowmelt component (more details also see section 2.4.2.2). In general, snowmelt was represented well with a six-weeks snowmelt approach. Especially the fast decline of $\delta^{18}O$ at the onset of snowmelt was reproduced quite well by weighting the $\delta^{18}O$ values of snow with the accumulated snow depths. Nevertheless, very sharp stream water peaks during snowmelt in March and April could not be modeled adequately in all cases. We measured, for example, a -15 ‰ $\delta^{18}O$ signal in the streams in 2010 in the Chämleten, Wallenboden and Bonegg micro catchments. These samples do not represent base flow samples by definition. But in this nival runoff regime, snowmelt takes place during several weeks and snow constitutes a substantial part of the water cycle in our micro catchments, especially in runoff throughout the months of May to August. Therefore, we included them in the modeling procedure. The probably shorter snowmelt period in 2010 can especially be seen in the Laubgädem micro catchment where we have a very large decrease of $\delta^{18}O$ to about -17 ‰, which increases to -14 ‰ after 14 days only. This phenomenon can also not be reproduced by the model. After the six

weeks of snowmelt in the lower parts of the catchments, the residual accumulated snow of the upper parts presumably slowly refills the reservoirs.

The steeper increase of $\delta^{18}O$ values of stream water in summer 2010 in Chämleten was not clearly reproduced by the model. It underestimates the variability of $\delta^{18}O$, which is higher in spring/summer 2010 in Chämleten and Bonegg than in Wallenboden and especially Laubgädem. Thus, MTT for Chämleten is probably lower compared to Wallenboden even if their range for parameter sets C, D and E are similar for the best model fits (Figure 2.6).

Generally, we think the applied exponential model could satisfactorily reproduce the measured stable isotope values of stream water and it also implicitly gives useful insights into the flow systems. However, it could not reproduce the relatively "short" snowmelt peaks (about 10 weeks) and the subsequent quick onset of more positive $\delta^{18}O$ values with low variability throughout summer, autumn and winter. This is probably due to the time-invariant modeling approach and the fact that MTTs can be shorter and the dynamics in the aquifers can be higher during snowmelt periods.

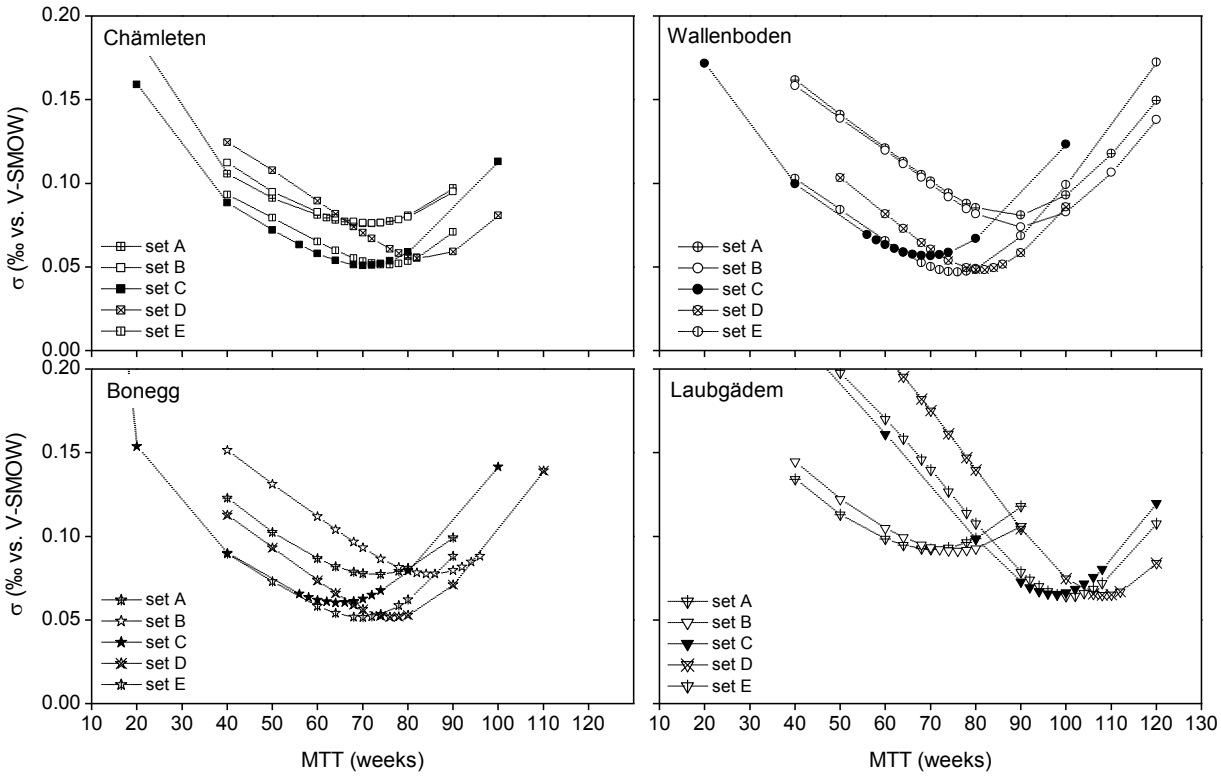

Figure 2.6: Uncertainty analysis of MTT calculation for the micro catchments with different input parameter sets.

Table 2.3: Mean water transit times (MTT) and hydrogeological parameters of the micro catchments (means ± standard deviations calculated for parameter sets C to E).

	Chämleten	Wallenboden	Bonegg	Laubgädem
mean $\delta^{18}O_{base\ flow}$ (‰)	-12.90	-13.09	-13.64	-13.83
MTT (weeks)	76 ± 7	75 ± 5	70 ± 6	102 ± 5
V_{H_2O} (m^3)	$5 \times 10^4 \pm 5 \times 10^3$	$1 \times 10^5 \pm 7 \times 10^3$	$3 \times 10^5 \pm 2 \times 10^4$	$2 \times 10^5 \pm 9 \times 10^3$
V_{rocks} (m^3)	1×10^6	2×10^8	2×10^8	2×10^6
porosity n_{mean} (-)	$4 \times 10^{-2} \pm 3 \times 10^{-3}$	$7 \times 10^{-4} \pm 5 \times 10^{-5}$	$2 \times 10^{-3} \pm 1 \times 10^{-4}$	$8 \times 10^{-2} \pm 4 \times 10^{-3}$
K ($m\ s^{-1}$)	3×10^{-7}	8×10^{-8}	1×10^{-7}	1×10^{-6}

V_{H_2O} = mobile catchment storage; V_{rocks} = volume of rocks; K = hydraulic conductivity

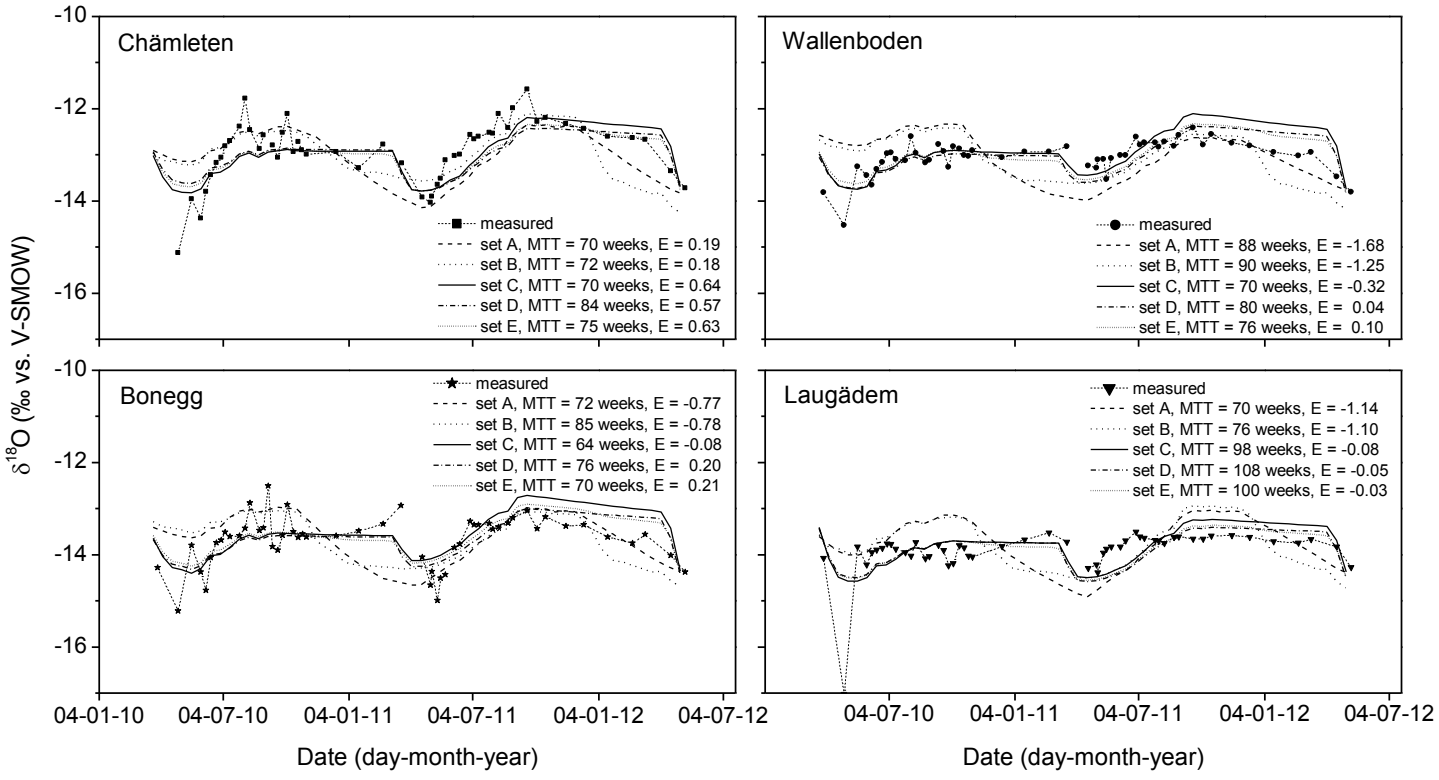

Figure 2.7: Measured and modeled stable isotopes ($\delta^{18}O$ of H_2O) in stream water base flow in the four micro catchments. The best fit according to Figure 2.6 for each input parameter set and the model efficiency (E) according to Nash and Sutcliffe (1970) are shown.

2.4.2.2 Fractionation of stable isotopes

Evaporation of soil water

Evaporation of soil water can alter isotopic signals (Zimmermann et al., 1967). Viville et al. (2006) and Stumpp et al. (2009b) stated that the stable isotope input function for modeling MTTs can be improved by taking evapotranspiration into account. According to Barnes and Turner (1998), the influence of evaporation on stable isotopes signals is rather small in humid areas since other processes are prevailing (e.g. mixing and dispersion). Water uptake by plants does not alter isotope signatures of soil water (e.g. Dawson and Ehleringer, 1991; Ehleringer and Dawson, 1992; Zimmermann et al., 1967), but it could of course reduce amounts of precipitation water entering the deeper soil layers and the bedrock. In our micro catchments the volume weighted stable isotope signal of the precipitation input equals the mean stable isotope signal of the stream water output. Thus, the evapotranspiration from the north-facing slopes most likely played a negligible role in shifting isotopic values. Moreover, the $\delta^{18}O$ vs. $\delta^{2}H$ plot does not indicate substantial evaporation since base flow, precipitation and snow samples plot near the global meteoric water line.

Evaporation through interception

Evaporation of water by interception can also change isotope signals in precipitation. Generally, throughfall enrichment is between 0.1 to 1.2 ‰ (e.g. Ingraham, 1998; Saxena, 1986), but there are also studies in which throughfall was depleted in ^{18}O compared to bulk precipitation (Saxena, 1986). In our study we found some samples of throughfall in shrub sites to be enriched in ^{18}O by about 1.5 ‰, but more samples to be depleted in ^{18}O by about 0.6 ‰ compared to bulk precipitation samples in grassland sites. Since there was no general pattern, the differences were small and micro catchments include different surface cover types from vegetation (grass and shrubs) to bare rocks, we concluded that a possible influence of evaporation through interception should play a minor role for the modeling..

Fractionation of stable isotopes in snow

Snowmelt water input into the system could also be a critical input component in MTT modeling. Evaporation of water from the snowpack during the winter and fractionation processes during melt can alter isotopic composition of the water infiltrating into the soil (Moser and Stichler, 1975). Again, we assume that substantial evaporation during the winter can be excluded because no shift from the global meteoric water line was measured for the bulk snow samples. These were taken a few days before the onset of snowmelt. Moreover, evaporation in March and April in our micro catchments is estimated to be very low (Baumgartner et al., 1983).

The bulk snow samples show slight enrichment of the heavier isotopes with time towards the end of the winter from about -17 to -15 ‰. But the samples shortly after snowmelt, that were taken on some shadowed locations where snow still was available, only showed a small enrichment of the heavier isotope compared to the samples before the onset of snowmelt. Moreover, they plot around the local meteoric water line even after snowmelt in the lower parts of the micro catchments occurred (Figure 2.3). These facts indicate that evaporation (under equilibrium) during melt occurred to a certain extent. But for model parameter set C (Table 2.2) we assumed that the isotope signal from our depth integrating bulk snow samples just before the onset of snowmelt could be regarded as our input signal in our modeling interval of two weeks. Water balance estimates suggest that the major fraction of the total accumulated snow recharges to the aquifer, and since we are not looking at short temporal variations during snowmelt we can assume that the mean stable isotope signal of our bulk snow samples represents the model input signal that recharges into the aquifer. Nevertheless, since the first meltwater can be depleted in the heavier isotope (e.g. Taylor et al., 2001), uncertainty is introduced to the model results by taking bulk snow samples as the model input. In order to estimate the influence of the fractionation processes during snowmelt on our modeled data we also considered a modified parameter set D (Table 2.2) where we estimated the first meltwater to be depleted in the heavier isotope by about 2 ‰ (Taylor et al., 2001). The results are discussed in section 2.4.1.

2.4.2.3 Length of data record

McGuire and McDonnell (2006) argued that the length of the data record for the input function should exceed the MTT by a factor of 4 to 5. This would ensure that tracer mass recovery would be nearly 100 %. According to Hrachowitz et al. (2011), the required minimum length of the data record in their study was 3 times the MTT in order to maximize tracer mass recovery. Our record is about 2 yr and MTTs are 1.2 to 2.1 yr. We therefore extended our input record backwards in time by correlating stable isotopes in precipitation with air temperature measured at the valley bottom. Although stable isotopes of precipitation are not solely dependent on air temperature (e.g. Ingraham, 1998), we obtained a good linear correlation between stable isotope values of precipitation and air temperature for the Urseren Valley ($\delta^{18}O = 0.73 \bullet T$ (°C) - 16.89, $r^2 = 0.84$, $p < 0.0001$, $n = 145$). Extending the stable isotope time series by this technique has been successfully used by other authors and has proved to be a valuable tool to extrapolate stable isotope data (Burns and McDonnell, 1998; Hrachowitz et al., 2011; Uhlenbrook et al., 2002). With this prolongated time series we tested the modeling procedure for the Laubgädem and the Chämleten micro catchments. We could not improve our model results of MTT calculation with the longer data record. Therefore, we used our measured input record of about 2 yr for the modeling, as described above.

2.4.3 Influences on mean water transit time

2.4.3.1 Effect of vegetation cover and topography

The two largest micro catchments Wallenboden and Bonegg with a shrub cover of 13.8 % and 38.5 %, respectively, and the smallest micro catchment Chämleten with the highest shrub cover of 82.2 % have a similar range of MTTs of 64 to 90 weeks (Figure 2.6 and Figure 2.7). Moreover, the micro catchments Laubgädem and Wallenboden with a similar fraction of shrub cover have MTTs of 102 and 75 weeks, respectively (average MTT of parameter sets C to E). The correlation between MTT and shrub cover is weak and statistically not significant ($r^2 = 0.17$, $p = 0.59$, Figure 2.8) and we therefore conclude that shrub cover most likely does not influence base flow MTT in these steep alpine headwater catchments. We are aware that the evaluation of a data set of four points with spearman correlation is critical. However, we feel that visualization in giving r^2 and p is helpful if interpretation is done with caution.

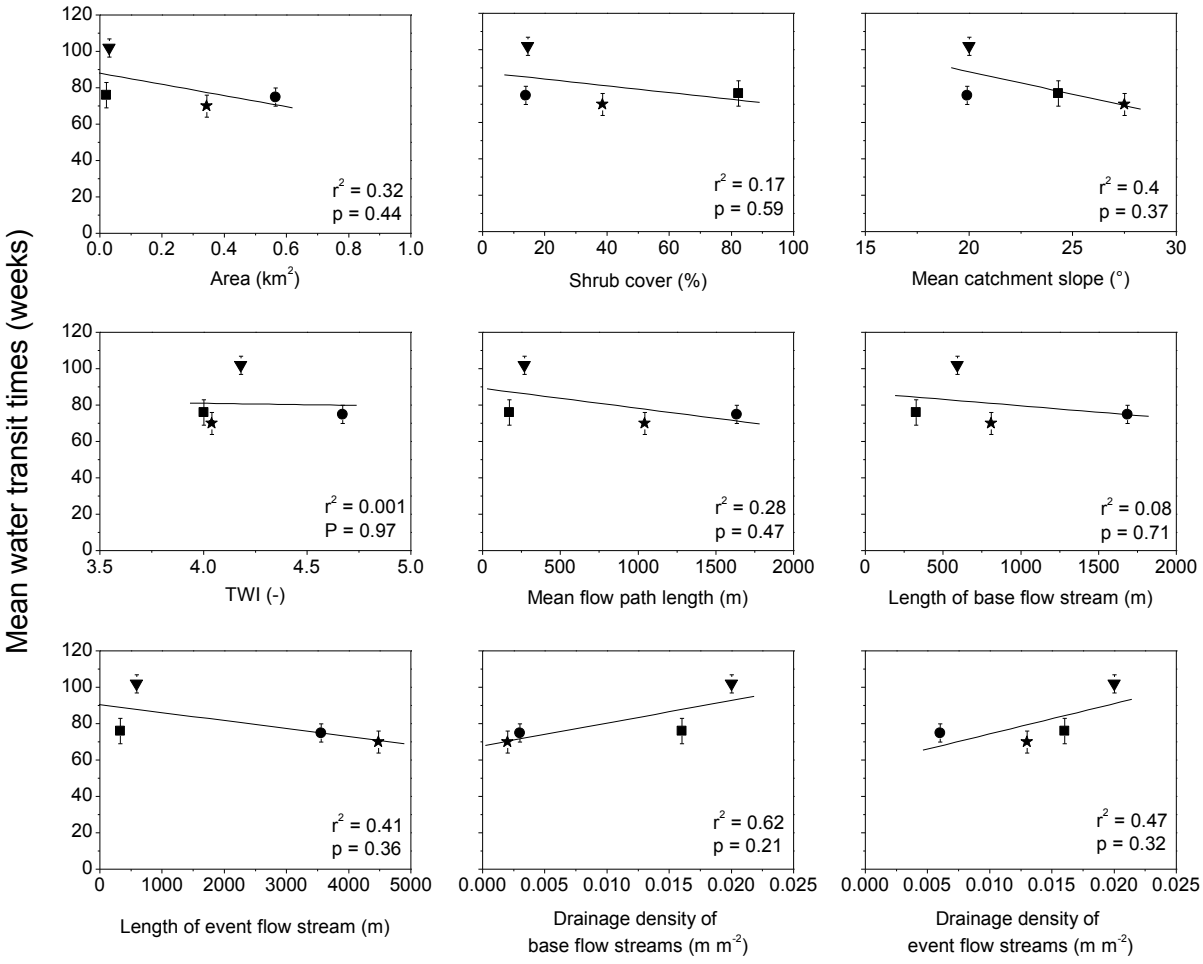

Figure 2.8: Correlation of MTT with topographic indices and shrub cover. Average MTTs of parameter sets C to E are shown. ■ = Chämleten, ● = Wallenboden, ★ = Bonegg, ▼ = Laubgädem. Micro catchment area and shrub cover data from Fercher (2013) and van den Bergh et al. (2011), modified.

Infiltration/recharge and transpiration could also be out of phase, which would affect the influence of vegetation on the water balance and its isotopic characteristics (Brooks et al., 2010). The seasonality of precipitation and its stable isotope signals and the seasonality of transpiration could produce different water pools (i.e. soil water vs. groundwater) with different isotopic characteristics, analogous to the findings of Brooks et al. (2010) and Goldsmith et al. (2012). Brooks et al. (2010) found that evaporation changed stable isotope values of soil water. However, soil water pools, which were used by plants, did not substantially contribute to stream water in their study. The latter showed no evidence of evaporative enrichment. These processes might be present at our sites since there exists a strong seasonality of water input, which is manifest in the snow dynamics. However, we consider it to be of minor importance with regard to the overall hydrological balance of precipitation and stream water and their stable isotope characteristics. Alaoui et al. (2013) also estimate that effect of vegetation cover (i.e. evapotranspiration) on the hydrological balance plays a minor role at our sites, especially on the investigated north-facing slopes.

Roa-Garcia and Weiler (2010) found the vegetation cover (i.e. the percentage of wetlands and forest) to increase the transit time of water. The authors argued that wetlands and forests have a higher water storage capacity. This is in contrast to our findings where the Chämleten micro catchment, which includes some wetland sites, revealed the highest dynamic of stream water stable isotope values and the shortest MTT. The wetland sites in Chämleten were nearly water saturated throughout the year. Thus, the function of these wetlands of buffering inflowing water and subsequently the transit time of water can be reduced.

Overall, we estimate the influence of the vegetation cover on the MTT of base flow to be negligible in our catchments. The increase of soil hydraulic conductivity, induced by invading shrubs (Alaoui et al., 2013), seems to be of minor importance since high stone content and texture of the soils can mask the effect of roots.

Since the influence of vegetation cover on MTT seems to be of minor importance, we were also interested in possible influence of other factors (e.g. topography) on MTT. In contrast to the findings of McGlynn et al. (2003), McGuire et al. (2005), Rodgers et al. (2005) and Soulsby and Tetzlaff (2008), MTT in our study is not related to any of the calculated topographic indices (Figure 2.8). Slight trends can be seen, but since in our study the range of MTT is small (Figure 2.7 and Figure 2.8) and the range of most of the calculated topographic indices is relatively high, we conclude that at our sites, with catchments smaller than 1 km^2, MTT does not depend on any of the calculated topographic indices. In contrast to McGuire et al. (2005) for example, we found no relation of MTT with mean catchment slope or the topographic wetness index (TWI). In accordance with several other studies (McGlynn et al., 2003; McGuire et al., 2005; Rodgers et al., 2005; Soulsby and Tetzlaff, 2008; Tetzlaff et al., 2009), MTT is not related to catchment size in our study. The larger (Wallenboden and Bonegg) and the smaller micro catchments (Chämleten and Laubgädem) have both relatively long and short MTTs. A qualitative comparison of the

pattern of stream water stable isotopes of the Reuss River with the four micro catchments (Figure 2.4 and Figure 2.5) also suggests that there exists no relation between catchment size and MTT. However, the range of our catchment size is small compared to other studies (e.g. Tetzlaff et al., 2009) and we considered the time series of the larger Reuss subcatchment too short for quantitative modeling.

Tetzlaff et al. (2011) stated that a greater contribution of groundwater inputs weakens the influence of topographic controls. The importance of groundwater contribution, inferred from geochemical data and estimated hydrogeological parameters, will be discussed below.

2.4.3.2 Implications from geochemical and hydrogeological aspects

Mean concentrations of total dissolved Ca, Mg, Na and K (Table 2.4) are higher than can be expected from similar geological and climatological settings with mainly granitic or gneiss materials (e.g. Drever and Zobrist, 1992; Ofterdinger, 2001; Tardy, 1971). Ofterdinger (2001) and Ofterdinger et al. (2004) studied stable isotopes and other geochemical parameters of groundwater in the western Gotthard massif (granitic Rotondo massif) only a few km south-west of our sites. They measured, for example, calcium concentrations of up to 9 mg L^{-1} for surface waters, springs and groundwaters. Mean sulfate concentrations at our sites range from 7.3 to 19.7 mg L^{-1} (Table 2.4), which is also slightly higher than we would expect from a mere magmatic or metamorphic geological setting (1 to 8 mg L^{-1}) (e.g. Drever and Zobrist, 1992; Ofterdinger, 2001; Tardy, 1971). Sulfate rich minerals seem to be dissolved by the percolating water. Mean silicon concentrations (Table 2.4) are slightly lower than compared to other granitic or gneiss regions with comparable climate (e.g. Drever and Zobrist, 1992; Tardy, 1971). Silicon could be a product of weathering of quartz veins, which are very common in this zone of fractured rocks (Winterhalter, 1930). Overall, our data show that dissolution of magmatic or metamorphic minerals alone cannot account for the measured concentrations of solutes. The pH of stream water of more than 7 suggests dissolution of evaporative minerals, i.e. karst formation, in the deeper bedrock. Moreover, soil pH in our micro catchments is about 4 to 5. Therefore, infiltrating precipitation must be strongly buffered in the deeper aquifer below the soils. Low pH of water leaching from the soil, in turn, could accelerate weathering of rocks.

Ofterdinger et al. (2004) concluded that water can percolate in the fractured granitic rocks of the Rotondo massif (only a few km south-west of our sites), which will lead to a strong dampening of the stable isotope input signal. Additionally, the phenomenon of strong isotope signal dampening is also known from karstic environments (e.g. Bakalowicz et al., 1974; Maloszewski et al., 1992; Maloszewski et al., 2002; Perrin et al., 2003). This suggests that the rocks in our test sites are highly fractured and have a high porosity and storage capacity. Water percolating in these systems will have relatively longer transit times compared to an unfractured system with low storage capacity. Of course water storage capacity, water flow and consequently the MTT will then also depend on the form, the

extent and the connectivity of fractures and fissures and not only on their frequency (e.g. Banks et al., 2009).

We estimated porosities of 7 x 10^{-4} to 8 x 10^{-2} (Table 2.3), which are in the same order of magnitude as values given by Frick (1994) and Himmelsbach et al. (1998) for a geological complex in the Aar massif containing fault zones. They measured porosities between 7.4 x 10^{-3} and 1.3 x 10^{-3}, respectively. Porosity in the intact Rotondo granite with moderate fracturation are lower and range from 2.4 x 10^{-5} to 2.9 x 10^{-4} (Ofterdinger, 2001). Our estimates for hydraulic conductivities (Table 2.3) are at the upper end together with fault zone and sedimentary rocks (Ofterdinger, 2001). Ofterdinger (2001) gave hydraulic conductivities for different rock types in the Rotondo area, ranging from 5.3 x 10^{-9} to 4.0 x 10^{-7} m s^{-1}. This strongly supports the conclusion of fractured rocks in the micro catchments in which water can percolate into the deeper bedrock. The lack of relation between mean mobile catchment storage and catchment surface area indicates that surface and subsurface catchment area are not equal and water can be delivered via subsurface flow paths from the upslope bedrock to the micro catchments. This in turn could mask possible influences of topographic indices on MTTs since these indices were calculated for the surface catchment areas.

Consequently, the strong attenuation of the stable isotope input signal can be explained by a combination of water flowing in the fractures and fissures of the rocks and in cavities that can be produced by dissolution of readily soluble minerals (gypsum, dolomite or calcite). Our findings support the conclusions of, e.g. Gabrielli et al. (2012) and Asano and Uchida (2012), who underlined the importance of water flow in the subsurface and bedrock and its control on MTT.

Table 2.4: Means and standard deviations of geochemical parameters of stream base flow samples (mg L^{-1}).

	Chämleten	Wallenboden	Bonegg	Laubgädem
Ca (n = 20)	16.3 (1.8)	27.4 (3.6)	22.8 (3.7)	19.4 (1.7)
Mg (n = 20)	0.9 (0.1)	1.6 (0.1)	2.2 (0.3)	0.8 (0.1)
Na (n = 20)	0.9 (0.1)	1.0 (0.1)	1.3 (0.1)	0.7 (0.1)
K (n = 20)	1.1 (0.2)	2.1 (0.2)	2.6 (0.3)	1.7 (0.1)
Si (n = 29)	2.6 (0.8)	2.4 (0.7)	3.0 (1.0)	1.9 (0.6)
SO_4^{2-} (n = 27)	10.8 (1.5)	14.7 (1.4)	19.7 (3.2)	7.3 (0.7)
pH (summer)	7.35 (0.18)	7.65 (0.25)	7.55 (0.14)	7.35 (0.32)
pH (winter)	7.30 (0.26)	7.54 (0.26)	7.56 (0.25)	7.68 (0.13)

2.5 Conclusions

We investigated the influence of differing percentage of shrub cover on MTTs in four mountainous micro catchments. Stream water stable isotope signals during base flow conditions over two years point to mixing of waters of different ages, resulting in MTTs of at least 1 yr. Our data suggest that neither shrub vegetation cover nor topography nor catchment size influence the MTT of base flow. The shrub encroachment does not seem to

increase MTTs and other factors than other surficial catchment characteristics mainly controlled MTTs at our sites.

The snowmelt input into the micro catchments and its release during spring was identified as an important influence on mean stable isotope signals and for MTT modeling. Geochemical data from stream water suggest that water percolates through partially karstified deeper bedrock at all four investigated catchments. This in turn favors mixing of water and storage in the deeper bedrock, which leads to a strong attenuation of the $\delta^{18}O$ signal of precipitation input in our alpine headwater catchments. Furthermore, our estimates of hydrogeological parameters indicate that subsurface storage and flow paths strongly control MTTs. The major part of the precipitation input enters the bedrock systems rather quickly, which leads to a sustained discharge of this bedrock groundwater to base flow in our micro catchments.

We therefore conclude that, in our mountainous headwater catchments with relatively shallow soil layers, the hydrogeological and geochemical patterns and snow dynamics influence storage, mixing and release of precipitation in a stronger way than vegetation cover does. The effect of vegetation on MTT can be masked at the catchment scale in such a setting.

Acknowledgements

We would like to thank Mark Rollog and Marianne Caroni for laboratory analyses and Claude Schneider for technical support. We also thank Thijs van den Bergh (Group of Botany, Section Plant Ecology, University of Basel) and Mathias Fercher (Institute of Geography, Group of Hydrology, University of Bern) for providing data of catchment sizes and vegetation cover, Abdallah Alaoui, Susanne Lagger and Philipp Schmidt (Institute of Geography, Group of Hydrology, University of Bern) for providing discharge data and estimates on evapotranspiration rates, and Katrin Meusburger (Environmental Geosciences, University of Basel) for calculating the TWI. Lothar Schroeder, Yannick Bucher, Robin Nager, Jonas Gessler and Gyula Csato helped during the sampling campaigns. We also would like to thank the anonymous referees for their constructive comments and suggestions, which helped to improve our manuscript, and Christine Stumpp as the editor of this manuscript.

This work was part of the project “The ecological and socio-economic consequences of land transformation in alpine regions: an interdisciplinary assessment and VALuation of current changes in the Ursern Valley, key region in the Swiss central Alps”, funded by the Swiss National Science Foundation, grant no. CR30I3_124809.

3 Tracking water pathways in steep hillslopes by $\delta^{18}O$ depth profiles of soil water

Mueller, M. H.[1,], Alaoui, A.[2], Kuells, C.[3,#], Leistert, H.[3], Meusburger, K.[1], Stumpp, C.[4], Weiler, M.[3], and Alewell, C.[1]*

[1]Environmental Geosciences, University of Basel, Bernoullistrasse 30, 4056 Basel, Switzerland

[2]Centre for Development and Environment (CDE), University of Bern, Hallerstrasse 10, 3012 Bern, Switzerland

[3]Chair of Hydrology, University of Freiburg, Fahnenbergplatz, 79098 Freiburg, Germany

[4]Helmholtz Zentrum München, Institute of Groundwater Ecology, Ingolstädter Landstr. 1, 85764 Neuherberg, Germany

[*]present address: Applied and Environmental Geology, University of Basel, Bernoullistrasse 32, 4056 Basel, Switzerland

[#]present address: University of Applied Sciences, Mönkhofer Weg 239, 23562 Lübeck, Germany

This chapter is accepted for publication in the Journal of Hydrology, 2014, doi: http://dx.doi.org/10.1016/j.jhydrol.2014.07.031

3.1 Abstract

Assessing temporal variations in soil water flow is important, especially at the hillslope scale, to identify mechanisms of runoff and flood generation and pathways for nutrients and pollutants in soils. While surface processes are well considered and parameterized, the assessment of subsurface processes at the hillslope scale is still challenging since measurement of hydrological pathways is connected to high efforts in time, money and personnel work. The latter might not even be possible in alpine environments with harsh winter processes. Soil water stable isotope profiles may offer a time-integrating fingerprint of subsurface water pathways. In this study, we investigated the suitability of soil water stable isotope ($\delta^{18}O$) depth profiles to identify water flow paths along two transects of steep subalpine hillslopes in the Swiss Alps. We applied an one-dimensional advection-dispersion model using $\delta^{18}O$ values of precipitation (ranging from -24.7 to -2.9 ‰) as input data to simulate the $\delta^{18}O$ profiles of soil water. The variability of $\delta^{18}O$ values with depth within each soil profile and a comparison of the simulated and measured $\delta^{18}O$ profiles were used to infer information about subsurface hydrological pathways. The temporal pattern of $\delta^{18}O$ in precipitation was found in several profiles, ranging from -14.5 to -4.0 ‰. This suggests that vertical percolation plays an important role even at slope angles of up to 46°. Lateral subsurface flow and/or mixing of soil water at lower slope angles might occur in deeper soil layers and at sites near a small stream. The difference between several observed and simulated $\delta^{18}O$ profiles revealed spatially highly variable infiltration patterns during the snowmelt periods: The $\delta^{18}O$ value of snow (-17.7 ± 1.9 ‰) was absent in several measured $\delta^{18}O$ profiles, but present in the respective simulated $\delta^{18}O$ profiles. This indicated overland flow and/or preferential flow through the soil profile during the melt period. The applied methods proved to be a fast and promising tool to obtain time-integrated information on soil water flow paths at the hillslope scale in steep subalpine slopes.

3.2 Introduction

Knowledge about soil water flow paths is important to assess mechanisms of runoff generation (Stewart and McDonnell, 1991), which include for example overland and subsurface flow (Dunne, 1978). These processes subsequently have important implications for the generation of floods (Beven, 1986), recharge of groundwater (Barnes and Allison, 1988), soil erosion dynamics (e.g. Konz et al., 2010; Lindenmaier et al., 2005; Uchida et al., 2001) and transport of nutrients and pollutants (Schmocker-Fackel, 2004; Weiler and McDonnell, 2006). These processes are of special interest in headwater catchments in mountainous regions, because of their great hydrological importance for the adjacent lowlands (Viviroli et al., 2011; Weingartner et al., 2007).

Hydrological processes at the hillslope scale are influenced by a complex interplay of different factors, including input characteristics, vegetation, geological, morphological and pedological characteristics, all acting on different spatial and temporal scales (Bachmair and Weiler, 2011). Among the topographic controls, slope angle has been identified as a crucial factor influencing hillslope hydrology, i.e. water flows paths (e.g. Hopp and McDonnell, 2009; Lv et al., 2013; Penna et al., 2009). Further, Sayama et al. (2011) found that storage of water was increased with increasing catchment slope. This was due to a greater extent of hydrological active (permeable) bedrock, which is available for water storage in steeper catchments. This underpins the hydrological importance of headwater catchments and the necessity to obtain information on (subsurface) water pathways in these areas. Moreover, Vereecken et al. (2008) and UNESCO-IHE (2011) highlight the importance of knowledge about spatial distribution of hydrological processes and characteristics in the subsurface at different spatial scales.

A great variety of techniques has been applied to study soil hydrological processes. Soil water content can be monitored e.g. by time-domain reflectrometry (TDR), electrical resistivity measurements, heat pulse sensors or capacitive sensors (for a review see Vereecken et al., 2008). However, to obtain information on soil water content dynamics at the hillslope scale using these techniques, a high number of sensors has to be deployed during a relatively long time period measuring with high temporal resolution (see review of Dobriyal et al., 2012; Zehe et al., 2010). In addition, the use of hydrometric equipment may be limited in stony soils (Coppola et al., 2013) or due to harsh winter conditions, which often occur in steep hillslopes in alpine headwater catchments. Spatially distributed information on areas where water flow potentially concentrates, can be derived from the topographic wetness index TWI (Beven and Kirkby, 1979), calculated from a digital elevation model. However, Penna et al. (2009) found that flow-related topographic variables (e.g. slope, contributing area and wetness index) could only explain up to 42 % of the spatial variation of soil moisture in steep mountainous terrain during two summer seasons. In addition to surface topography, the subsurface topography also plays a crucial role for water flow paths (Freer et al., 2002). Ground penetrating radar (GPR) or electrical resistivity

tomography (ERT) can indirectly provide information about possible flow paths in the subsurface, soil water contents, hydraulic properties and soil water dynamics (Jadoon et al., 2012; Lunt et al., 2005; Steelman and Endres, 2012). However, heterogeneities in soils can limit accurate assessment of subsurface characteristics by GPR (Jadoon et al., 2012). All these techniques require a high effort in time, work and economic resources if a monitoring of water fluxes in various compartments over several seasons is investigated (e.g. long-term high-frequency measurements).

Alternatively, soil water stable isotopes can be a valuable tool to track movement of soil water and to gain integrative information about subsurface flow processes like mixing, preferential flow and hydrodynamic dispersion (Asano et al., 2002; Barnes and Allison, 1988; Dusek et al., 2012; Klaus et al., 2013; McDonnell et al., 1991; Stewart and McDonnell, 1991; Stumpp and Maloszewski, 2010; Stumpp et al., 2009b). The seasonally varying stable isotope signals of precipitation and the subsequent potential attenuation or propagation of distinct peaks in the soil water can be used to determine recharge rates (Adomako et al., 2010; McConville et al., 2001; Saxena and Dressie, 1983), soil water movement (Gehrels et al., 1998) and to calculate soil water transit times (Stewart and McDonnell, 1991; Stumpp et al., 2012). As such, pore water stable isotope signals have the potential to give a fingerprint integrating over time (one season to several years) and a certain space.

Soil water for stable isotope analysis can be extracted by suction lysimeters (Stewart and McDonnell, 1991), centrifugation of soil samples (Gehrels et al., 1998) or distillation techniques (Ingraham and Shadel, 1992), which are time-consuming and prone to isotopic fractionation (Wassenaar et al., 2008). Wassenaar et al. (2008) developed a fast and effective method for soil water stable isotope analysis, which is based on H_2O_{liquid} - H_2O_{vapor} equilibration laser spectroscopy. Garvelmann et al. (2012) applied this approach and used a combination of soil water stable isotope profiles along two relatively smooth hillslope transects and digital terrain analysis to investigate subsurface hydrological processes. With these methods they were able to deduce the relative importance of dominant subsurface flow paths (vertical percolation and lateral subsurface flow) at the hillslope scale. Their approach offers a way to generate a time-integrated overview of soil water flow paths in the subsurface without the need of extensive hydrometric equipment. However, a more physically based description of soil water flow and transport processes to support their conceptual model was not realized in their study. The Richards equation for variably-saturated flow combined with advection-dispersion equations can be used to quantitatively describe water flow and solute transport in soils (e.g. van Genuchten and Simunek, 2004). More complex models to account for non-equilibrium and preferential flow include for example dual-porosity and dual-permeability approaches (for reviews see Beven and Germann, 2013; Simunek et al., 2003). Stable isotopes of soil water in combination with modeling tools were successfully used to describe soil hydrological processes at the plot scale (e.g. Shurbaji and Phillips, 1995; Stumpp et al., 2012) and the hillslope scale (e.g. Dusek et al., 2012). Studies on the plot scale using lysimeters give detailed information on

transport parameters on the one hand (e.g. Stumpp et al., 2012). Studies on hillslope hydrographs provide integrated information at the hillslope scale (e.g. Dusek et al., 2012), missing the spatial variability of e.g. transport parameters on the other hand. A method linking this gap could provide important additional information that can be included in detailed spatial hydrological models at the hillslope scale. The aims of the presented study were therefore: (i) to use depth profiles of soil pore water stable isotopes as an indicator of water flow paths and its heterogeneity at the hillslope scale, (ii) to combine measurements of stable water isotopes of soil profiles with a numerical model of the Richards equation coupled with the advection-dispersion equation including fractionation processes to identify water pathways and transport processes in the shallow subsurface and (iii) to apply this method in steep hillslopes in a remote alpine headwater catchment, where installation of more conventional equipment to investigate water flow and solute transport would not only be extremely time consuming, but also very difficult (e.g. due to harsh winter conditions, which can impede continuous measurements or due to high stone contents, which might hamper proper installation of TDR probes). The method was tested with 28 depth profiles of soil water $\delta^{18}O$ values at a transect of a north- and a south-facing subalpine hillslope in the Swiss Alps. The suggested method is designed as a diagnostic tool to obtain a time-integrated overview of hillslope hydrology, without the necessity to collect long time series data of hillslope hydrology.

3.3 Material and Methods

3.3.1 Study site

Soil samples for analysis of soil water stable isotopes were taken on two opposing hillslopes in the Urseren Valley in the Central Alps, Switzerland (Figure 3.1). The U-shaped valley is characterized by a rugged terrain. Its main axis is parallel to a geological fault line which separates the granites of the Aar massif and the gneisses of the so-called Altkristallin from the paragneisses and granites of the Gotthard massif (Labhart, 1977). The two massifs are separated by softer Permocarbonic and Mesozoic sediments, the so-called Urseren Zone (Labhart, 1977). These vertically dipping layers consist of Permocarbonic sandy-clay sediments and Mesozoic sandstones, rauhwackes, dolomites, dark clay-marl, marl, clays and limestones. Quaternary alluvium can be found at the lower parts of the valley slopes. The south-east-facing hillslope (named south-facing in the following) includes the gneisses of the Altkristallin and the sediments of the Urseren Zone in the lower part. The north-west-facing hillslope (named north-facing in the following) is underlain by the paragneissic rocks of the Gotthard massif. In the summers 2006, 2009 and 2010 Carpentier et al. (2012) collected data with ground penetrating radar (GPR), electrical resistivity tomography (ERT) and direct observations in soil trenches at a section of the south-facing hillslope (Figure 3.1). They detected a xenolithic schist layer starting mostly at 1 m depth followed by a clay layer at about 2 m depth. They also detected some vertical structures which were interpreted as faults/fractures in the bedrock or vertically dipping layers due to interbedding in the schistose rocks. These structures can enhance infiltration of water into deeper zones of the

bedrock, which starts at 2.5 m depth in the upper part and 10 m depth in the lower part of the investigated hillslope section. Slope angles of the investigated sites range from 5° to 29° and from 3° to 46° at the north and the south-facing hillslope, respectively.

The dominant soil types in the Urseren Valley according to the world reference base (IUSS Working Group WRB, 2006) are Podsols and Cambisols (Meusburger and Alewell, 2008). Leptosols developed at higher elevations and steeper slopes. Clayey gleyic Cambisols, Histosols, Fluvisols and Gleysols are commonly associated with the valley bottom and downslope areas. Soils on the investigated north-facing hillslope can be described as Podsols partially with gleyic or slight histic properties. Soils on the south-facing hillslope are mainly Cambisols. The latter can partially be affected by a clay layer in deeper zones of about 2 m depth, possibly impeding downward water flow (Carpentier et al., 2012). Generally, soils in the Urseren Valley are high in silt and sand content with relatively low content of clay (Gysel, 2010).

The hydrometeorological conditions in the Urseren Valley are characterized by an alpine climate with precipitation rather evenly distributed over the year. Mean annual air temperature at the MeteoSwiss climate station in Andermatt (1442 m a.s.l., years 1980 to 2012) is 4.1 ± 0.7 °C and mean annual precipitation is 1457 ± 290 mm, with ~30 % falling as snow (MeteoSwiss, 2013). The period of snow cover lasts usually from November to April.

Vegetation was strongly influenced by pasturing for centuries (Kägi, 1973). An invasion of shrubs after reduced grazing was identified for both, the north and south-facing slopes along the valley. Particularly on the north-facing slopes shrubs are predominant (Kägi, 1973; Küttel, 1990; Wettstein, 1999). The south-facing slopes are dominated by dwarf-shrub communities (Kägi, 1973; Küttel, 1990) and diverse herbs and grass species. Both investigated hillslopes of this study are mainly covered by grassland.

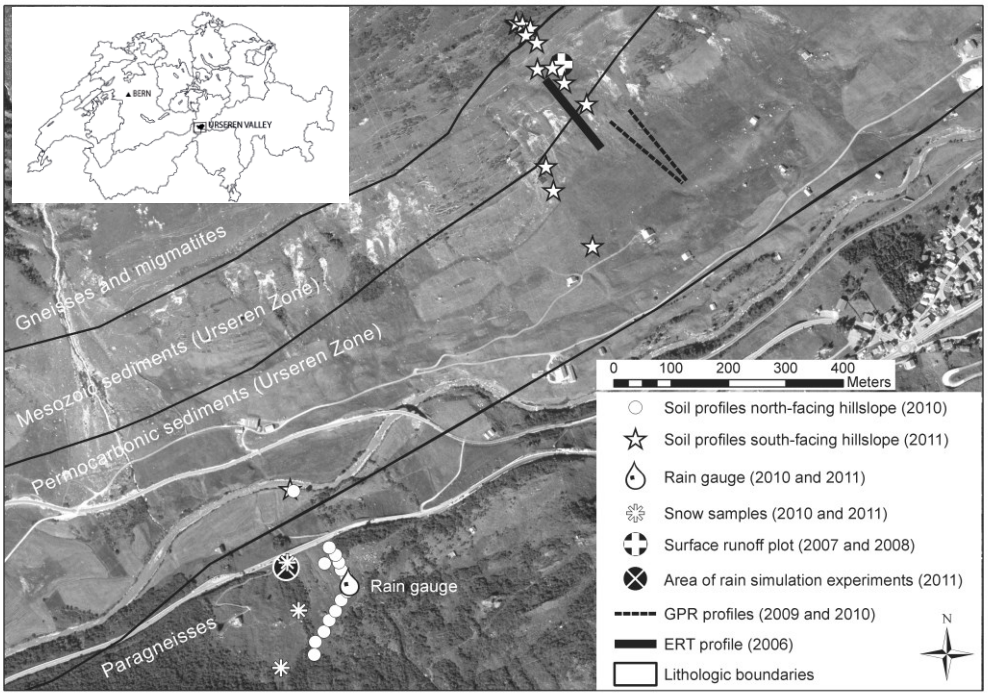

Figure 3.1: Location of the Urseren Valley and the investigated hillslopes. Locations of selected ground penetrating radar profiles (GPR) and the electrical resistivity tomography profile (ERT) are indicated; data from Carpentier et al. (2012). Air photograph reproduced by permission of Swisstopo (BA13058).

Table 3.1: Soil texture classes of the sampled depth profiles from the north- and south-facing hillslope according to Soil Survey Division Staff (1993).

profile No.	hillslope	0 to 0.3 m depth	> 0.3 m depth
1	S	silt loam	silt loam
2, 5	S	sandy loam	sandy loam
3	S	silt loam	silt loam
4	S	silt loam	sandy loam
5	S	sandy loam	sandy loam
6, 10, 11	S	silt loam	silty clay loam
7	S	silt loam	sandy clay loam
8, 9	S	silt loam	loam
12	S	silt loam	sandy loam
13 and 15 to 26	N	silt loam	sandy loam
14	N	loamy sand	sandy loam
27a, 27b	flat site	silt loam	silt loam

3.3.2 Sampling and analysis

3.3.2.1 $\delta^{18}O$ of precipitation

We monitored $\delta^{18}O$ values in precipitation (volume integrated) at the north-facing hillslope and used these $\delta^{18}O$ data as input data to simulate the $\delta^{18}O$ profiles of soil water (described in section 3.3.2.3). Precipitation was sampled biweekly with a 0.02 m^2 seasonal rain gauge and a buried and covered 5 L bottle to protect the water from evaporation. Snow

was collected as bulk samples on a monthly basis during the winter with a plastic tube of 2 m length and a diameter of 0.035 m at the lowest point of the north-facing hillslope. In March 2010 and 2011, we additionally sampled snow spatially distributed over several kilometers along the valley slopes from 1500 to 2700 m a.s.l. to account for spatial heterogeneity of stable isotopes in snow. The south-facing hillslope was not sampled for snow due to high avalanche risk in the lower parts of the south-facing slopes. However, snow samples from May 2011 of an avalanche-safe area at a south-facing slope at 2400 m a.s.l. (about 8 km west from the investigated hillslope) were available. These samples were used to estimate the $\delta^{18}O$ values in snow cover at the south-facing hillslope. $\delta^{18}O$ values in precipitation (snow was melted) were measured with a Thermo Finnigan GasBench II connected to a Thermo Finnigan DELTAplus XP continuous flow mass spectrometer (CF-IRMS, DELTAplus XP, Thermo, Bremen, Germany) and a liquid water isotope analyzer (Los Gatos Research, Inc. (LGR), Mountain View, USA). Results are reported as $\delta^{18}O$ in ‰ vs. the V-SMOW (Vienna Standard Mean Ocean Water) standard. Precisions were 0.05 ‰ with the IRMS and 0.1 ‰ with the LGR instrument. The precisions are calculated based on long term performance of the instruments, using multiple injections of the applied standards V-SMOW, SLAP and GISP. The measured samples were then calibrated to these standards.

3.3.2.2 $\delta^{18}O$ of soil water

In August 2010, we took soil samples from 15 soil profiles with a 0.9 m long soil corer of 0.055 m diameter. Samples were taken on two consecutive days along a transect at a north-facing hillslope (Figure 3.1). About 20 mm of rainfall occurred on the second sampling day (profiles 22 to 27a; more details will be discussed below). In June 2011, 13 profiles were taken along a south-facing hillslope transect (Figure 3.1). The samples at the foot of the south-facing hillslope were slightly relocated in relation to the samples from the upper part, which was due to agricultural land use in the lower area. Soil cores were transported to the laboratory in sealed plastic tubes to prevent evaporation. They were stored 3 days at 4 °C until analysis, due to practical constraints. For stable isotope analysis of soil water ($\delta^{18}O$), we followed the procedure described by Garvelmann et al. (2012), which is based on the H_2O_{liquid} - H_2O_{vapor} equilibration and laser spectroscopy method used by Wassenaar et al. (2008). We took subsamples of the soil cores at 0.05 to 0.1 m intervals and placed the fresh subsamples into two nested 1 L Ziplock plastic bags. In 2011, the Ziplock were replaced by laminated polyester bags (Weber Packaging, Germany), which were heat-sealed. The polyester bags we used in 2011 are easier to handle and less susceptible to gas losses. Prior to analysis each bag was filled with dried air and left for 15 hours in the laboratory to reach equilibrium of stable isotopes between soil water and water vapor in the bags. Stable isotope analysis of the headspace water vapor ($\delta^{18}O$) of the soil samples was performed via Wavelength-Scanned Cavity Ring Down Spectroscopy (WS-CRDS, Picarro, USA). Precision for this analysis was 0.16 ‰ vs. V-SMOW.

In 2010, the calibration of raw soil water $\delta^{18}O$ values from the north-facing hillslope was performed by using the fractionation factor α between H_2O_{liquid} and H_2O_{vapor}, the respective equilibration coefficients from Majoube (1971), and the measured equilibration temperature

in the laboratory. The coefficients from Majoube (1971) will be given below, together with the description of the soil water stable isotope model. With these values we calculated the $\delta^{18}O$ values of the soil pore water from the respective signals of the headspace water vapor.

In 2011, the calibration procedure was modified. For the standards, we applied water with a known $\delta^{18}O$ value to dried soil samples from the site (n = 23) and treated them in the same way as the actual samples. This allowed direct calculation of $\delta^{18}O$ values of soil water by relating the measured $\delta^{18}O$ value of the water vapor of the spiked calibration samples to the real, known $\delta^{18}O$ value of the applied liquid water of these spiked calibration samples. These spiked samples were used to re-check the calibration method from 2010 using the fractionation factors. The $\delta^{18}O$ value of the applied liquid water was reproduced with a mean standard error of 0.5 ‰ vs. V-SMOW, which is considered as the accuracy of our method. This cross-check of the calibration methods underpins the validity of the calibration method from 2010 using the fractionation factors. Additionally, repeated measurements on 15 selected samples within a few hours showed that the mean difference between the first and the second measurement of the same sample was 0.3 ‰ vs. V-SMOW.

Variability of the measured soil water $\delta^{18}O$ profiles was analyzed by comparing the coefficients of variation (CV) of the profiles. The CV was calculated according to the equation suggested by Fry (2003) which is used for natural abundance samples applying the stable isotope ratios R ($^{18}O/^{16}O$) of the samples:

$$\textbf{(11)}\quad CV = \left(\frac{R_{stdev}}{R_{mean}} \right) \cdot 1000‰ \ ,$$

where R_{stdev} is the standard deviation and R_{mean} is the mean of measured stable isotope ratios respectively.

3.3.2.3 Modeling of soil water $\delta^{18}O$ profiles

The soil water flow was modeled based on a numerical solution of the nonlinear Richards equation (Richards, 1931) for unsaturated water flow in the vadose zone:

$$\textbf{(12)}\quad \frac{\partial \theta(t)}{\partial t} = \frac{\partial}{\partial z}\left(k(\psi(\theta(t))) * \left(\frac{\partial \psi(\theta(t))}{\partial z} - 1 \right) \right) - ET_a \ ,$$

where θ is the water content, q is the water flux, $\psi(\theta)$ is the matrix potential as a function of water content, $k(\psi(\theta))$ is the unsaturated hydraulic conductivity as a function of the matrix potential and ET_a is the actual evapotranspiration.

Unsaturated hydraulic conductivity $k(\psi(\theta))$ and matrix potential $\psi(\theta)$ as functions of the water content θ were calculated based on the Mualem - van Genuchten approach (Mualem, 1976; van Genuchten, 1980). The Mualem - van Genuchten parameters, which include saturated and residual water contents and empirical parameters, were chosen based on the textural classes according to Sponagel et al. (2005) and Renger et al. (2009).

ET_a was calculated based on potential evapotranspiration (ET_p) and water availability according to the approach implemented in WASIM-ETH (Schulla and Jasper, 2007) and in TOPMODEL (Menzel, 1997). Thus, potential evapotranspiration (ET_p) was calculated using the Hargreaves equation (Hargreaves and Samani, 1982). Evapotranspiration was split into evaporation with isotope fractionation and transpiration without fractionation. The latter may still influence the stable isotope profile of soil water indirectly, as a result of partial removal of soil water and a subsequently modified soil water flow. Transpiration was set to 70 % of evapotranspiration during the growing season, and 10 % of evapotranspiration during the dormant season, which is based on estimates for alpine grasslands of Körner et al. (1989). Transpiration was implemented with a linear root water uptake function with depth. The amount of precipitation or snowmelt that exceeds the infiltration capacity is allocated to a runoff component. As the model is one dimensional this runoff component is not redistributed downhill.

The one-dimensional differential advection-dispersion equation was used to calculate isotope transport:

$$\frac{\partial \theta C}{\partial t} = \frac{\partial}{\partial z}(\theta D \frac{\partial C}{\partial z}) - \frac{\partial (qC)}{\partial z} - (EC_f + TC), \quad (13)$$

where C corresponds to the ^{18}O content of soil water (in atom %) and C_f is the fractionated evaporation concentration (atom %, description see below), E represents the soil evaporation, T the plant transpiration, q the water flux and D the dispersion coefficient. The latter was calculated as:

$$D = \frac{\lambda \cdot q}{\theta}, \quad (14)$$

with λ= dispersivity.

Conversion of the isotope values, given as delta values ($\delta^{18}O$), into atom % ratios and back calculation after the simulation runs, was done using the isotope ratios of the standard V-SMOW, using the following equation:

$$C(atom\%) = \frac{\left(\frac{\delta^{18}O}{1000} + 1\right) \cdot R_{std}}{1 + \left(\frac{\delta^{18}O}{1000} + 1\right) \cdot R_{std}} \cdot 100\%, \quad (15)$$

with R_{std} being the isotope ratio $^{18}O/^{16}O$ of the standard.

Equilibrium and kinetic isotope fractionation were considered and solved for. Therefore, the equilibrium fractionation factor $\alpha_{^{18}O\_liquid\text{-}vapor}$ was calculated according to the coefficients $a_{^{18}O}$ = 1.137, $b_{^{18}O}$ = -0.4156 and $c_{^{18}O}$ = -2.0667, determined by Majoube (1971) as a function of ambient temperature T:

(16) $$\alpha_{^{18}O\_liquid-vapor} = \exp\left[\left(\frac{a_{^{18}O}\cdot 10^6}{T^2} + \frac{b_{^{18}O}\cdot 10^3}{T} + c_{^{18}O}\right)\cdot\frac{1}{10^3}\right]$$

Additional kinetic fractionation by non-equilibrium fractionation for ^{18}O was calculated based on the approximation of Gonfiantini (1986) as a function of humidity h (available from the MeteoSwiss station in Andermatt) and then converted to a kinetic fractionation factor $\alpha_{k\_^{18}O}$ using the enrichment factor $\varepsilon_{k\_^{18}O}$ (see equations **(17)** and **(18)**). Kinetic fractionation is assumed to occur only in the upper 0.1 m of the soil.

(17) $$\varepsilon_{k\_^{18}O} = 14.2\cdot(1-h)$$

(18) $$\alpha_{k\_^{18}O} = \alpha_{^{18}O\_liquid-vapor} + \left(\frac{\varepsilon_{k\_^{18}O}}{1000}\right)$$

The fractionated evaporation concentration C_f was then calculated using the isotope ratios R ($^{18}O/^{16}O$) of water vapor and liquid water and the fractionation factor $\alpha_{k\_^{18}O}$ as:

(19) $$R_{vapor} = \frac{R_{liquid}}{\alpha_{k\_^{18}O}}.$$

The soil profile was subdivided into 12 cells of 0.1 m depth each and the model was run with a daily time step. Daily $\delta^{18}O$ values of precipitation were calculated from air temperature data and their correlation to the biweekly measured stable isotope signature of precipitation from the period March 2010 to March 2012 ($\delta^{18}O = 0.73 \bullet T$ (°C) - 16.89, $r^2 = 0.84$, $p < 0.0001$, $n = 145$). For the regression analysis, the precipitation-weighted arithmetic mean of air temperature of the respective biweekly interval was calculated by using measured daily air temperatures and daily precipitation volumes. This was done in order to consider only days with precipitation in the regression analysis. For the model input of the soil water stable isotopes in this study, the $\delta^{18}O$ values were weighted with precipitation volume via equations **(12)** and **(13)**. Infiltration of precipitation into the soil was set to zero during the winter seasons, when snow accumulated. The daily snowmelt volume in spring was estimated according to the degree-day-method (Linsley, 1943) using daily air temperatures. We slightly modified the degree-day-method by scaling the sum of calculated total snowmelt volume to the total measured snow water equivalent at the MeteoSwiss station in Andermatt. We obtained daily snowmelt rates of 10 ± 13 mm day^{-1} (mean ± standard deviation) for the south-facing hillslope (year 2011) and 13 ± 13 mm day^{-1} for the north-facing hillslope (year 2010). Fractionation effects during the snowmelt period were introduced by assuming that the first melt water was depleted by 2 ‰ compared to the measured $\delta^{18}O$ values of the bulk snow samples for the north- and the south-facing hillslope. These estimates are based on comparison of measured bulk snow samples at the beginning and the end of the snow accumulation period and following the estimates of Taylor et al. (2001), who investigated the stable isotope fractionation during snowmelt.

Two different input parameter sets were considered for the simulation runs to test the influence of the snowmelt component on the $\delta^{18}O$ profiles. The first input set ("sim1") refers to the $\delta^{18}O$ input as described above, including the snowmelt component. The second input set "sim2" refers to a data set from which we excluded the entire snowmelt component, which might not have entered (e.g. overland flow) or bypassed the soil matrix. We consider the two data sets "sim1" and "sim2" as extreme scenarios.

The model efficiency was evaluated using the Nash-Sutcliffe efficiency coefficient (NSE) (Nash and Sutcliffe, 1970):

$$\textbf{(20)}\quad NSE = 1 - \frac{\sum_{z=1}^{n}(\delta^{18}O_{z,\,obs} - \delta^{18}O_{z,\,sim})^2}{\sum_{z=1}^{n}(\delta^{18}O_{z,\,obs} - \delta^{18}O_{mean,\,obs})^2},$$

where $\delta^{18}O_{z,\,sim}$ is the simulated $\delta^{18}O$ value at depth z, $\delta^{18}O_{z,\,obs}$ is the measured $\delta^{18}O$ value at depth z, $\delta^{18}O_{mean,\,obs}$ is the mean of the observed values, and n is the number of measured and simulated $\delta^{18}O$ values. Additionally, measured and simulated $\delta^{18}O$ profiles were compared using the root mean squared error (RMSE):

$$\textbf{(21)}\quad RMSE = \sqrt{\frac{1}{n}\sum_{z=1}^{n}(\delta^{18}O_{z,\,sim} - \delta^{18}O_{z,\,obs})^2}\,.$$

A good agreement between measured and simulated $\delta^{18}O$ profiles (NSE close to 1 and low RMSE) consequently indicates a good model performance and that vertical soil water flow can be simulated well within a soil profile. Poor model efficiency suggests that either other flow processes take place which are not captured by the applied one dimensional model or that the chosen parameters for vertical flow are not representative.

3.3.2.4 Physical and hydrological soil properties

Homogenized, dried and sieved (2 mm) soil samples from 0 to 0.55 m depth from locations of the north- and south-facing slopes across the Urseren Valley were used for grain size analyses. We used sieves for grain sizes between 32 to 2000 µm and a Sedigraph 5100 (Micromeritics) for grain sizes between 1 to 32 µm. Samples were treated with H_2O_2 to oxidize organic carbon and sodium hexametaphosphate to break soil aggregates prior to analysis (König, 2009). Soil texture classes of the sampled depth profiles of the two hillslopes were estimated in the laboratory by a quick finger method described by Sponagel et al. (2005). Skeleton content, i.e. particles > 2 mm, was determined gravimetrically. Saturated hydraulic conductivity (K_{sat}) of undisturbed soil samples from grassland sites on the north-facing hillslope from 0 to 0.15 m and 0.2 to 0.35 m depth was determined in the laboratory with a constant head permeameter (Klute and Dirksen, 1986). 12 samples were measured for each depth interval.

Additional soil hydrological information of the investigated sites was available from earlier studies. In 2007 and 2008, Konz et al. (2010) measured surface runoff and soil water

content at a plot on the south-facing hillslope (Figure 3.1). On the north-facing hillslope, in-situ rain simulation experiments were performed on 1 m^2 plots on grassland sites in 2010 and 2011 to investigate overland flow on the plot scale (Figure 3.1). The duration of each rain simulation was 1 hour with an intensity of 36 mm h^{-1}. For a more detailed description of the measurement techniques, the reader is referred to Konz et al. (2010) and Alaoui and Helbling (2006).

3.3.2.5 Topographic analysis

Topographic analysis of the hillslopes was performed with a digital elevation model with a cell size of 2 x 2 m (Swisstopo). Accuracy in X, Y and Z direction is ± 0.5 m (1σ) in open terrain. We used the geographic information system software SAGA GIS (version 2.1.0) to calculate the topographic wetness index as

(22) $$TWI = \ln \frac{A}{\tan \beta},$$

where A is the upslope area per unit contour length and tan *ß* is the local slope (Beven and Kirkby, 1979). The triangular multiple flow direction algorithm (Seibert and McGlynn, 2007) was used to calculate the upslope area. The TWI can be used to gain information on potential spatial soil moisture patterns and hydrological flow paths, related to the topography of the investigated site (Moore et al., 1991).

3.4 Results

3.4.1 Physical and hydrological soil properties

Sampled soils across the Urseren valley are dominated by sand (50 ± 13 %) and silt fractions (41 ± 9 %) whereas the clay fraction plays a minor role (9 ± 5 %) (n = 106) (Gysel, 2010 and own data). The texture classes according to Soil Survey Division Staff (1993) of the sampled depth profiles from the two hillslopes are given in Table 3.1. Highly fractured and weathered stone fragments of up to 0.3 m length within the soils have been observed at our sites. Skeleton content in the soils ranged from 1 % to 45 % dry weight (dw) with a mean of 20 % dw (n = 100) on the north-facing slopes and from 3 % to 65 % dw with a mean of 19 % dw (n = 28) on the south-facing slopes (Konz et al., unpublished data).

Saturated hydraulic conductivity (K_{sat}) ranged from 2.3 x 10^{-6} to 2.4 x 10^{-4} m s^{-1} with a harmonic mean of 1.1 x 10^{-5} m s^{-1} (n = 24) over both depth intervals in soils from the north-facing hillslope near the rain simulation experiments (Figure 3.1). K_{sat} can be classified as moderately high to high according to the Soil Survey Division Staff (1993) and precipitation can therefore quickly pass the upper soil layers and percolate towards deeper soil zones. This is supported by the results from the rain simulation experiments at the north facing hillslope. During these experiments, surface runoff was absent or low at all sites, resulting in low runoff coefficients (RC) of 0 to 0.1 (RC = total surface runoff in mm / total precipitation in mm).

3.4.2 Air temperature, precipitation and its $\delta^{18}O$ values

Mean daily air temperature strongly varied between seasons and ranged from -16.2 to +19.8 °C (Figure 3.2, top). Mean monthly precipitation was 98 ± 55 mm between September 2009 and June 2011 (MeteoSwiss, 2013). Measured (weekly and biweekly) $\delta^{18}O$ signals in precipitation strongly varied seasonally and ranged from -24.7 to -2.9 ‰ (Figure 3.2, bottom). The volume weighted mean $\delta^{18}O$ value in precipitation at the north-facing hillslope was -13 ‰. The precipitation sample with a $\delta^{18}O$ value of -24.7 ‰ (Figure 3.2) represents freshly fallen snow at the beginning of the winter season. The depth integrating bulk snow samples from March 2011 had a mean $\delta^{18}O$ value of -17.7 ± 1.9 ‰ (± standard deviation). The depth integrating bulk snow samples from May 2011of a south-facing slope at 2400 m a.s.l. (about 8 km west from the investigated hillslope) had a mean $\delta^{18}O$ value of -17.6 ± 0.4 ‰ (n = 5). We therefore used these measured $\delta^{18}O$ values of snow as input data for the south-facing hillslope. This was considered a feasible approach, comparing our spatially distributed stable isotope data of snow (data not shown) and the fact that aspect had a minor influence on stable isotope values of snow in a study conducted by Dietermann and Weiler (2013) in the Swiss Alps.

The calculated daily $\delta^{18}O$ signals in precipitation strongly varied between seasons ranging from -28 ‰ in winter to -2.5 ‰ in summer (Figure 3.2). The measured $\delta^{18}O$ values

of precipitation were reproduced by the calculated daily $\delta^{18}O$ values of precipitation with a coefficient of determination of $r^2 = 0.64$ ($p < 0.0001$).

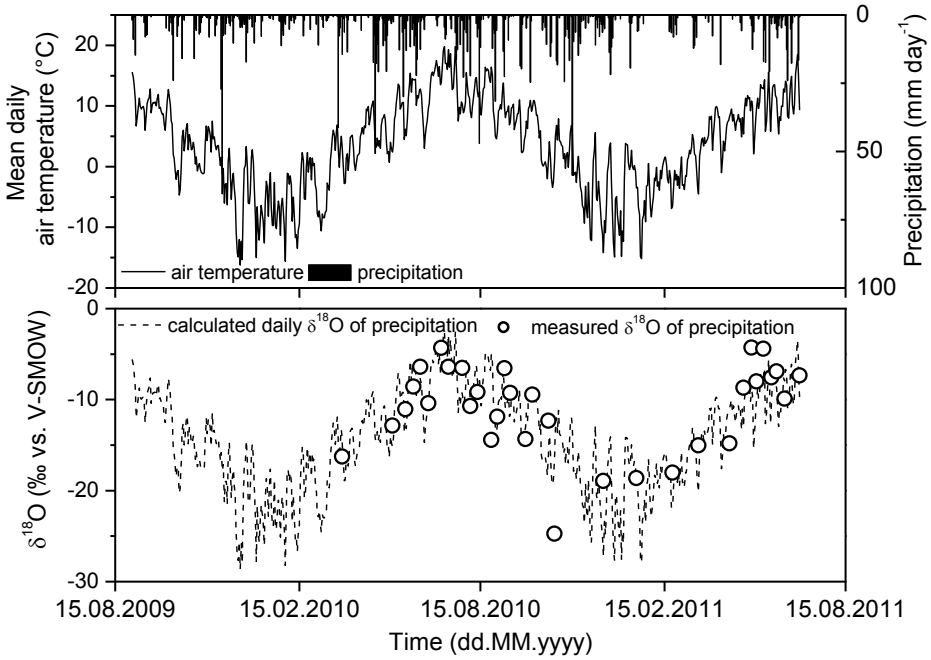

Figure 3.2: Mean daily air temperature and daily precipitation volume at the MeteoSwiss station in Andermatt (upper panel, MeteoSwiss (2013)). Lower panel: measured (bi)weekly (summer) and monthly (winter) and calculated daily $\delta^{18}O$ values of precipitation. Calculated data was derived from correlation of $\delta^{18}O$ values of precipitation with air temperature. Summer precipitation was obtained as aggregate (bi)weekly samples and winter precipitation was obtained as monthly bulk snow samples.

3.4.3 Measured and simulated soil water $\delta^{18}O$ profiles

3.4.3.1 South-facing hillslope: measured $\delta^{18}O$ profiles

Most of the profiles at the south-facing hillslope (1, 2 and 4 to 12) have similar $\delta^{18}O$ depth distributions among each other (Figure 3.3). Namely, we measured relatively higher $\delta^{18}O$ values close to the surface (-6 to -8 ‰), which decreased to about -11 to -12 ‰ in the deeper soil layers. The variability of $\delta^{18}O$ values decreased in the deeper soil layers (> 0.3 m) and the strong seasonal variation of precipitation was reduced. The variability of $\delta^{18}O$ of soil water in the upper soil layers points to vertical percolation even at high slope angles. In the profiles 2 and 3 the coefficient of variation was clearly lower (CV = 1.5 and 0.9 ‰, Figure 3.4) compared to the CV of the profiles 1 and 4 to 12, which ranged from about 1.7 to 2.8 ‰ (Figure 3.4). Profile 3 had the lowest variability (CV = 0.9 ‰) and a dampened and attenuated $\delta^{18}O$ pattern. The topographic wetness index (TWI) was not correlated to the standard deviation of $\delta^{18}O$ of soil water within each profile ($r^2 = 0.11$). This is in contrast to the study of Garvelmann et al. (2012) who found a correlation of the TWI with the standard deviation of soil water stable isotopes (δ^2H) within the profiles.

The $\delta^{18}O$ value from winter precipitation of about -17.7 ‰ (depth integrating bulk snow samples from north-facing slopes across the Urseren Valley) was not detected in terms of a clear winter peak in the measured profiles. If we take fractionation processes during winter and the snowmelt period (e.g. Taylor et al., 2001) at the south-facing slopes into account, the lowest $\delta^{18}O$ value of soil water of about -14.5 ‰ of profile 1 at the south-facing hillslope could be regarded as representing the isotopically lighter snowmelt component. Profiles with the lowest $\delta^{18}O$ value of about -10 ‰ suggest that the meltwater component was not present in these profiles. Precipitation volume of the period starting from snowmelt until the date of soil sampling in June 2011 was substantially lower (164 mm) than the amount of meltwater (approximately 284 mm snow water equivalent, SWE). We therefore expected the soil water $\delta^{18}O$ values in the lower horizon generally to be more negative in the case of a substantial contribution of snowmelt to the soil water pool. Possible explanations for the absent snowmelt peak in the $\delta^{18}O$ profiles will be discussed in detail below.

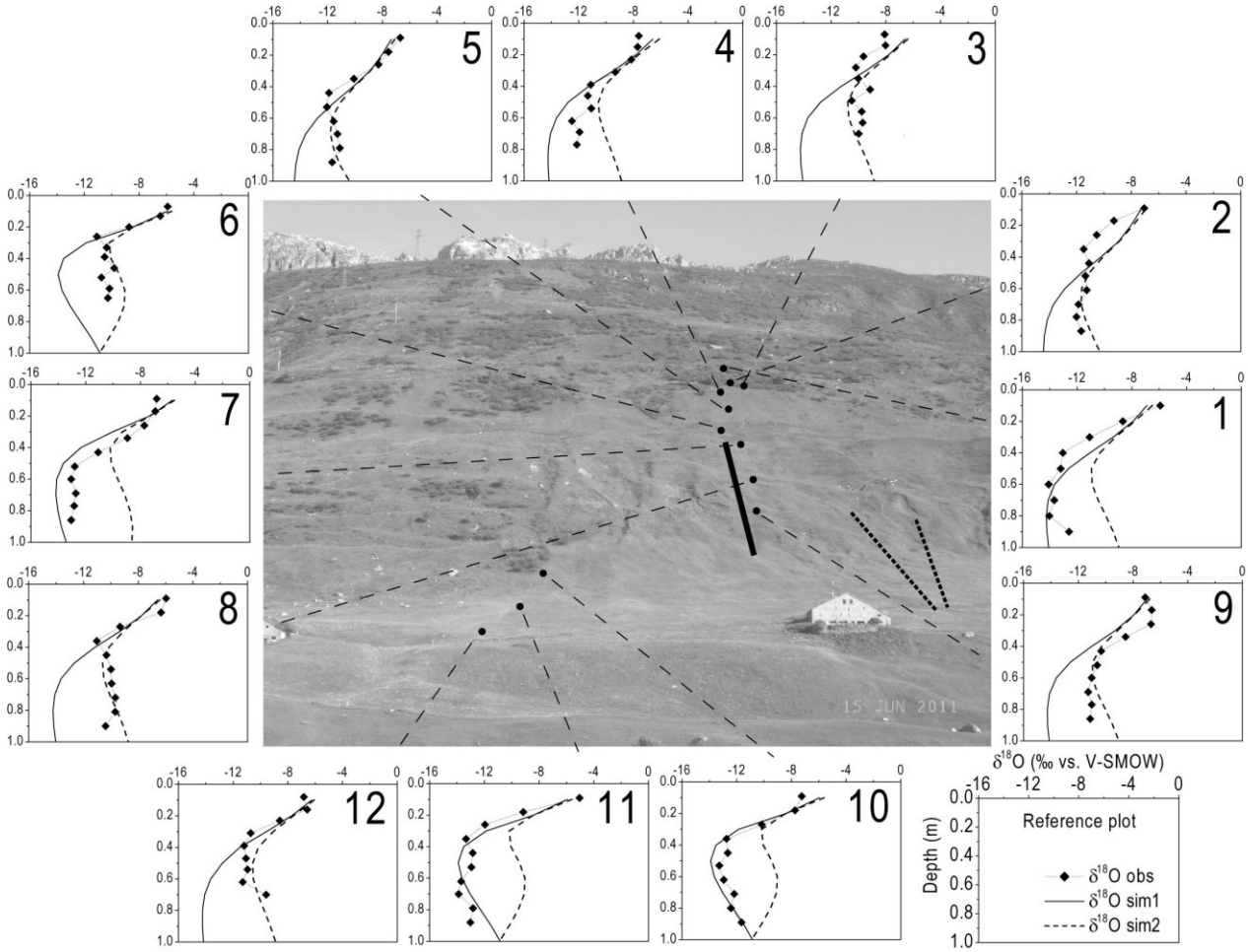

Figure 3.3: Measured ("obs") and simulated ("sim") soil water $\delta^{18}O$ isotope profiles at the south-facing hillslope from June 2011. X-axes show $\delta^{18}O$ values of soil water from -16 to 0 ‰ and y-axes show depth from 0 to 1 m. Axes are the same for each plot. A reference plot with axes labels is shown. "sim1" refers to the model which includes snowmelt; "sim2" refers to the model which excludes snowmelt. Locations of the ERT profile (▬) and selected GPR profiles (┅) from the study of Carpentier et al. (2012) are also given.

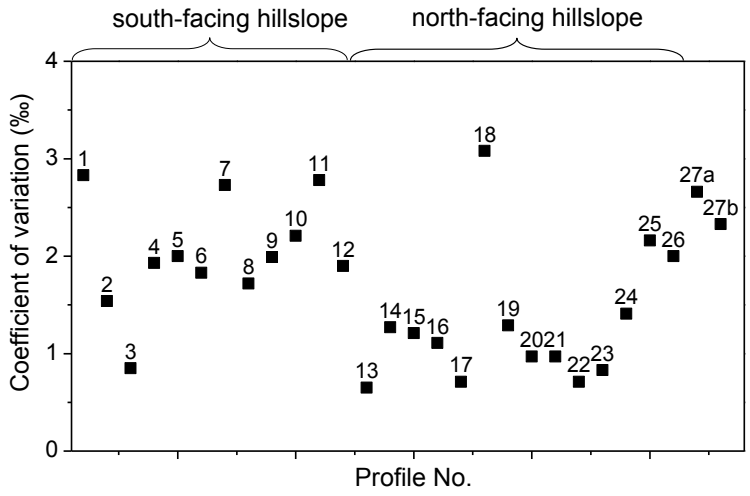

Figure 3.4: Coefficient of variation of measured $\delta^{18}O$ of soil water profiles. Data labels indicate the number of the respective profile.

3.4.3.2 South-facing hillslope: simulated $\delta^{18}O$ profiles

$\delta^{18}O$ values of the simulated profiles ranged from -14.4 ‰ in the deeper soil layers to -5.5 ‰ in the upper soil layers (Figure 3.3). Dispersivity λ was 0.02 m for all profiles, which is comparable to values of other soil hydrological studies (Pachepsky et al., 2004; van Genuchten and Wierenga, 1986; Vanderborght and Vereecken, 2007). The Nash-Sutcliffe efficiency coefficient (NSE) ranged from -11.9 (profile 3, Figure 3.5) to 0.9 (profile 5, Figure 3.5). If only the respective best fit (either data set "sim1" or "sim2") of each profile is considered, the median NSE is 0.73. Further, 83 % of the simulated profiles have a NSE of 0.5 and above. The latter is considered as "satisfactory" according to Moriasi et al. (2007). The root mean squared errors (RMSE) ranged from 0.52 ‰ (profile 5, Figure 3.6) to 3.18 ‰ (profile 11, Figure 3.6). Application of the input data set without the snowmelt component ("sim2") reduced the RMSE of several simulated profiles. Taking only the respective best fit (either data set "sim1" or "sim2") of each profile into account, the average RMSE was 1.0 ± 0.3 ‰ (mean ± standard deviation). For the profiles 1, 7, 10 and 11 we were able to reproduce the measured profile with the input parameters "sim1", including the snowmelt component (Figure 3.3). For the remaining profiles, the exclusion of the snowmelt component from the input ("sim2") could reduce the high deviation of about -4 ‰ of the simulated from the measured profiles. With this approach, it was possible to reproduce the measured profiles 2, 3, 5, 8, 9 and 12, in which the isotopically light winter precipitation seemed to be absent (Figure 3.3). We also tested other input parameter sets (e.g. considering higher dispersivities), which however were not able to compensate for the mismatch of 4 ‰ between the simulated and the measured profiles (data not shown).

Comparing the NSE with the CV visualizes that the model only performs efficiently above a certain threshold of the CV (Figure 3.7). Of course, a low model efficiency (NSE)

for profiles with a low CV can be expected, since both parameters decrease with decreasing sum of squared deviations from the mean observed values. However, high variations of $\delta^{18}O$ values within a profile (high CV) can most likely be associated with vertical percolation.

For a wide range of slope angles at the south-facing hillslope, the NSE (considering the best fit; either "sim1" or "sim2") was between 0.46 and 1 (Figure 3.8). This suggests that vertical percolation was not restricted to low slope angles. Even at a slope angle of about 46° the water can percolate vertically within the soil profile to deeper soil layers.

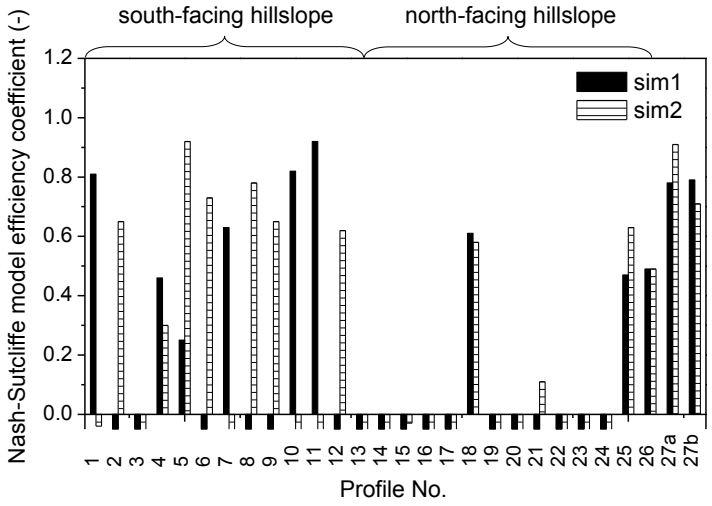

Figure 3.5: Nash-Sutcliffe model efficiency coefficient (NSE) for simulated $\delta^{18}O$ of soil water profiles. Data labels indicate the number of the respective profile. "sim1" refers to the model which includes snowmelt; "sim2" refers to the model which excludes snowmelt. For reasons of clarity the y-axis (NSE) is scaled from -0.05 to 1.2.

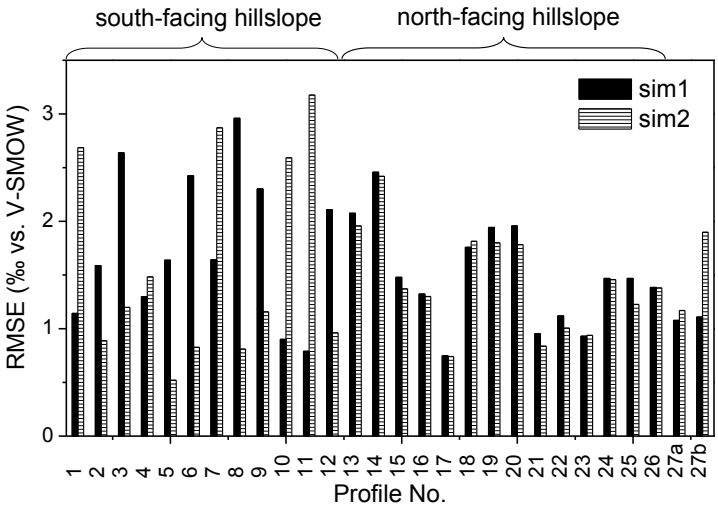

Figure 3.6: Root mean squared error of simulated $\delta^{18}O$ soil water stable isotope profiles of the north- and south-facing hillslope. Data labels indicate the number of the respective profile. "sim1" refers to the model which includes snowmelt; "sim2" refers to the model which excludes snowmelt.

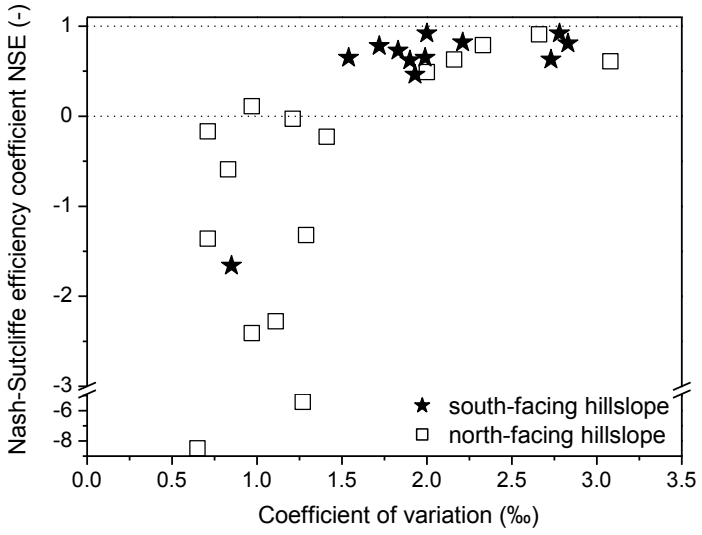

Figure 3.7: Comparison of Nash-Sutcliffe model efficiency (NSE) to the coefficient of variation (CV). For orientation the dashed lines refer to NSE = 1 (simulated data match the observed data) and NSE = 0 (model simulations are as accurate as the mean of the observed data). Please note the break on the y-axis.

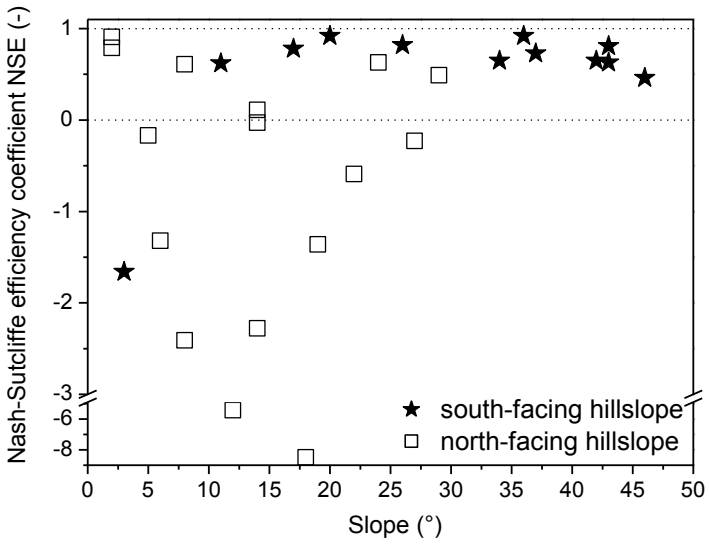

Figure 3.8: Nash-Sutcliffe model efficiency (NSE) versus slope angle. For orientation, the dashed lines refer to NSE = 1 (simulated data match the observed data) and NSE = 0 (model simulations are as accurate as the mean of the observed data). Please note the break on the y-axis.

3.4.3.3 North-facing hillslope: measured $\delta^{18}O$ profiles

The measured profiles 18 and 25 to 27b were highly variable with depth, with a coefficient of variation (CV) of 1.4 to 3.1 ‰ (Figure 3.9 and Figure 3.4). The pattern of these profiles indicates a direct imprint of the temporal highly variable $\delta^{18}O$ values of

incoming precipitation (Figure 3.2). A second group with a relatively low variability (CV ≤ 1.4 ‰), indicating redistribution and mixing of soil water from various precipitation events, comprises the profiles 14 to 17, 19, 20 and 24. Within this group the variability of $\delta^{18}O$ values clearly decreased with depth in some profiles (e.g. 14, 15, 19 and 20). Redistribution and mixing of water due to lateral subsurface flow of soil or groundwater can be an important process in the profiles 13 to 19 since a small stream passes about 10 to 20 m upslope to the profiles from right to left (Figure 3.9). Profiles 21, 22 and 23 can be regarded as intermediate profiles of these groups. Even though their CV is only 0.7 to 1.0 ‰, their pattern was qualitatively similar to the profiles 24 to 27a, but strongly dampened. These different patterns highlight the spatial heterogeneity of soil hydrological processes at the hillslope scale. Like on the south-facing hillslope, the TWI was not correlated to the standard deviation of $\delta^{18}O$ of soil water within each profile on the north-facing hillslope (r^2 = 0.01).

On the second sampling day (5 August 2010, profiles 22 to 27a), there were about 20 mm of rainfall with a $\delta^{18}O$ value of -10.4 ‰, whereas the rainfall of the 5 preceding days (22 mm) had a more positive $\delta^{18}O$ value of -6.9 ‰. The imprint of the rainfall from 5 August 2010 was visible in the profiles 22 to 27a (Figure 3.9), which tend to "bend" to more negative values $\delta^{18}O$ values in the upper 0.1 m interval compared to the profiles 13 to 21. There was no significant difference (p = 0.35) in the CV between the profiles taken on the first day (4 August 2010, profiles 13 to 21) and the profiles taken on the second day (5 August 2010, profiles 22 to 27a).

For plots 27a and 27b of Figure 3.9, the same site was sampled in August 2010 and June 2011, respectively. The distinct $\delta^{18}O$ summer peak of about -4.5 ‰ of profile 27a was not visible in the deeper soil layers of profile 27b, taken 10 months later. Assuming only vertical percolation at this site, the diverse patterns of these two profiles indicate that soil water was replaced in the upper 1 m at least within one year.

No clear winter peak was detected in the $\delta^{18}O$ profiles at the north-facing hillslope, and the ratios were more positive than the annual average in precipitation (-13 ‰). This suggests that the transit time of soil water in the upper 1 m was eventually shorter than 4 months, which is the approximate time span from snowmelt to the sampling date.

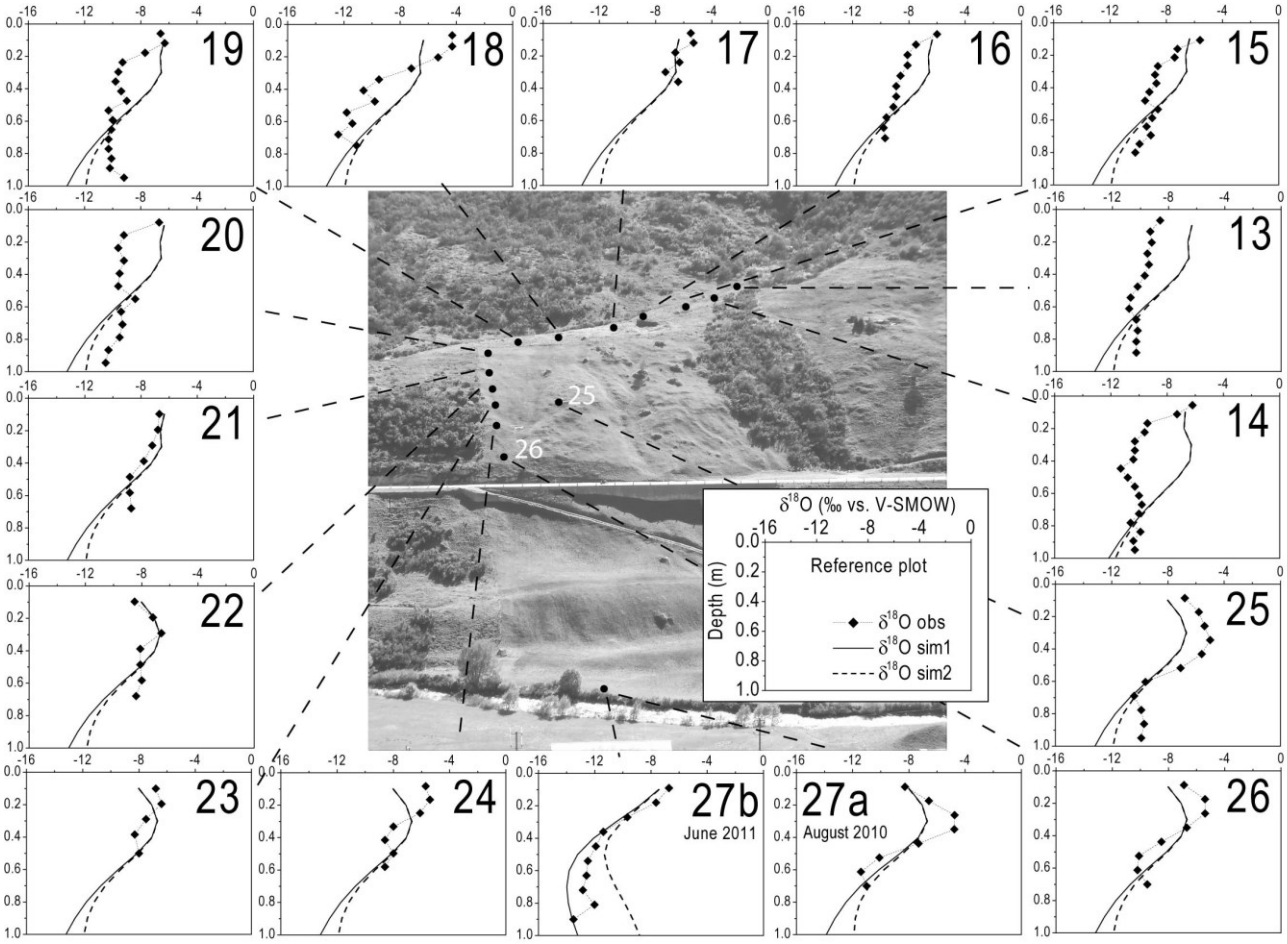

Figure 3.9: Measured ("obs") and simulated ("sim") $\delta^{18}O$ values of soil water stable isotope profiles at the north-facing hillslope from August 2010. X-axes show $\delta^{18}O$ of soil water from -16 to 0 ‰, y-axes show depth from 0 to 1 m. A reference plot with axes labels is shown. Plots 27a and 27b show the profiles from the same site taken in August 2010 and June 2011, respectively. "sim1" refers to the simulation run which includes snowmelt; "sim2" refers to the simulation run, which excludes snowmelt.

3.4.3.4 North-facing hillslope: simulated $\delta^{18}O$ profiles

The two simulation input sets "sim1" and "sim2" yielded similar profiles, which only deviated slightly from each other in the lower soil layers (Figure 3.9). This was supported by the similar root mean squared error (RMSE, Figure 3.6) and Nash-Sutcliffe model efficiency (NSE, Figure 3.5) for each respective profile. The small differences between the profiles simulated with "sim1" and "sim2" indicate a low potential and de facto influence of snowmelt at that sampling date in the year (4 and 5 August 2010 on the north-facing hillslope). At the north-facing hillslope, only the profiles 18, 21, 25, 26, and 27a and 27b had a NSE > 0. The mean RMSE for the respective best fits of all profiles from this hillslope was 1.4 ± 0.5 ‰. The distinct simulated $\delta^{18}O$ peak of about -6 ‰ at 0.4 m depth was observed in profiles 22, 25 and 27a, but the variability of the simulated profiles was more dampened.

The poor reproduction of measured isotope profiles 13 to 17, 19, 20, 22, 23 and 24 by the simulations (NSE < 0, Figure 3.5) indicates that vertical percolation is not the dominant water flow process at these sites, at least in the lower soil layers below 0.2 m depth. The simulated $\delta^{18}O$ values in the upper 0.1 m interval matched the measured values at least for the profiles 14, 16, 19, 21 and 22. Comparing the neighboring profiles 21 (taken on 4 August 2010) and 22 (taken on 5 August 2010) suggests that the applied model was able to reproduce the $\delta^{18}O$ values of soil water induced by the infiltration of rainfall on 5 August 2010. We consider the impact of the rainfall event of minor importance for the overall $\delta^{18}O$ patterns in the deeper soil layers, which is supported by the applied model using daily time steps.

Comparison of the NSE and the CV for the north-facing hillslope supports the findings from the south-facing hillslope (Figure 3.7). Above a threshold of the CV of about 1.5 ‰ (Figure 3.7) the model performed more efficient than for profiles with a CV < 1.5 ‰. In other words, vertical percolation was most likely dominant in profiles with a CV > 1.5 ‰. Further, a NSE > 0.49 was found for profiles at low and at high slope angles of the north-facing hillslope (Figure 3.8). This suggests that vertical percolation within the soil profile was not restricted to low slope angles.

3.5 Discussion

3.5.1 Physical and hydrological soil properties

Similar to our results from the rain simulation experiments, fast and nearly complete infiltration was observed at the south facing hillslope in an earlier study under natural rainfall conditions (Konz et al., 2010). The authors found that soil water content in 0.10 to 0.35 m below ground quickly responded to incoming precipitation (Figure 7 of Konz et al. (2010)). The reaction to precipitation inputs often started within 10 minutes in 0.35 m and it was often several hours faster in 0.35 m than in 0.10 m depth (data not shown). Additionally, the absolute change in volumetric soil water content was higher 0.35 m than in 0.10 m depth. This can be indicative for preferential vertical percolation and bypass flow. Only small amounts of surface runoff of 0 to 3.5 mm per month were detected during April to November 2007 and the runoff coefficient was only 0.02 for the observation period from April to November 2007 (Konz et al. (2010); precipitation volume during this period was comparable to our observation period). Furthermore, Scherrer (1996) studied runoff generation processes in rain simulation experiments very near to our sites at the south-facing hillslope and he showed that preferential bypass flow can occur at these sites. He associated the preferential bypass flow to animal burrows, which he observed in soil profiles and soil trenches. Our soil physical and hydrological data are in accordance with the study of Carpentier et al. (2012), who state that the overlaying soil material in the Urseren Valley allows fast drainage of water.

3.5.2 Subsurface water pathways as indicated by $\delta^{18}O$ depth profiles

Gazis and Feng (2004) investigated stable isotopes of soil water at sites with comparable climate (which influences temporal dynamics of stable isotopes in precipitation) and soil characteristics (e.g. texture). They found vertical subsurface flow to be important at their sites, which they inferred from abrupt changes in the stable isotope profile with depth. These changes can be produced by successive precipitation events with distinct stable isotope signatures if infiltrating precipitation pushes "old" soil pore water downward (e.g. Klaus et al., 2013). In our study, distinct $\delta^{18}O$ peaks from snowmelt and summer precipitation were identified in several investigated soil profiles. The relatively high variability (CV > 1.5 ‰) of $\delta^{18}O$ of soil water in several measured profiles combined with a "satisfactory" model efficiency (NSE > 0.5) for the respective simulated profiles point to vertical percolation and stable isotope transport within the soil profile even at high slope angles of up to 46° (Figure 3.4 and Figure 3.8). Hence, vertical percolation can predominate over other flow processes (e.g. lateral subsurface flow) at certain positions on a steep hillslope. In case of a permeable bedrock layer (like in the Urseren valley), the water can subsequently be routed directly to deeper zones and recharge into the bedrock. Since a larger volume of bedrock is available for water storage in steep watersheds (Sayama et al., 2011), a vertical percolation within a drainable soil can therefore be hydrologically even more important for recharge into bedrock in mountainous headwater catchments compared to watersheds with a smooth topography. Vertical structures at the south-facing hillslope in the Urseren valley, which Carpentier et al. (2012) interpreted as faults/fractures or vertically dipping layers, supports infiltration of water into deeper zones of the bedrock.

Nevertheless, there were also profiles at the investigated hillslopes in which the $\delta^{18}O$ peaks from snowmelt or summer precipitation were strongly dampened and the variability of $\delta^{18}O$ values within a soil profile was relatively low (CV < 1.5 ‰). For strongly dampened $\delta^{18}O$ profiles at the north-facing hillslope, the applied one-dimensional model using the Richards equation coupled with the advection-dispersion equation was not able to reproduce the measured $\delta^{18}O$ values of soil water, even on relatively flat sites (Figure 3.7 and Figure 3.8). Processes like lateral subsurface flow, mixing of waters, the influence of groundwater, and/or highly dispersive transport can reduce the variability in the deeper layers resulting in constant isotope signatures with depth (Barnes and Turner, 1998; Garvelmann et al., 2012; Gazis and Feng, 2004; Gehrels et al., 1998; Stumpp and Hendry, 2012). In the study of Garvelmann et al. (2012), profiles with a low variability of soil water stable isotopes – interpreted as indication of lateral subsurface flow – had a high TWI. This indicated accumulation of water at the respective site in their study. The authors therefore used the TWI to infer information on subsurface hydrological processes. In contrast, in our study the TWI is not correlated to the standard deviation of $\delta^{18}O$ of soil water within each profile. This points to decoupling of subsurface and surface water flow patterns at our sites. We conclude that information on subsurface hydrology cannot necessarily be obtained by only using the TWI at our sites.

Furthermore, the simulations revealed spatially heterogeneous snowmelt inputs into the soils. Several (interacting) processes, which would need further investigations, might act at our sites. The absent $\delta^{18}O$ value of the meltwater in the soil profiles can be partially explained by preferential subsurface flow of meltwater, which bypasses the soil layer and subsequently recharges into the bedrock (Brooks et al., 2010; Buttle and Sami, 1990; Darling and Bath, 1988; Gehrels et al., 1998; Stewart and McDonnell, 1991). The rock fragments of up to 0.3 m at our sites can promote funneling of water flow along their walls, which increases water flow velocity (Bogner et al., 2008) and results in fast water transport to deeper soil layers. Further, preferential flow within partially frozen soils might occur (Lundin and Johnsson, 1994; Stähli et al., 1996). Preferential bypass flow might also be explained by animal burrows (mice) which have been frequently observed visually at the soil surface of our sites after snowmelt (see photo 1 in appendix 2 in chapter 7). Furthermore, surface runoff of meltwater over frozen (Granger et al., 1984) or water saturated soils (infiltration/saturation excess overland flow) can lead to a low fraction of infiltrating meltwater. Surface runoff during the snowmelt periods was not quantitatively determined at our sites, but it was observed visually during field campaigns in early spring at the onset of snowmelt (see photo 2 in appendix 2 in chapter 7). Soil temperatures at our sites can decrease to 0 °C during winter (data not shown) promoting possible surface runoff of meltwater over these frozen soils. Spatial heterogeneous snowmelt inputs were also observed in studies of Litaor et al. (2008) and Williams et al. (2009). They were mostly associated to redistribution of snow by wind or spatially variable melt patterns controlled by elevation, aspect and vegetation. Spatial snow redistribution due to avalanches was frequently observed at our sites and might further enhance spatially heterogeneous snowmelt inputs into the soils (see photo 3 in appendix 2 in chapter 7).

We propose a conceptual flow model, which can be used to understand the main flow processes in this study (Figure 3.10). The comparison of measured and simulated $\delta^{18}O$ profiles can be used as a diagnostic tool for a relatively quick characterization of spatial heterogeneity of water inputs into the soil and transport processes at the hillslope scale. For highly permeable soils with low dispersivities like in our study, we suggest two main classes of $\delta^{18}O$ profiles that can be observed (profiles A1 to A3 versus profile B in Figure 3.10). In regions with seasonally varying $\delta^{18}O$ values in precipitation, a preservation of this variability in the $\delta^{18}O$ values in the soil water indicates vertical percolation within the soil (profiles A1 to A3 in Figure 3.10). Profile A3 in Figure 3.10 still implies vertical percolation, even if the $\delta^{18}O$ value of snowmelt water is absent. The latter was inferred from the simulated profiles using different input parameters. The second class is represented by profile B in Figure 3.10, which has a nearly constant $\delta^{18}O$ value of soil water with depth. The latter suggests a minor role of vertical percolation and a stronger influence of, for example, lateral subsurface flow, which can be due to near-surface groundwater flow in the vicinity of streams (Figure 3.10) or if recharge to the bedrock is hampered. Classification of our measured profiles (1 to 27b) according to the suggested conceptual model (Figure 3.10)

is given in Table 3.2. 64 % of the profiles correspond to type A profiles, indicating a predominant role of vertical percolation within these soils.

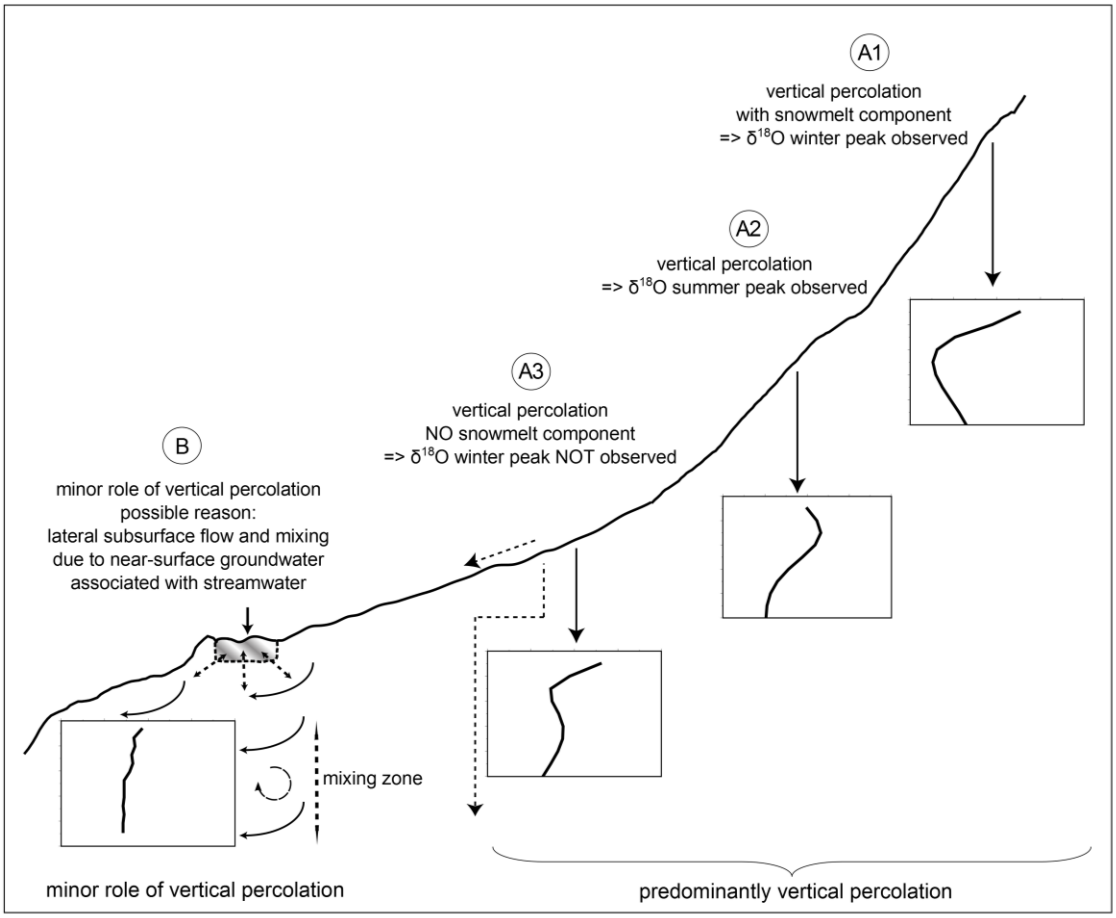

Figure 3.10: Conceptual subsurface water flow model. See text for detailed explanations.

Table 3.2: Classification of the measured $\delta^{18}O$ soil water profiles (profile numbers are given) according to the conceptual flow model of Figure 3.10.

schematic profile A1	schematic profile A2	schematic profile A3	schematic profile B
1	18	2	13
4	24	3	14
7	25	5	15
10	26	6	16
11	27a	8	17
27b		9	19
		12	20
			21
			22
			23

3.6 Conclusions

The temporal high variation of $\delta^{18}O$ values in precipitation and its subsequent attenuation in soil pore water was successfully used to track the water flow in the unsaturated zone and to estimate the relative importance of vertical percolation versus lateral subsurface flow in two steep subalpine hillslopes. In some profiles, $\delta^{18}O$ values of soil pore water indicate fast infiltration into the soil layers and subsequent vertical percolation into deeper zones even at steep slopes. This is supported by physical soil data (sandy soil texture and high skeleton contents) and surface runoff measurements during rain simulations. The high infiltration capacity can be explained by the relatively high values of K_{sat}, which we measured at selected undisturbed soil samples in the laboratory. Overland flow during summer rain events, which can cause sheet erosion of soil, therefore plays a minor role in our study area. The vertical transport processes were confirmed by an one-dimensional soil physical model coupled with the advection-dispersion equation, which was used to simulate the measured $\delta^{18}O$ profiles. In other profiles, however, the $\delta^{18}O$ values of soil pore water also suggest that processes, like for example lateral subsurface flow or mixing of water occurred at the investigated sites, which was most likely due to near-surface groundwater at one hillslope. Non-equilibrium flow processes can lead to poor model performance, since the applied model is at the present stage designed for uniform equilibrium flow and transport. Furthermore, the model simulations suggest a spatial heterogeneity of snowmelt input into the soils at the hillslope scale.

The applied soil sampling and stable isotope analysis proved to be a fast (one single sampling campaign) and suitable approach to investigate actual soil water flow paths at steep subalpine hillslopes. Within 1 to 2 days of sampling and 3 days of soil water stable isotope measurements only, we were able to generate a quick time-integrating overview of subsurface hydrological processes at the hillslope scale. In combination with a physically based soil model, we suggest this method as a tool to investigate hillslope hydrology at sites were more conventional soil moisture equipment cannot be easily installed (e.g. in stony soils or during harsh winter conditions) or if time is a limiting factor.

Acknowledgements

We would like to thank Barbara Herbstritt, Benjamin Gralher, and Jakob Garvelmann for their great support and background information during stable isotopes measurements at the laboratory of the Chair of Hydrology, University of Freiburg, Germany. We also would like to thank Björn Probst and Gregor Juretzko for their assistance during soil sampling in the field and Marianne Caroni for soil texture analyses. Susanne Lagger and Philipp Schmidt are kindly acknowledged for their help during the irrigation experiments and we thank Silvia Hunkeler for measuring saturated hydrologic conductivity of soil samples. Finally, we would like to thank the three anonymous reviewers for their constructive comments, which greatly helped to improve our manuscript. Peter K. Kitanidis is gratefully acknowledged for handling the review process.

This work was part of the project “The ecological and socio-economic consequences of land transformation in alpine regions: an interdisciplinary assessment and VALuation of current changes in the Urseren Valley, key region in the Swiss central Alps”, funded by the Swiss National Science Foundation (SNF), grant no. CR30I3_124809. (The SNF was not involved in study design; in the collection, analysis and interpretation of data; and in the writing of the report.)

4 Green alder shrubs and wetland soils influence stream water geochemistry during a storm event and a snowmelt period in headwater catchments

Mueller, M. H.[1,], Alaoui, A.[2], and Alewell, C.[1]*

[1]Environmental Geosciences, University of Basel, Bernoullistrasse 30, 4056 Basel, Switzerland

[2]Centre for Development and Environment (CDE), University of Bern, Hallerstrasse 10, 3012 Bern, Switzerland

[*]present address: Applied and Environmental Geology, University of Basel, Bernoullistrasse 32, 4056 Basel, Switzerland

This chapter is in preparation for submission.

4.1 Abstract

Stream water geochemistry can be influenced by various external and internal factors such as atmospheric inputs and catchment characteristics, e.g. soil and vegetation cover. In the Swiss Alps, shrubs (e.g. *Alnus viridis subsp. viridis*) are encroaching into formerly open habitats. The shrub encroachment might affect soil hydrological properties, which in turn influences runoff generation. Moreover, alder species (*Alnus spp.*) are known to affect chemical soil properties and can therefore alter the export of nutrients via stream water.

In our study, we investigated four small alpine headwater catchments to assess the influence of shrub encroachment and wetland soils on stream water geochemistry during storm and snowmelt runoff. Stream water was sampled (bi)weekly during 2 years, at hourly intervals during a rainfall event in the growing season, and on a daily basis during a snowmelt period. Stream geochemistry was strongly influenced by the land cover, i.e. soil and shrub cover. Riparian wetland soils were flushed by a high proportion of event water, which increased dissolved organic carbon export during the rainfall event and the snowmelt period. An increase in nitrate export during the rainfall event is likely due to the encroachment of green alder shrubs.

4.2 Introduction

Headwater catchments in mountainous regions provide freshwater for lowland areas (Viviroli et al., 2011; Weingartner et al., 2007) and therefore play an important role for groundwater recharge and subsequent sustenance of high quality drinking water production. Moreover headwater stream characteristics, e.g. stream geochemistry, strongly influence ecological integrity of downstream rivers (Bishop et al., 2008; Freeman et al., 2007). It is well known that stream water geochemistry can be influenced by various factors such as geology (Drever, 1982), chemical soil characteristics (Billett and Cresser, 1992), topography, which in turn influences hydrological response (McGuire et al., 2005), atmospheric inputs (Gibbs, 1970), land use (e.g. agricultural use) (Hill, 1978) and land/vegetation cover (Andersson and Nyberg, 2009). These factors can act on both the long and the short term scale, i.e. at base flow and storm flow conditions. Williams et al. (1990) showed that base flow geochemistry was mainly influenced by deep and shallow groundwater geochemistry in an alpine catchment, whereas Neff et al. (2012) found that stream water geochemistry, including both base and event flow conditions, was mainly influenced by soil and vegetation variables in their study.

In the Swiss Alps, current land use changes due to changing agricultural practices induce a shrub encroachment into formerly open habitats (Tasser et al., 2005; Wettstein, 1999). An invasion of shrubs, mainly green alder (*Alnus viridis subsp. viridis*), was for example identified in the Urseren Valley in the Swiss Central Alps (Kägi, 1973; Küttel, 1990; Wettstein, 1999). The shrub encroachment might affect the hydrological and geochemical functioning of headwater catchments in this area. Since alder species (*Alnus spp.*) are known to alter chemical soil properties (e.g. Mitchell and Ruess, 2009), stream geochemistry might be affected. Nitrogen dynamics can be altered through a symbiotic relationship with the nitrogen-fixing bacterium *Frankia alni* (Benecke, 1970; Pawlowski and Newton, 2008). Mitchell and Ruess (2009) observed elevated carbon and nitrogen contents in soils under green alder stands (*Alnus viridis subsp. fruticosa*) and Rhoades et al. (2001) measured increased extractable soil nitrate under green alder trees (*Alnus viridis subsp. crispa*). Bühlmann (2011) measured increased nitrate concentrations in soil water under green alder stands (*Alnus viridis subsp. viridis*) in the Urseren Valley in the Swiss Central Alps. Shaftel et al. (2012) showed that nitrate concentrations in streams of headwater catchments, which are covered by alder species (*Alnus viridis subsp. fruticosa*, *Alnus viridis subsp. sinuate* and *Alnus incana subsp. tenuifolia*), were increased.

Along with the possible direct influence of green alder encroachment on stream water geochemistry, it might additionally alter hydrologic pathways and components of the water cycle. Hydrological pathways in turn directly influence stream water geochemistry during summer rainfall events and snowmelt periods (Bishop et al., 2004; Creed et al., 1996; Fiebig et al., 1990; Grabs et al., 2012; Hornberger et al., 1994; Inamdar et al., 2004; McGlynn et

al., 1999; Pacific et al., 2010). In the Urseren Valley, the influence of invading shrubs on the total water balance (Alaoui et al., 2013) and mean water transit times and geochemistry at base flow conditions (i.e. long term scale) was negligible (Mueller et al., 2013). However, the short term scale hydrology, i.e. the generation of storm or snowmelt runoff, might be affected by higher soil hydraulic conductivities of soils under green alder stands (Alaoui et al., 2013). Decaying plant roots of shrubs can establish preferential flowpaths (Jarvis, 2007), which can be an important component in generating runoff at the plot and the catchment scale (Hrachowitz et al., 2013; Sidle et al., 2000; van der Heijden et al., 2013), when connection to the stream water can be established. This connection is especially known to occur via riparian wetland zones, which strongly interact with streams and therefore support exchange of water and nutrients during snowmelt (Kendall et al., 1999; Sebestyen et al., 2008) or rainfall events during the growing season (Fiebig et al., 1990). Rapid flow of event water through preferential flowpaths can then for example transport dissolved organic carbon from riparian zones to the streams (Fiebig et al., 1990; McGlynn and McDonnell, 2003).

In this study, we investigated four alpine headwater catchments, with differing percentage of green alder cover and wetland soils in order to assess the temporal geochemical evolution (i.e. dissolved organic carbon and inorganic solutes) during a rainfall event in the growing season and a snowmelt period. Stable water isotope ratios ($\delta^{18}O$ values), calcium and silicon were used to infer information on runoff generation mechanisms and water flow paths. We hypothesize that the encroachment of green alder shrubs increases concentrations of nitrate in stream water during high flow periods of rainfall and snowmelt events. We further hypothesize that the connection of the zones where green alder shrubs grow with the streams is established via riparian wetlands, which subsequently increase the export of dissolved organic carbon from the catchments.

4.3 Material and Methods

4.3.1 Study site

The study sites are located in the Urseren Valley in Central Switzerland (Figure 4.1). The Urseren Valley is a glacially influenced U-shaped valley with steep, rugged slopes and a flat valley bottom, ranging from 1400 to 3200 m a.s.l. The southern mountain ridge is built by the “Gotthard massif” which mainly includes paragneisses and granites. The northern crests are formed by granites, granitoids, gneisses and migmatites of the Aar system, which is divided into the “Aar granite” and the gneiss/migmatite complex of the “Altkristallin” (Labhart, 1977). The Aar and Gotthard massifs are separated by the “Urseren Zone”, which is formed by vertically dipping Permocarbonic and Mesozoic layers along a geological fault line. The latter corresponds to the valley axis. These layers comprise sandstones, rauhwackes, dolomites, dark clay-marls and limestones and they are outcropping at the lower parts of the south-facing slopes. Throughout the formation of the Alps the material was metamorphosed to schists (Labhart, 1977). Limestones, dolomites and/or gypsum rich

rocks can underlie or can be incorporated as lenses in the outcropping rocks of the Gotthard and the Aar systems (Ambuehl, 1929; Buxtorf, 1912; Labhart, 1977; Winterhalter, 1930). Ambuehl (1929) reports a high carbonate content in a serpentinite pit near the Chämleten catchment (Figure 4.1). Mullis (2011) also reports sulfate bearing minerals in veins of the Gotthard system.

Dominant soil types in the valley according to the world reference base (IUSS Working Group WRB, 2006) are Podsols, Podzocambisols and Cambisols (Meusburger and Alewell, 2008). Leptosols can be found at higher elevations and on steeper slopes. Clayey gleyic Cambisols, Histosols, Fluvisols, and Gleysols predominantly developed at the valley bottom and lower slopes. Organic carbon content can be elevated up to 34 weight % at sites where riparian wetland soils and peat bogs developed (Schroeder, 2012).

Mean annual air temperature at the MeteoSwiss climate station in Andermatt (1442 m a.s.l., years 1980 to 2012) is 4.1 ± 0.7 °C and mean annual precipitation is 1457 ± 290 mm, with ~30 % falling as snow (MeteoSwiss, 2013). The period of snow cover is usually from November to April and runoff is usually dominated by snowmelt in May and June.

Vegetation shows a strong anthropogenic influences due to pasturing for centuries (Kägi, 1973). Shrubs are encroaching into formerly open habitats (Tasser et al., 2005; Wettstein, 1999). The invasion of shrubs, mainly *Alnus viridis subsp. viridis* (green alder) together with *Sorbus aucuparia* (mountain-ash), was identified on both the north and south-facing slopes in the Urseren Valley (Kägi, 1973; Küttel, 1990; Wettstein, 1999). The shrub cover increased by 32 % between 1965 and 1994 (Wettstein, 1999) and again by 24 % between 1994 to 2004 (van den Bergh et al., unpublished data) and is predominant at the north-facing slopes. On the south-facing slopes, dwarf-shrub communities and diverse herbs and grass species can be found (Kägi, 1973; Küttel, 1990).

Four steep micro catchments (< 1 km^2) located on north-east and north-west facing slopes in the Urseren Valley were chosen with regard to their differing percentage of shrub cover, ranging from 14 to 82 % (Table 4.1 and Figure 4.1). Catchment characteristics were assessed by van den Bergh et al. (2011), Fercher (2013) and Schroeder (2012) by a combination of satellite images and field observation, and modified after additional field observations. Topographic analysis was performed with a digital elevation model with a cell size of 2 x 2 m below 2000 m a.s.l. and 25 x 25 m above 2000 m a.s.l.

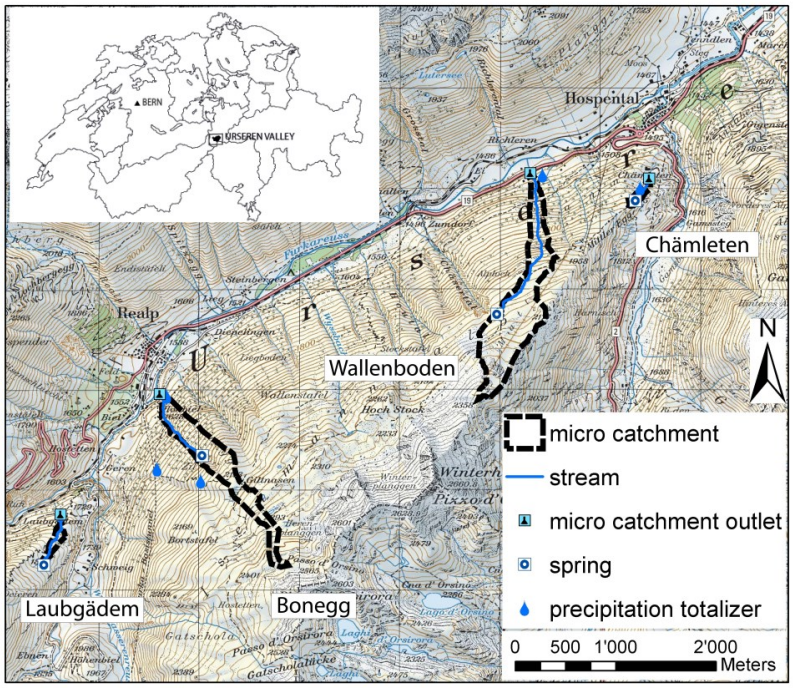

Figure 4.1: Location of the micro catchments in the Urseren Valley. Micro catchment limits from van den Bergh et al. (2011) and Fercher (2013), modified. Figure according to Mueller et al. (2013). Geodata reproduced by permission of swisstopo (BA13109).

Table 4.1: Characteristics of micro catchments. Vegetation data from van den Bergh et al. (2011) and Fercher (2013) (modified), discharge data from Lagger (2012) and Schmidt (2012).

	Chämleten	Wallenboden	Bonegg	Laubgädem
projected area (km^2) [a]	0.01981	0.56431	0.34302	0.02981
vegetation cover (%) [a]	100	79	96	100
grassland (%)	10	47	35	13
dwarf shrubs (e.g. *Calluna vulgaris*) (%)	8	19	23	73
bare rocks (%)	0	19	3	0
forest (%)	0	0	0.1	0
shrub cover (mainly *Alnus viridis subsp. viridis* and *Sorbus aucuparia*) (%) [a]	82	14	39	15
Riparian wetlands (incl. peat bog sites) (%) [b]	15 to 20	2 to 5	3 to 6	10 to 15
elevation range (m a.s.l.) [a]	1669 – 1810	1501 – 2354	1551 – 2492	1721 – 1915
mean elevation (m a.s.l.) [a]	1740	2082	2026	1836
slope range (°) [a]	4 .0 – 55.7	0.6 – 60.5	0.5 – 73.1	0.3 – 49.3
mean catchment slope (°) [a]	24	20	28	20
aspect [a]	NE	NNW	NW	NE
range of discharge ($L\ s^{-1}$) [a]	0.1 – 36.0	0.5 – 44.0	2.0 – 93.5	0.1 – 14.6
mean discharge ($L\ s^{-1}$) [a] (summer 2010 and 2011)	1.1	2.4	6.3	2.9
mean water transit time of base flow (years) [a]	1.5 ± 0.1	1.4 ± 0.1	1.3 ± 0.1	2.0 ± 0.1

[a] Data taken from Mueller et al. (2013)

[b] Please note that riparian wetlands are mainly covered by what we summarized as grassland and sometimes also by (dwarf) shrubs.

4.3.2 Sampling and analysis of precipitation and stream water

Precipitation volume was continuously measured with a Davis Vantage pro2 weather station at the MeteoSwiss station Andermatt by the Swiss Federal Office of Meteorology and Climatology (MeteoSwiss, 2013). During the growing season, precipitation was also measured with rain gage tipping buckets (model 52203, Young, USA) in the four micro catchments by the Group of Hydrology of the University of Bern, Switzerland, and with ECRN-50 rain gage tipping buckets (Decagon Devices, USA) distributed across the Urseren Valley. Discharge in the four micro catchments was measured with pressure transducers (PDCR1830, Campbell Scientific) and a radar sensor (Vegapuls61, VEGA) by the Group of Hydrology of the University of Bern, Switzerland. Availability of discharge data was restricted to summer months because streams and installed weirs were completely snow covered and/or frozen during winter.

Precipitation and stream water was sampled biweekly from March 2010 to May 2012. A 0.02 m^2 totalizer was used to collect precipitation near the catchment outlets. After determination of precipitation volume, a subsample was transferred into a 250 ml poly ethylene (PE) bottle. Stream water was sampled by hand with 250 ml PE bottles, which were filled completely to protect the samples against evaporation. Samples were taken at base flow conditions, defined as the "baseline" of the hydrograph when discharge was not increased by the influence of precipitation events. Stream water was also sampled hourly during a rainfall event in July 2011 with an automatic water sampler (ISCO 6700, Isco Inc., USA) to investigate runoff generation processes and stream water geochemistry of storm runoff. Sampling was started several hours before the onset of rainfall and continued until discharge receded to pre-event conditions. We also sampled stream water in the Wallenboden and Bonegg catchments on a daily basis during five weeks from April to May 2012 (except during high avalanche risk) to capture snowmelt runoff. Source water samples were collected in the upper part of each catchment at the spring of the stream after a period of two weeks without precipitation in October 2011.

We measured various geochemical parameters, which served as geogenic tracers. Total dissolved Ca, Mg, K, Na and Si were measured by Inductively Coupled Plasma Optical Emission Spectrometry (ICP-OES, Spectro Genesis, Spectro Analytical Instruments, Germany). Nitrate (NO_3^-) and Sulfate (SO_4^{2-}) where measured by ion chromatography (761 Compact IC, Metrohm, Switzerland). Samples were calibrated to known standards and precision for ICP-OES and IC measurements was 0.1 mg L^{-1}. Stable water isotopes ($\delta^{18}O$ values) were used as a time-oriented tracer and measured with a Thermo Finnigan GasBench II connected to a DELTAplus XP continuous flow mass spectrometer (CF-IRMS, DELTAplus XP, Thermo, Bremen, Germany) and a liquid water isotope analyzer (Los Gatos Research, Inc. (LGR), Mountain View, USA). Results are reported as $\delta^{18}O$ in ‰ vs. the V-SMOW standard. Precisions are 0.05 ‰ with the IRMS and 0.1 ‰ with the LGR instrument respectively. Samples were calibrated to known standards (V-SMOW, SLAP and GISP). PH was measured continuously during the summer periods with a CS525 ISFET pH

Probe (Campbell Scientific, UK, accuracy 0.1 pH unit) and on a monthly basis during winter with a portable pH 340i probe (WTW, Weilheim, Germany). Electrical conductivity of precipitation was determined with a SevenMulti probe (Mettler Toledo Seven Multi, Germany) in the laboratory. A LF 92 – TetraCon 96 probe (WTW, Weilheim, Germany; reference temperature was 25 °C) was used in the field during the snowmelt campaign to determine electrical conductivity of stream water. Dissolved organic carbon (DOC) was determined in acidified samples with a TOC Analyzer (Shimadzu, Tokyo). Samples were calibrated to known standards and precision for DOC measurements was 0.1 mg L^{-1}. Samples were filtered with 0.45 µm filters (Rotilabo-filter, PVDF, Roth, Switzerland), cooled during transport to the laboratory, and kept frozen at -20 °C until analysis.

4.3.3 Hydrograph separation

Storm hydrograph separation was performed via a two component analysis to calculate proportions of pre-event (e.g. groundwater and soil water) and event water (rainfall) in stream runoff during the rainfall event (McDonnell et al., 1990; Sklash and Farvolden, 1979). We used $\delta^{18}O$ values and the approach of incremental mean of precipitation inputs to account for its variation during the rainfall event (McDonnell et al., 1990). The mean $\delta^{18}O$ value of stream water at base flow conditions was used as the $\delta^{18}O$ value of pre-event water (Munoz-Villers and McDonnell, 2012) and it was assumed to be time-invariant. Event water fraction was calculated according to Genereux (1998) as:

(23) $$f_{event} = \frac{\delta_{pre-event} - \delta_{stream}}{\delta_{pre-event} - \delta_{event}}$$

f_{event} = fraction of event water

$\delta = \delta^{18}O$ value of event, pre-event and stream water

event water = rainfall

pre-event water = groundwater and soil water

stream = stream water

The $\delta^{18}O$ values of event water for each time step i (precipitation volume P was measured every 3 hours) was calculated as:

(24) $$\delta_{event} = \frac{\sum_{i=1}^{n} P_i \cdot \delta_{event}}{\sum_{i=1}^{n} P_i}$$

Uncertainty of the two component mixing analysis was validated using the error propagation technique of Genereux (1998):

(25)

$$W_{fe} = \sqrt{\left(\frac{\delta_{pre-event} - \delta_{stream}}{(\delta_{pre-event} - \delta_{event})^2} W_{\delta\_event}\right)^2 + \left(\frac{\delta_{stream} - \delta_{event}}{(\delta_{pre-event} - \delta_{event})^2} W_{\delta\_pre-event}\right)^2 + \left(\frac{-1}{(\delta_{pre-event} - \delta_{event})} W_{\delta\_stream}\right)^2}$$

W_{fe} = uncertainty of fraction of event water

$W_{\delta\_pre\text{-}event}$ = uncertainty of $\delta^{18}O$ value of pre-event water

W_{δ_event} = uncertainty of $\delta^{18}O$ value of event water

W_{δ_stream} = uncertainty of $\delta^{18}O$ value of stream runoff

We used the analytical error of ± 0.1 ‰ for the stream water samples (W_{δ_stream}) according to Genereux (1998). The standard deviation of the base flow stream water samples was taken as the uncertainty of the pre-event water for every micro catchment ($W_{\delta\_pre\text{-}event}$ = ± 0.55 to 0.2 ‰). The $\delta^{18}O$ values of rainfall decreased from about -3 to -7.5 ‰ during the whole event. For each time step we estimated the uncertainty of the event water (W_{δ_event}) to be about ± 1.5 ‰ as a maximum value, accounting for spatial and temporal variability.

4.4 Results and Discussion

4.4.1 Geochemistry of rainfall, spring and stream water

4.4.1.1 Rainfall and spring water

Rainfall was relatively low in solute concentrations (Table 4.2 and Table 4.3), which is comparable to other areas in the Alps (Rogora et al., 2006). Comparison of rainfall and spring water (Table 4.4) indicates that geochemical processes along the flow paths of rainfall increased most of the solute concentrations in Chämleten, Wallenboden and Laubgädem (Ca, K, Na, Si and SO_4^{2-}). Solute concentrations of spring water in Bonegg were low and comparable to rainfall geochemistry (Table 4.4). This points to less water-rock interaction and less geochemical buffering of spring water in Bonegg. NO_3^- and DOC were mostly lower in the spring water than in rainfall samples (except NO_3^- in Bonegg), suggesting biogeochemical degradation and/or consumption of DOC and NO_3^- along the flow paths in deeper zones, e.g. via denitrification or microbial uptake (Cooper, 1990; Knowles, 1982).

Table 4.2: Geochemistry of rainfall in the Urseren Valley. Solute concentrations in mg L^{-1}; electrical conductivity (EC) in µS cm^{-1}. Aggregate samples from two sampling dates in summer 2011. Each data point represents the mean of all four micro catchments.

Collecting period		P (mm)	Ca	K	Mg	Na	NO_3^-	SO_4^{2-}	pH	EC
10 to 24 Aug 2011	mean	12	5.8	0.9	0.8	0.7	2.2	1.2	na	na
	standard deviation	2	1.0	0.3	0.3	0.2	0.4	0.2	na	na
24 to 31 Aug 2011	mean	53	7.3	0.9	0.6	0.7	2.4	2.6	6.1	44.5
	standard deviation	7	0.3	0.4	0.1	< 0.1	0.1	0.1	0.1	8.7

na: not available

Table 4.3: Geochemistry of rainfall on 13 July 2011. Solute concentrations in mg L^{-1}.

	7-day antecedent P (mm)	3-day antecedent P (mm)	13 July 2011 P (mm)	Ca	K	Mg	Na	Si	NO_3^-	SO_4^{2-}	DOC
Chämleten	36	3	48	0.8	0.1	0.1	0.1	0.1	1.7	0.6	0.9
Wallenboden	31	na	48	0.4	0.1	< 0.1	< 0.1	0.1	1.2	0.5	0.9
Bonegg	30	3	45	0.3	0.1	< 0.1	< 0.1	0.1	1.1	0.4	0.8
Laubgädem	38	3	44	0.4	0.1	< 0.1	< 0.1	0.1	1.6	0.5	0.6

Table 4.4: Geochemistry of spring water in the four micro catchments in mg L-1. Sampling on 6 October 2011 after two weeks without precipitation (n = 1).

	Ca	K	Mg	Na	Si	NO_3^-	SO_4^{2-}	DOC
Chämleten	16.8	1.5	0.8	1.1	2.4	0.4	12.5	0.9
Wallenboden	6.1	1.1	0.3	0.9	1.8	0.4	8.4	< 0.1
Bonegg	3.5	0.9	0.4	0.6	1.6	3.6	3.5	0.7
Laubgädem	23.3	1.9	0.8	1.0	2.5	0.5	7.2	0.1

4.4.1.2 Stream water during base flow conditions

As discussed in an earlier study (Mueller et al., 2013), pH values, concentrations of SO_4^{2-} and concentrations of total dissolved Ca, Mg, Na and K (Table 4.5) were higher than can be expected from similar geological and climatological settings with mainly granitic or gneiss materials (e.g. Drever and Zobrist, 1992; Ofterdinger, 2001; Tardy, 1971). In contrast, mean silicon concentrations (Table 4.5) were slightly lower than compared to other granitic or gneiss regions with comparable climate (e.g. Drever and Zobrist, 1992; Tardy, 1971). The relatively high SO_4^{2-} concentrations in base flow stream water (Table 4.5) and the low SO_4^{2-} input via precipitation (Table 4.2 and Table 4.3) suggest that SO_4^{2-} concentrations in stream water are mainly controlled by geological factors in our catchments (sulfate bearing minerals), whereas atmospheric inputs play a minor role. As pointed out in our earlier study (Mueller et al., 2013), the low soil pH in the micro catchments of about 4 to 5 and the low pH of precipitation samples (Table 4.2) compared to the relatively high stream water pH of about 7 to 7.7 (Table 4.5) suggests that infiltrating precipitation is geochemically strongly

buffered by dissolution of evaporative minerals, i.e. karst formation, in the deeper bedrock (Mueller et al., 2013).

Mean DOC concentrations were in general relatively low in stream water base flow (0.6 to 1.8 mg L^{-1}, Table 4.5), which is comparable to headwater catchments in the Prealps of Central Switzerland (Hagedorn et al., 2000) and the Italian Alps (Balestrini et al., 2013). In Chämleten, the DOC concentrations were significantly higher than in the other catchments ($p < 0.0001$, $n = 51$). This can be attributed to an influence of 15 to 20 % (area) of riparian wetland and peat bog sites, which are hydrologically well connected to the stream in Chämleten (Schroeder, 2012). However, the low DOC concentrations in all four catchments suggest that stream water during base flow conditions was mainly fed by groundwater inputs with low DOC concentrations. This is in accordance with a study of Kawasaki et al. (2008) who found DOC concentrations of groundwater to be the main contributor to stream water during base flow conditions.

Mean NO_3^- concentrations of base flow ranged from 0.2 to 2.3 mg L^{-1} (Table 4.5), which is comparable to other headwater catchments with comparable land use in the Swiss Alps (Drever and Zobrist, 1992). NO_3^- concentrations were low in Laubgädem (0.2 ± 0.2 mg L^{-1}), suggesting mainly groundwater contributions to the stream water in this catchment. Despite the high percentage of shrub cover (Table 4.1) and a measured increase in NO_3^- concentrations of soil water due to green alder shrubs in Chämleten (Bühlmann, 2011), the influence on NO_3^- concentrations in stream water seems of minor importance during base flow. This might be due to the peat bog sites and riparian wetland soils in Chämleten (Schroeder, 2012), which can reduce nitrate export through denitrification (Cooper, 1990).

Table 4.5: Means and standard deviations of geochemical parameters of stream base flow samples (mg L^{-1}).

	Chämleten		Wallenboden		Bonegg		Laubgädem	
	mean	stddev	mean	stddev	mean	stddev	mean	stddev
Ca (n = 20) [a]	16.3	1.8	27.4	3.6	22.8	3.7	19.4	1.7
Mg (n = 20) [a]	0.9	0.1	1.6	0.1	2.2	0.3	0.8	0.1
Na (n = 20) [a]	0.9	0.1	1.0	0.1	1.3	0.1	0.7	0.1
K (n = 20) [a]	1.1	0.2	2.1	0.2	2.6	0.3	1.7	0.1
Si (n = 29) [a]	2.6	0.8	2.4	0.7	3.0	1.0	1.9	0.6
SO_4^{2-} (n = 27) [a]	10.8	1.5	14.7	1.4	19.7	3.2	7.3	0.7
pH (summer) [a]	7.35	0.18	7.65	0.25	7.55	0.14	7.35	0.32
pH (winter) [a]	7.30	0.26	7.54	0.26	7.56	0.25	7.68	0.13
DOC (n = 51)	1.8	0.5	1.0	0.3	0.9	0.3	0.6	0.3
NO_3^- (n = 47)	1.5	1.2	2.3	0.6	2.1	0.7	0.2	0.2

[a] Data from Mueller et al. (2013)

4.4.2 Geochemistry of storm runoff and snowmelt

4.4.2.1 Hydrograph separation and runoff generation

The investigated storm event rainfall intensity was approximately 45 mm within 12 hours with a peak intensity of 30 mm within 3 hours, which represents the highest intensity within the observation period. The $\delta^{18}O$ values of precipitation decreased from -2.3 to -7.7 ‰ during the event (Figure 4.2). The influence of precipitation on the stream water $\delta^{18}O$ values (Figure 4.2) and discharge (Figure 4.3) was detected within only 30 to 60 minutes after the beginning of rainfall. This indicates a fast reaction of runoff to event water input. Despite the fast reaction of $\delta^{18}O$ values in stream water, event water only contributed 15 to 29 % to total runoff in the first phase of the rainfall event until the significant increase of discharge at about 5:00 p.m. (Figure 4.2 and Figure 4.3). $\delta^{18}O$ values and fractions of event water then strongly increased up to maximum values of 61 to 72 % (Figure 4.2 and Table 4.6). The maximum of event water fractions (Table 4.6) were relatively high, compared to most other studies, where event water only contributed about 10 to 40 % to storm runoff (Genereux and Hooper, 1998; Turner and Barnes, 1998). Nevertheless, event water was also found to be the dominant contributor to storm runoff (75 %) on the catchment scale in a study by Turner et al. (1991). Leaney et al. (1993) found that subsurface storm flow was dominated by event water by > 90 % on the plot scale, which they attributed to preferential macropore flow. Bengtsson et al. (1991) and Buttle and Sami (1990) also associated high fractions of event water with preferential macropore flow, which can be enhanced during high intensity rainfall events (Jarvis, 2007). Irrigation experiments in the Urseren Valley showed that overland flow in grassland and green alder sites plays a negligible role (Lagger, 2012; Schmidt, 2012). Therefore, water infiltration rates are high and water can be quickly delivered via subsurface flow paths to the streams.

We found only small differences of event water fraction between the four micro catchments during the whole event. The event water fraction of total runoff during the rainfall event was on average about 41 ± 2 %, integrated over the whole rainfall event in all four catchments. The estimated mean uncertainty of the pre-event and event water fraction in stream runoff according to equation **(25)** was about ± 6 % (range of 4 to 13 % for all micro catchments), which might mask possible small differences between the catchments. The maximum event water fraction was 8 to 11 % higher in Laubgädem compared to Chämleten, Wallenboden and Bonegg, which however is within the uncertainty (Table 4.6). The stronger increase of event water fraction and $\delta^{18}O$ values in Chämleten at the beginning of rainfall (compared to Wallenboden, Bonegg and Laubgädem, Figure 4.2) might be due to the higher percentage of shrub cover, promoting preferential macropore flow in Chämleten. Macropore flow was visually observed in soil profiles in riparian wetland and peat bog sites in Chämleten, which also can enhance the flushing of event water. The more smoothened recession of event water fraction and $\delta^{18}O$ values in Chämleten highlights the good hydrological connectivity of the wetlands to the stream, which enhances outflow of event water.

Despite only small differences in event water fractions between the four catchments, the temporal pattern of $\delta^{18}O$ values and event water fractions suggest that an areal increase in shrub cover combined with riparian wetlands can enhance the flushing of event water through a catchment. This in turn will affect nutrient dynamics on the event scale.

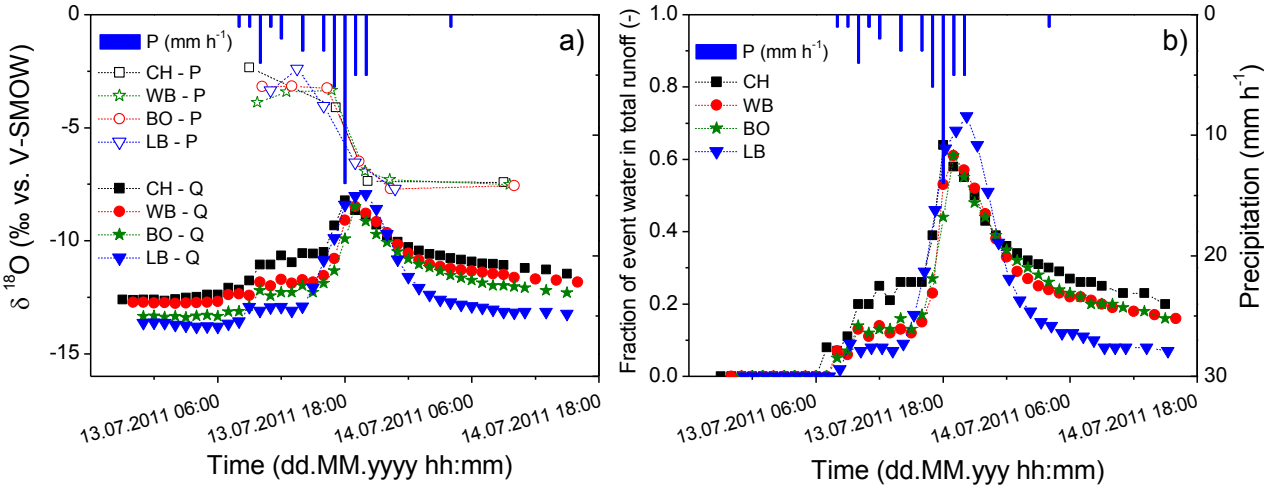

Figure 4.2: a) $\delta^{18}O$ values of stream water (Q) and precipitation (P). b) Fraction of event water, and precipitation volume during the event sampling on 13 July 2011. Precipitation data from the Bonegg micro catchment.

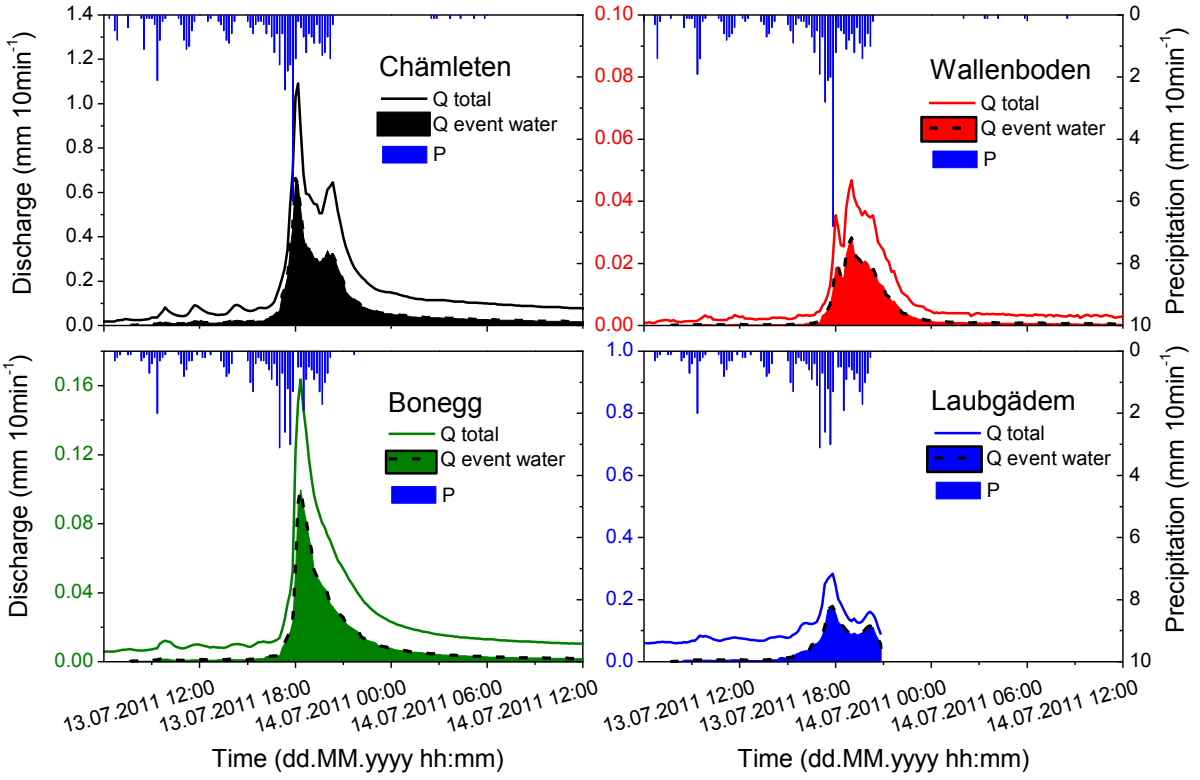

Figure 4.3: Fraction of event water of total discharge and precipitation volume during the event sampling on 13 July 2011. Please note that the discharge data of the falling limb in Laubgädem are excluded because of measurement artifacts during discharge recession.

Table 4.6: Maximum fraction of event water.

Catchment	Maximum fraction of event water (%)	Error according to equation **(25)** (%)
Chämleten	64	14
Wallenboden	61	12
Bonegg	61	11
Laubgädem	72	13

4.4.2.2 Sources of solutes during the rainfall event

The fast and marked decrease of Ca, Si and SO_4^{2-} concentrations during peak discharge to about 25 to 50 % of the base flow concentrations (Figure 4.4) points to a dilution effect by incoming event water with low solute concentrations (Table 4.3). Moreover, the decrease of pH during the rainfall event, which indicates arrival of event water in the stream, is consistent with the low soil pH and the low pH of rainfall (Table 4.2 and Table 4.3). Please note that Mg, K, Na concentrations are not shown, but display the same temporal pattern as Ca during the rainfall event. The pattern of a clear minimum concentration shortly after the

highest precipitation intensity and during peak discharge is similar for all four micro catchments.

DOC concentration in all four catchments increased between 500 to 1700 % of base flow concentrations (Figure 4.4) and peaked synchronically with discharge (for comparison with discharge timing, see Figure 4.3). Comparing micro catchments among each other reveals that from both, Laubgädem and Chämleten, relatively high DOC concentrations of up to 9 mg L^{-1} were leached. Dosskey and Bertsch (1994) reported that riparian wetlands were the dominant source of DOC in runoff in their study, which is due to the hydrological connectivity of wetlands to streams (Roa-Garcia and Weiler, 2010). Riparian wetland soils contributed 68 % of organic carbon to the stream, despite their small areal fraction of only 6 % of the catchment area in the study of Dosskey and Bertsch (1994). In our study, the soil organic carbon (SOC) content in green alder (3.3 ± 1.4 wt %) and grassland sites (4.0 ± 2.4 wt %) was significantly lower compared to peat bog sites and riparian wetland soils (up to 34 wt %, Schroeder (2012)). We therefore attribute the increase in stream DOC to the 10 to 20 % (area) of peat bog sites and riparian wetland soils in Chämleten and Laubgädem. The earlier increase of DOC and the more dampened recession in Chämleten compared to Wallenboden, Bonegg and Laubgädem, highlights the good hydrological connectivity of the riparian wetland soils in Chämleten (Figure 4.4).

NO_3^- concentrations in Chämleten peaked about 2 hours after the discharge peak (Figure 4.4). Concentrations still were relatively low, but the increase from 1 to 3 mg L^{-1} corresponds to an increase by about 200 % within 2 hours in Chämleten. We suggest that NO_3^- is mobilized from the soil layers where it was accumulated due to the activity of the nitrogen-fixing bacterium Frankia alni associated with the high fraction of green alder in Chämleten (Bühlmann, 2011). In Wallenboden, Bonegg and Laubgädem NO_3^- concentrations decreased during rainfall (Figure 4.4). At the end of the rainfall event, only a flat peak was detected about 6 to 12 hours after the respective discharge peak in Wallenboden, Bonegg and Laubgädem. This can be explained by the substantially lower green alder cover in Wallenboden, Bonegg and Laubgädem compared to Chämleten (Table 4.1).

Bishop et al. (2004) used the transmissivity feedback mechanism to explain increasing DOC concentrations and decreasing Ca concentrations in stream water, which can be coupled to a mobilization of pre-event water by a rising groundwater table during storm events. In several studies (e.g. Creed et al., 1996; Inamdar et al., 2004; Rusjan et al., 2008), the peak of NO_3^- concentration was also associated with rising water tables, flushing pre-event water with elevated NO_3^- concentrations to the streams. This flushing of pre-event water is not completely consistent with our hydrograph separation using $\delta^{18}O$ data, which clearly points to a high proportion of up to 62 to 72 % of event water in storm runoff. The associated strong increase of DOC concentrations and the decrease of Ca, Si and SO_4^{2-} concentrations indicate that the event water flushed through the shallow soil layers, e.g. via preferential flow paths (Jarvis, 2007; Leaney et al., 1993; Nimmo, 2012; van der Heijden et

al., 2013). DOC, which can accumulate during the dry period before the event (Kalbitz et al., 2000), can then be mobilized during the rainfall event (Fiebig et al., 1990; Worrall et al., 2008). In a study in small peat land catchments Worrall et al. (2008) concluded that DOC diffuses from the internal sites of peat aggregates to their external sites during dry periods, from where it can be flushed by mobile (event) water during storm events. We conclude that DOC export is mainly controlled by periodic flushing events of peat bog sites and riparian wetland soils. Furthermore, we suggest that NO_3^- is also mobilized by the event water, but the lag time between the NO_3^- and DOC peaks suggests different source areas of these two solutes (Mitchell et al., 2006). While DOC is flushed from the riparian wetland soils, NO_3^- is leached from the areas further away from the stream, where green alder shrubs increases the NO_3^- concentrations in soil water.

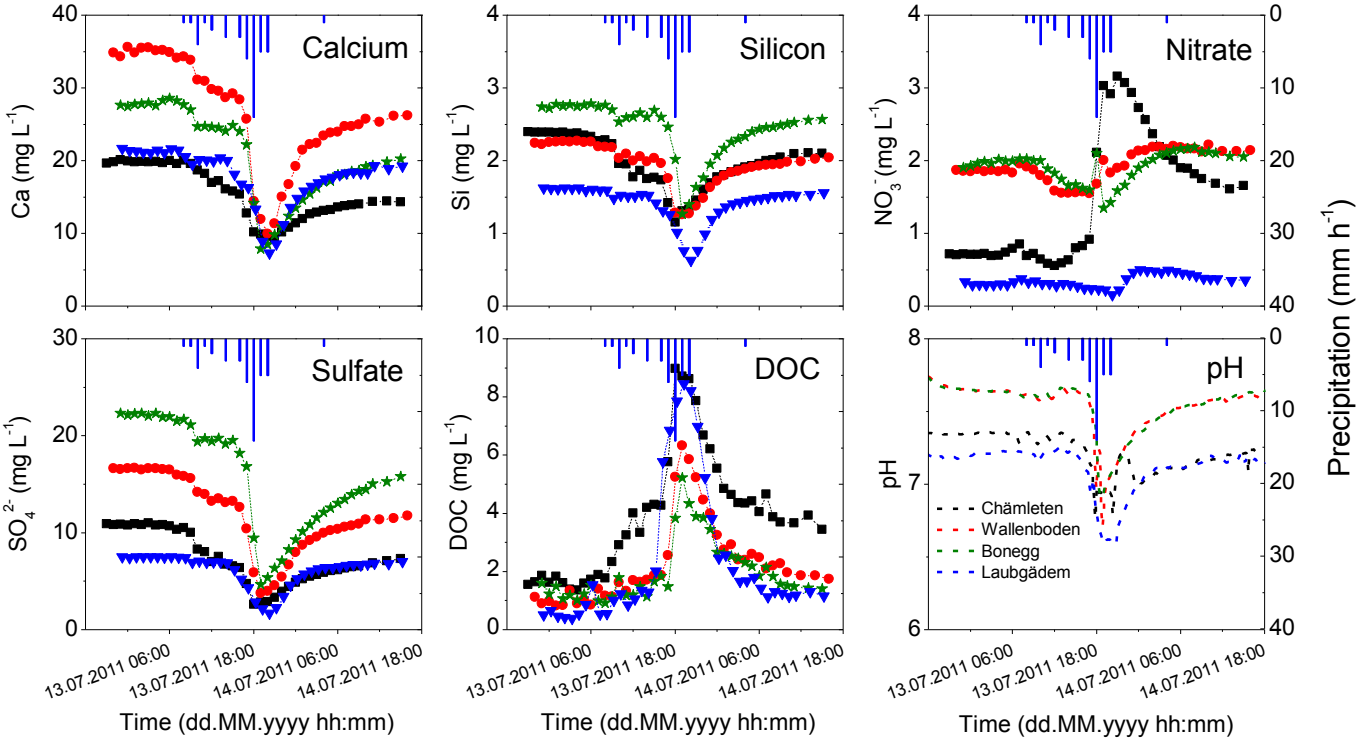

Figure 4.4: Stream water geochemistry during the event sampling on 13 July 2011. Chämleten (■), Wallenboden (●), Bonegg (★), Laubgädem (▼). Precipitation data from the station Bonegg is shown; stations Chämleten, Wallenboden and Laubgädem are comparable in precipitation amount and timing at the hourly scale.

4.4.2.3 Concentration vs. discharge relations

Concentration-discharge relations have been widely applied to gain information about runoff generation during episodic hydrological events and therefore give additional information about sources and timing of solute flushing (e.g. Evans and Davies, 1998).

The curvilinear concentration-discharge relations (Figure 4.5) of Ca, Si, SO_4^{2-} and pH were fitted with exponential decay models. An exponential growth model was used for the

curvilinear concentration-discharge relations of DOC. The coefficients of determination (r^2) were higher than 0.89 for all fitted concentration-discharge relations, except for pH in Chämleten and NO_3^-, which will be discussed below. The curves for K, Mg and Na from this study are not shown, but they have the same exponential decay pattern as Ca or Si. According to Evans and Davies (1998), a curvilinear pattern of the concentration-discharge relation can be interpreted using a two component mixing model, where two components, e.g. event water and soil water, have equal solute concentrations. The authors modeled concentration-discharge relations of stream water for a single-peaked rain event with different solute concentrations in surface event water (representing precipitation), soil water and groundwater. Our observed curvilinear concentration-discharge relations therefore underpin that the application of a two component hydrograph separation was justified. The solutes, for which the exponential decay function was applied to describe the curvilinear concentration-discharge relation (Figure 4.5), tend to have higher concentrations in the pre-event water fraction than in the event water fraction (rainfall). In the case of DOC, we can mathematically consider rainfall and soil water as one component, which has a higher DOC concentration than the groundwater, in order to explain the exponential growth function (cf. Figure 4a in Evans and Davies, 1998). The increase of DOC concentrations with increasing discharge up to a catchment specific plateau (Figure 4.5) indicates that DOC release from the catchments can be controlled by physico-chemical processes as shown by Worrall et al. (2008). The diffusion of DOC to the external sites of peat aggregates controlled the supply of leachable DOC on the event timescale up to two days (Worrall et al., 2008). The rate of production of DOC, which is mainly biologically controlled (Kalbitz et al., 2000), becomes relevant primarily on longer timescales between different events Worrall et al. (2008).

Variations of NO_3^- concentrations were clearly detectable, but with only small changes in Wallenboden, Bonegg and especially Laubgädem (Figure 4.5). Therefore NO_3^- concentrations do not correlate with discharge (Figure 4.5) in these catchments. Variations with discharge were higher in Chämleten, creating a hysteresis loop which could not be fitted with an exponential decay or growth model. Similar to DOC, a three component mixing model with two components having the same NO_3^- concentrations, can be assumed to create the observed hysteresis loop (c.f. Figure 4b in Evans and Davies, 1998). In the case of NO_3^-, rainfall and base flow water can be considered as one component. The considered NO_3^- concentrations were not equal, but both low in rainfall (1.7 mg L^{-1}) and base flow (0.7 mg L^{-1}) on 13 July 2011. NO_3^- concentrations in soil water in green alder stands range from 8.4 to 28.8 mg L^{-1} (Bühlmann, 2011), which is substantially higher than in rainfall and base flow. The exceptional concentration-discharge pattern of NO_3^- in Chämleten, compared to the other catchments, underpins the importance of different source areas of NO_3^- compared to the other solutes, e.g. DOC (Mitchell et al., 2006).

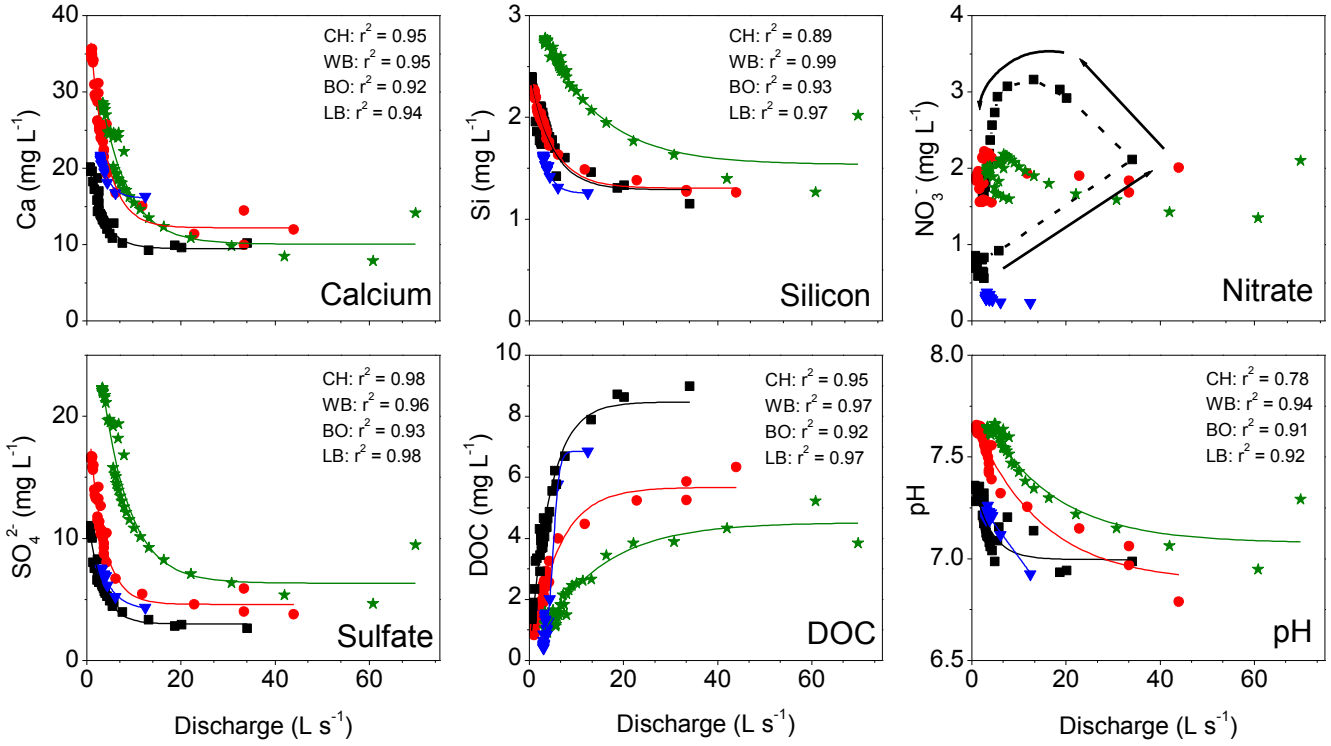

Figure 4.5: Discharge-concentration relations during the event sampling on 13 July 2011. Chämleten (CH) (■), Wallenboden (WB) (●), Bonegg (BO) (★), Laubgädem (LB) (▼). Exponential decay fit: $y = y_0 + A \cdot e^{-x/t}$ for Ca, Si, SO_4^{2-} and pH. Exponential growth fit (Box-Lucas model) for DOC with $y = a \cdot (1 - e^{-bx})$ and a Boltzmann growth function for DOC of Laubgädem (LB) catchment. Arrows in die NO_3^- plot indicate temporal dynamics of NO_3^- concentrations. Please note that the concentration-discharge relations for Laubgädem only include data from the rising limb because of measurement artifacts for discharge during the falling limb.

4.4.2.4 Sources of solutes during snowmelt

Solute concentrations in bulk snow samples were generally low (Table 4.7), which is comparable to other studies on snow chemistry of the Alps (Parriaux et al., 1990). Snow height data from the weather station in Andermatt (MeteoSwiss, 2013) are given as a proxy for the timing of snowmelt (Figure 4.6). Maximum snow height was about 2100 mm at the end of March 2012 (MeteoSwiss, 2013), which corresponds to a snow water equivalent (SWE) of about 840 mm. Snow cover lasted from 5 December 2011 to 4 May 2012 in the valley bottom (station in Andermatt). The snowmelt period can be divided in three phases. A first intensive decrease in snow height took place from 23 March to 6 April, which we think is partially also associated with wetting and compaction of the snowpack and an increase in snow density (Jonas et al., 2009). The melt rate was at most 365 mm SWE in 15 days in the first period. This was followed by a "stagnant" period with low temperatures and precipitation falling as snow from 7 to 24 April, which slowed down the decrease in snow height. The melt rate was only about 150 mm SWE during these 17 days. The third phase

took place from 25 April to 3 May and had a high melt rate of approximately 325 mm SWE in 9 days.

Please note that the intensive stream water sampling could only be performed in Wallenboden and Bonegg. Chämleten and Laubgädem were sampled on a monthly basis at that time. Also, it was not always possible to sample at the same time of day in Wallenboden and Bonegg. We might therefore have missed the full range of solute concentrations during the snowmelt period.

The temporal pattern of snowmelt is reflected in the evolution of the geochemical parameters during the melt period (Figure 4.6). SO_4^{2-} concentrations and $\delta^{18}O$ values decreased with the onset of snowmelt. The strongest decrease of SO_4^{2-} concentrations and $\delta^{18}O$ values was observed during the third phase of the snowmelt period, when also Ca concentrations and electrical conductivity (EC) started to decrease. Ca and SO_4^{2-} concentrations decreased by about 20 to 50 % of the winter base flow concentrations in the last phase of the snowmelt. The data indicate a strong and quick response of stream water geochemistry to the input of meltwater with low solute concentrations and $\delta^{18}O$ values.

With the onset of snowmelt, DOC concentrations increased by 90 to 100 % compared to the winter base flow in Wallenboden and Bonegg and peaked in the last phase of the snowmelt period (Figure 4.6). In Chämleten and Laubgädem, the DOC concentrations also strongly increased, but due to the lower sampling frequency, we might have missed the concentration peak around peak snowmelt on 28 April 2012. The increase of DOC concentrations indicates flushing of leachable DOC from the shallow soil layers (Hornberger et al., 1994; Kendall et al., 1999). In comparison to the rainfall event during the growing season (Figure 4.4), DOC concentrations were substantially lower during the snowmelt (Figure 4.6). This suggests that the pool of potentially leachable DOC was lower in spring than during the growing season, due to a reduced biological activity during the dormant winter season (Kalbitz et al., 2000). DOC concentrations in March, April and May 2012 in Chämleten were higher than in Wallenboden, Bonegg and Laubgädem, taking only the sampling days into account, when all four catchments were sampled. Since Chämleten has abundant riparian wetland soils, we suggest that these wetland soils contribute to the export of DOC from the catchments.

NO_3^- concentrations increased by about 100 % in Wallenboden and Bonegg during the first phase of the melt period. In Wallenboden, the NO_3^- concentrations were less variable with only minor peaks during the second and third phase of the snowmelt period compared to Bonegg. The pattern of NO_3^- concentrations suggest that accumulated NO_3^- from the shallow soil layer was flushed with the onset of the snowmelt, since NO_3^- concentrations in stream base flow and snow were relatively low (Table 4.5 and Table 4.7). In comparison to the rainfall event during the growing season (Figure 4.4), NO_3^- concentrations also increased in Wallenboden and Bonegg during the snowmelt (Figure 4.6). This suggests that the amount of potentially leachable NO_3^- was higher during the spring snowmelt period than

during the growing season. This could be explained by lower biological activity with less uptake of NO_3^- and denitrification during the dormant winter season, which can lead to accumulation of leachable NO_3^- (Burns et al., 1998). At the end of the snowmelt period, NO_3^- concentrations in Chämleten were lower than in Wallenboden and Bonegg, despite the higher green alder shrub cover in Chämleten. This can be explained by denitrification processes in the peat bog sites and riparian wetland soils in Chämleten (Cooper, 1990). In Laubgädem NO_3^- concentrations were nearly constant throughout the period from January to May 2012, which indicates very low amounts of accumulated and leachable NO_3^- in this catchment. This can be due to the low percentage of green alder shrubs combined with NO_3^- removal in the riparian wetland soils.

A hydrograph separation according to equation **(23)**, using $\delta^{18}O$ values of bulk snow samples and stream water, suggests that snow contributed up to about 20 % during the first melt period and about 50 to 60 % during the peak intensity of the third phase of the snowmelt period (28 April 2012) to total runoff in Wallenboden and Bonegg. Therefore, flushing of pre-event water, i.e. shallow groundwater, via a rising water table most likely influences solute concentrations during the first melt period (Hornberger et al., 1994; Kendall et al., 1999; McGlynn et al., 1999; Pacific et al., 2010). This is consistent with the first increase of DOC and Ca concentrations, whereas as SO_4^{2-} concentrations suggest dilution effect by event water (meltwater) also in the first melt period. However, low SO_4^{2-} concentrations in flushed pre-event water, having less contact with sulfate bearing minerals, could also explain the decrease of SO_4^{2-} concentrations in the first melt period. In the third phase of the snowmelt period, event water flushed the shallow soil layers and became the main factor controlling stream geochemistry. The increase of DOC concentrations combined with the increased fraction of event water again points to activation of preferential flow paths in riparian zones. This is comparable to the rainfall event during the growing season.

Table 4.7: Mean geochemistry of bulk snow samples across the Urseren Valley in March 2012 (n = 24). Solute concentrations in mg L^{-1}; $\delta^{18}O$ in ‰; electrical conductivity (EC) in µS cm^{-1}.

	Ca	K	Mg	Na	NO_3^-	SO_4^{2-}	DOC	$\delta^{18}O$	pH	EC
mean	0.8	0.8	0.1	0.8	0.3	0.1	1.3	-18.3	4.6	6.9
standard deviation	0.4	0.7	0.1	0.7	0.1	0.0	1.7	0.7	0.3	1.8

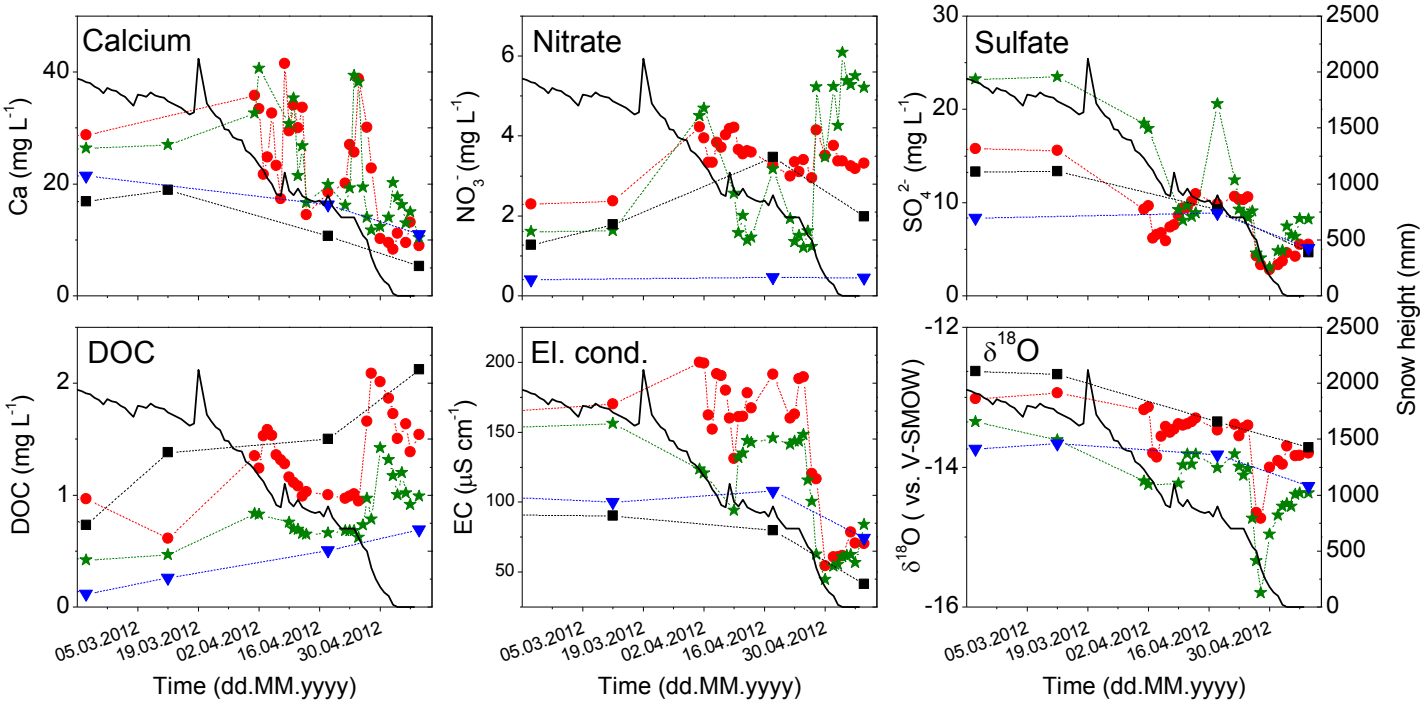

Figure 4.6: Geochemistry of stream water during snowmelt in 2012 in Chämleten (■), Wallenboden (●), Bonegg (★), Laubgädem (▼). EC and $\delta^{18}O$ data from Bucher (2013). Snow height data (–) from the MeteoSwiss station in Andermatt (MeteoSwiss, 2013); rightmost axes for snow height apply to all plots.

4.5 Conclusions

We investigated four alpine headwater catchments to identify the role of wetland zones and shrub encroachment on stream water geochemistry during a rainfall event in the growing season and a spring snowmelt period. Base flow geochemistry before the rainfall event and snowmelt was mainly controlled by geochemical composition of the underlying bedrock (Figure 4.7), whereas the shallow soil cover strongly influenced runoff generation processes and temporal dynamics of storm and snowmelt geochemistry (Figure 4.7). The increase of DOC during the investigated rainfall event, coupled with high fractions of event water during the peak discharge suggest that preferential flow paths can be activated on the catchment scale, at least in small headwater catchments. As a consequence, event water can flush riparian wetland soils and quickly transport elevated amounts of DOC and mostly low concentrations of Ca, Si, and SO_4^{2-} to the streams (Figure 4.7). This was also observed during the snowmelt period. Green alder shrubs (*Alnus viridis subsp. viridis*), which are encroaching on abandoned pasture sites, likely lead to a slight intermittent increase of NO_3^- export due to flushing of oxic soils during rainfall and snowmelt events. However, denitrification and uptake processes keep NO_3^- concentrations low, especially during the growing season.

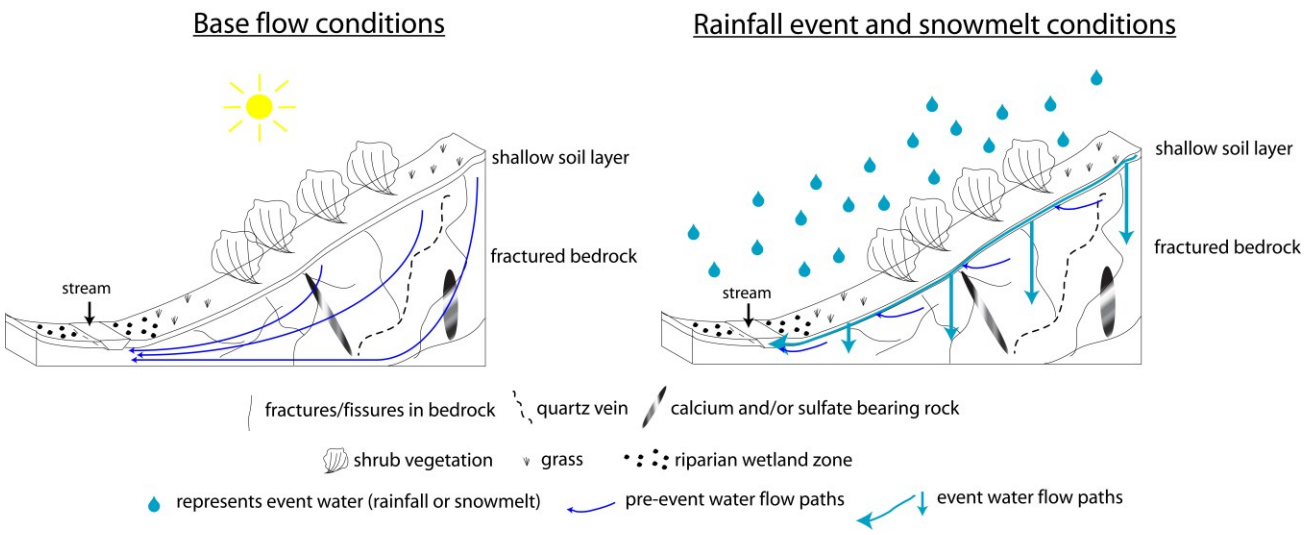

Figure 4.7: Conceptual model of water flow paths (see text for detailed description).

Acknowledgements

We would like to thank Mark Rollog and Marianne Caroni for laboratory analyses and Claude Schneider for technical support. We also thank Thijs van den Bergh (Group of Botany, Section Plant Ecology, University of Basel) and Mathias Fercher (Institute of Geography, Group of Hydrology, University of Bern) for providing data of catchment sizes and land cover, and Rolf Weingartner, Abdallah Alaoui, Susanne Lagger and Philipp Schmidt (Institute of Geography, Group of Hydrology, University of Bern) for providing discharge data. Robin Nager and Yannick Bucher helped during the snowmelt sampling campaigns.

This work was part of the project "The ecological and socio-economic consequences of land transformation in alpine regions: an interdisciplinary assessment and VALuation of current changes in the Ursern Valley, key region in the Swiss central Alps", funded by the Swiss National Science Foundation, grant no. CR30I3_124809.

5 Final conclusions and outlook

The main aim of this thesis was to investigate the influence of soil cover (i.e. wetland soils) and vegetation cover changes (i.e. encroachment of green alder shrubs on abandoned pastures and meadows) on the hydrological and geochemical functioning of contrasting alpine micro catchments. Geochemical tracers and modeling tools were used to track hydrological flow paths on the hillslope scale and micro catchment scale.

The physical soil data and stable isotope signals of soil water data pointed to well drained soils and vertical flow processes, which allows quick infiltration and percolation of water within the soil profiles, even at steep hillslopes. This can prevent overland flow during summer rain events on the hillslope scale and facilitate percolation of water into deeper zones, i.e. the bedrock, which is highly fractured in our region. The percolation, storage and subsequent outflow of this bedrock water was supported by stream water stable isotope signals during base flow conditions and the calculated relatively long mean water transit times (MTT). These data suggested that the surficial catchment characteristics, i.e. shrub vegetation cover, topography or catchment size did not influence the MTT of base flow. Instead, the hydrogeological and geochemical patterns of the bedrock and snow dynamics influenced storage, mixing and release of precipitation in a stronger way than vegetation cover did. The effect of vegetation on MTT might be masked at the catchment scale in mountainous headwater catchments with relatively shallow soil layers.

The short term hydrological and geochemical patterns of stream were clearly influenced by land/soil cover (i.e. wetland zones) and by vegetation cover (i.e. green alder shrub encroachment) during a rainfall event in the growing season and a snowmelt period. The increase of dissolved organic carbon (DOC) during the investigated rainfall event and snowmelt period, coupled with high fractions of event water during the peak discharge of the summer storm, suggested activation of preferential flow paths at the catchment scale. Encroaching green alder shrubs (*Alnus viridis subsp. viridis*) likely led to a slight intermittent increase of nitrate (NO_3^-) export due to flushing of oxic soils during the storm and snowmelt event. But denitrification and uptake processes most likely kept stream water NO_3^- concentrations low, especially during the growing season.

It can be concluded that, on the investigated scales, the bedrock geology and geochemistry plays a major role for the hydrology and geochemistry of base flow stream water. This can be explained by the much greater extend of the highly fractured bedrock compared to the shallow soil layers. The fractures in the bedrock allow recharge to and percolation of water within the bedrock, controlling therefore water transit times and the geochemical evolution of water. On the other hand, the land cover, i.e. the soil and vegetation cover, plays a major role for the hydrological and geochemical processes during rainfall or snowmelt event flow conditions. The shallow soil layers represent a very reactive "reservoir" for biogeochemical processes. They are mainly hydrologically connected to the

streams during rainfall and snowmelt events, which was shown by the geochemical data combined with discharge data. The rainfall and the snowmelt event resulted in strong temporal dynamics of stream water geochemistry and an increased export of DOC and NO_3^- during these events. Since duration of snow cover will be shortened and rainfall events during the growing season will become more frequent and intense (IPCC, 2007), it can be hypothesized that the importance of vegetation and soil characteristics for the export of nutrients might still increase in the future.

The results of the study also raised several questions, which could not be addressed during the project:

Additional measurements of soil water stable isotopes at different dates at hillslopes across the valley (including hillslopes with green alder shrubs) would for example be useful to track the water flow at a broader spatial and temporal scale. In a further study, piezometers could be installed at the steep hillslopes in order to directly observe possible (saturated) water flow at the hillslope scale.

With regard to the stream geochemistry, sampling of additional rainfall events with different pre-storm conditions would be desirable to survey the flushing of nutrients at different meteorological conditions. Additionally, groundwater/drinking water wells and the main stream at the valley bottom could be monitored in order to integrate the observation from the micro catchments into the larger meso scale catchment of the Urseren Valley. Monitoring of geochemical parameters (i.e. NO_3^- and its stable oxygen and nitrogen isotopes) in springs and drinking water wells across the valley might help to clarify whether or not the green alder encroachment is able to affect NO_3^- concentrations of drinking water.

Acknowledgements

I am deeply grateful to all the support throughout the years by Prof. Christine Alewell. Thank you for all the scientific inputs and discussions, and your personal encouragement related to all the challenges, which came up during the last four years within this project!

Thanks to all my colleagues from the Group of Environmental Geosciences and the Group of Biogeochemistry in the Bernoullianum, with whom I shared a great time in the last years!

Mark Rollog and Marianne Caroni (Group of Environmental Geosciences, University of Basel) did a lot of laboratory analyses and therefore produced a lot of data for me to work on. Thank you for all your support and your "down-to-earth way" to solve technical problems and lab logistics!

Apart from providing a lot of data of the Urseren Valley and information on how to use GIS-Software, I especially thank Dr. Katrin Meusburger (Group of Environmental Geosciences, University of Basel) for all non-science-related support during the last years.

I would also like to thank the whole *ValUrsern* project group for providing a lot of information on the valley, data and also infrastructure on the Furka Pass (Section of Plant Ecology, University of Basel). I especially like to thank the following persons:

- Thijs van den Bergh (Group of Botany, Section Plant Ecology, University of Basel) and Mathias Fercher (Institute of Geography, Group of Hydrology, University of Bern) provided data of catchment sizes and land cover.

- Prof. Rolf Weingartner, Dr. Abdallah Alaoui, Susanne Lagger, Philipp Schmidt, Matthias Flury and Matthias Fercher (Institute of Geography, Group of Hydrology, University of Bern) are kindly acknowledged for providing discharge data and help in interpreting hydrological data. Susanne Lagger and Philipp Schmidt are acknowledged for providing data from their irrigation experiments. Finally I thank Silvia Hunkeler for measuring saturated hydrologic conductivity of soil samples.

- Furthermore, I would like to thank the following individuals: Prof. Christian Körner, Dr. Erika Hiltbrunner, Tobias Bühlmann, Tobias Zehnder and Dr. Nicole Inauen (Group of Botany, Section Plant Ecology, University of Basel), Prof. Frank Krysiak and Dr. Markus Ludwig (Environmental Economics, University of Basel), Prof. Martin Schaffner and Rahel Wunderli (General Modern History, University of Basel).

Claude Schneider is kindly acknowledged for technical support.

Yannick Bucher, Robin Nager, Jonas Gessler and Gyula Csato helped during the snow sampling campaigns. Thanks to Jonas and Gyula, the two mountain guides, who always found the safest way on the steep snow covered slopes in the Urseren Valley. It was a lot of fun skiing down!

I also would like to thank Björn Probst, Gregor Juretzko and Lothar Schroeder for their assistance during soil sampling campaigns in the field. I can still hear us hammering the soil corer into the ground…

I gratefully like to acknowledge Barbara Herbstritt and Benjamin Gralher for their great support during stable isotopes measurements at the laboratory of the Chair of Hydrology, University of Freiburg, Germany.

Thanks to all farmers in the Urseren Valley who provided access to their field sites – an essential prerequisite for the realization of my thesis.

All co-authors are kindly acknowledged for their help during modeling of data and manuscript preparation: Dr. Christine Stumpp, Prof. Christoph Külls, Prof. Markus Weiler, Hannes Leistert, Dr. Abdallah Alaoui, Dr. Katrin Meusburger, and Prof. Rolf Weingartner.

Prof. Jan Seibert is kindly acknowledged for reviewing my thesis and acting as examiner during my PhD defense.

Thanks to my family for all their support throughout the ups and downs during my PhD thesis! Ich bin meinen Eltern Heidulf und Doris und meinen Geschwistern Martina, Judith, Barbara und Bernhard (und ihren jeweiligen Familien) zutiefst dankbar für ihre Unterstützung in all den Jahren!

Kathi, vielen lieben Dank für deine Geduld und deine Unterstützung in den vergangenen Jahren, in denen wir gemeinsam gewachsen sind!

References

Adomako, D., Maloszewski, P., Stumpp, C., Osae, S., and Akiti, T. T.: *Estimating groundwater recharge from water isotope (delta H-2, delta O-18) depth profiles in the Densu River basin, Ghana*, Hydrological Sciences Journal - Journal Des Sciences Hydrologiques, 55, 1405-1416, 10.1080/02626667.2010.527847, 2010.

Alaoui, A., and Helbling, A.: *Evaluation of soil compaction using hydrodynamic water content variation: Comparison between compacted and non-compacted soil*, Geoderma, 134, 97-108, 10.1016/j.geoderma.2005.08.016, 2006.

Alaoui, A., Willimann, E., Jasper, K., Felder, G., Herger, F., Magnusson, J., and Weingartner, R.: *Modelling the effects of land use and climate changes on hydrology in the Ursern Valley, Switzerland*, Hydrological Processes, 10.1002/hyp.9895, 2013.

Alexander, R. B., Boyer, E. W., Smith, R. A., Schwarz, G. E., and Moore, R. B.: *The role of headwater streams in downstream water quality*, Journal of the American Water Resources Association, 43, 41-59, 10.1111/j.1752-1688.2007.00005.x, 2007.

Ambach, W., Dansgaard.W, Eisner, H., and Moller, J.: *The altitude effect on isotopic composition of precipitation and glacier ice in the Alps*, Tellus, 20, 595-600, 1968.

Ambuehl, E.: *Petrographie und Geologie des zentralen Gotthardmassivs südlich Andermatt*, PhD Thesis, A.G. Gebr. Leemann, Zürich, 1929.

Amin, I. E., and Campana, M. E.: *A general lumped parameter model for the interpretation of tracer data and transit time calculation in hydrologic systems*, Journal of Hydrology, 179, 1-21, 10.1016/0022-1694(95)02880-3, 1996.

Andersson, J. O., and Nyberg, L.: *Using official map data on topography, wetlands and vegetation cover for prediction of stream water chemistry in boreal headwater catchments*, Hydrology and Earth System Sciences, 13, 537-549, 2009.

Angehrn, P.: *Hydrogeologische Grundlagen, Urserental*, Kanton Uri, Amt für Umweltschutz, Abteilung Gewässerschutz, 1996.

Asano, Y., Uchida, T., and Ohte, N.: *Residence times and flow paths of water in steep unchannelled catchments, Tanakami, Japan*, Journal of Hydrology, 261, 173-192, 10.1016/s0022-1694(02)00005-7, 2002.

Asano, Y., and Uchida, T.: *Flow path depth is the main controller of mean base flow transit times in a mountainous catchment*, Water Resources Research, 48, 10.1029/2011wr010906, 2012.

Asselman, N. E. M., Middelkoop, H., and van Dijk, P. M.: *The impact of changes in climate and land use on soil erosion, transport and deposition of suspended sediment in the River Rhine*, Hydrological Processes, 17, 3225-3244, 10.1002/hyp.1384, 2003.

Bachmair, S., Weiler, M., and Nützmann, G.: *Controls of land use and soil structure on water movement: Lessons for pollutant transfer through the unsaturated zone*, Journal of Hydrology, 369, 241-252, 10.1016/j.jhydrol.2009.02.031, 2009.

Bachmair, S., and Weiler, M.: *New Dimensions of Hillslope Hydrology*, in: Forest Hydrology and Biogeochemistry: Synthesis of Past Research and Future Directions, edited by: Levia, D. F., Carlyle-Moses, D., and Tanaka, T., Ecological Studies, Springer Netherlands, 455-481, 2011.

Bakalowicz, M., Blavoux, B., and Mangin, A.: *Use of natural isotopic tracers in studying functioning of a karstic system - oxygen-18 contents of 3 systems in Pyrenes, France*, Journal of Hydrology, 23, 141-158, 10.1016/0022-1694(74)90028-6, 1974.

Balestrini, R., Arese, C., Freppaz, M., and Buffagni, A.: *Catchment features controlling nitrogen dynamics in running waters above the tree line (central Italian Alps)*, Hydrology and Earth System Sciences, 17, 989-1001, 10.5194/hess-17-989-2013, 2013.

Banks, E. W., Simmons, C. T., Love, A. J., Cranswick, R., Werner, A. D., Bestland, E. A., Wood, M., and Wilson, T.: *Fractured bedrock and saprolite hydrogeologic controls on groundwater/surface-water interaction: a conceptual model (Australia)*, Hydrogeology Journal, 17, 1969-1989, 10.1007/s10040-009-0490-7, 2009.

Bariac, T., Millet, A., Ladouche, B., Mathieu, R., Grimaldi, C., Grimaldi, M., Hubert, P., Molicova, H., Bruckler, L., Bertuzzi, P., Boulegue, J., Brunet, Y., Tournebize, R., and Granier, A.: *Stream hydrograph separation on two small Guianese catchments*, in: Tracer Technologies for Hydrological Systems, edited by: Leibundgut, C., Iahs Publications, 229, 193-209, 1995.

Barnes, C. J., and Allison, G. B.: *Tracing of water-movement in the unsaturated zone using stable isotopes of hydrogen and oxygen*, Journal of Hydrology, 100, 143-176, 10.1016/0022-1694(88)90184-9, 1988.

Barnes, C. J., and Turner, J. V.: *Isotopic exchange in soil water*, in: Isotope Tracers in Catchment Hydrology, edited by: Kendall, C., and McDonnell, J. J., Elsevier Science, Amsterdam, 137–163, 1998.

Baumgartner, A., Reichel, E., and Weber, G.: *Der Wasserhaushalt der Alpen: Niederschlag, Verdunstung, Abfluß u. Gletscherspende im Gesamtgebiet d. Alpen im Jahresdurchschnitt für d. Normalperiode 1931-1960; mit 68 Tab*, Bd. 1, R. Oldenbourg Verlag, München, 1983.

Benecke, U.: *Nitrogen fixation by alnus-viridis (Chaix) DC*, Plant and Soil, 33, 30-&, 10.1007/bf01378194, 1970.

Bengtsson, L., Lepisto, A., Saxena, R. K., and Seuna, P.: *Mixing of meltwater and groundwater in a forested basin*, Aqua Fennica, 21, 3-12, 1991.

Bethke, C. M.: *Geochemical and Biogeochemical Reaction Modeling*, Cambridge University Press, United Kingdom, 543 pp., 2008.

Beven, K., and Germann, P.: *Macropores and water-flow in soils*, Water Resources Research, 18, 1311-1325, 10.1029/WR018i005p01311, 1982.

Beven, K., and Germann, P.: *Macropores and water flow in soils revisited*, Water Resources Research, 49, 3071-3092, 10.1002/wrcr.20156, 2013.

Beven, K. J., and Kirkby, M. J.: *A physically based, variable contributing area model of basin hydrology / Un modèle à base physique de zone d'appel variable de l'hydrologie du bassin versant*, Hydrological Sciences Bulletin, 24, 43-69, 10.1080/02626667909491834, 1979.

Beven, K. J.: *Hillslope runoff processes and flood frequency characteristics*, in: Hillslope processes, edited by: Abrahams, A. D., Allen & Unwin, Boston, 187-202, 1986.

BFS: *Arealstatistik Schweiz: Zahlen – Fakten – Analysen*, edited by: Bundesamt für Statistik (BFS), Neuchâtel, Switzerland, 104 pp., 2005.

Billett, M. F., and Cresser, M. S.: *Predicting stream-water quality using catchment and soil chemical characteristics*, Environmental Pollution, 77, 263-268, 10.1016/0269-7491(92)90085-o, 1992.

Bishop, K., Seibert, J., Koher, S., and Laudon, H.: *Resolving the Double Paradox of rapidly mobilized old water with highly variable responses in runoff chemistry*, Hydrological Processes, 18, 185-189, 10.1002/hyp.5209, 2004.

Bishop, K., Buffam, I., Erlandsson, M., Fölster, J., Laudon, H., Seibert, J., and Temnerud, J.: *Aqua Incognita: the unknown headwaters*, Hydrological Processes, 22, 1239-1242, 10.1002/hyp.7049, 2008.

Bogner, C., Engelhardt, S., Zeilinger, J., and Huwe, B.: *Visualization and analysis of flow patterns and water flow simulations in disturbed and undisturbed tropical soils*, in: Gradients in a Tropical Mountain Ecosystem of Ecuador, edited by: Beck, E., Bendix, J., Kottke, I., Makeschin, F., and Mosandl, R., Ecological Studies: Analysis and Synthesis, 387-396, 2008.

Botter, G., Bertuzzo, E., and Rinaldo, A.: *Catchment residence and travel time distributions: The master equation*, Geophysical Research Letters, 38, 10.1029/2011gl047666, 2011.

Brooks, J. R., Barnard, H. R., Coulombe, R., and McDonnell, J. J.: *Ecohydrologic separation of water between trees and streams in a Mediterranean climate*, Nature Geoscience, 3, 100-104, 10.1038/ngeo722, 2010.

Bucher, Y.: *Isotopendynamik des Abflusses in alpinen Einzugsgebieten im Urserntal während der Ablationsperiode*, Bachelor Thesis, Environmental Geosciences, University of Basel, Basel, Switzerland, in preparation, 2013.

Bühlmann, T.: *Alnus viridis increases the nitrogen concentration in the soil solution and leachate in the Swiss Alps*, Masters Thesis, Plant Ecology, University of Basel, Basel, Switzerland, 2011.

Bundt, M., Jaggi, M., Blaser, P., Siegwolf, R., and Hagedorn, F.: *Carbon and nitrogen dynamics in preferential flow paths and matrix of a forest soil*, Soil Science Society of America Journal, 65, 1529-1538, 2001.

Burns, D. A., and McDonnell, J. J.: *Effects of a beaver pond on runoff processes: comparison of two headwater catchments*, Journal of Hydrology, 205, 248-264, 10.1016/s0022-1694(98)00081-x, 1998.

Burns, D. A., Murdoch, P. S., Lawrence, G. B., and Michel, R. L.: *Effect of groundwater springs on NO3 concentrations during summer in Catskill Mountain streams*, Water Resources Research, 34, 1987-1996, 10.1029/98wr01282, 1998.

Burt, T., Pinay, G., and Sabater, S.: *What do we still need to know about the ecohydrology of riparian zones?*, Ecohydrology, 3, 373-377, 10.1002/eco.140, 2010.

Buttle, J. M., and Sami, K.: *Recharge processes during snowmelt - an isotopic and hydrometric investigation*, Hydrological Processes, 4, 343-360, 10.1002/hyp.3360040405, 1990.

Buttle, J. M.: *Fundamentals of small catchment hydrology*, in: Isotope Tracers in Catchment Hydrology, edited by: Kendall, C., and McDonnell, J. J., Elsevier Science, Amsterdam, The Netherlands, 1-49, 1998.

Buxtorf, A.: *Über die geologischen Verhältnisse des Furkapasses und des im Bau befindlichen Furkatunnels*, Eclogae Geologicae Helvetiae, 12, 176–178, 10.5169/seals-157268, 1912.

Buytaert, W., De Bievre, B., Wyseure, G., and Deckers, J.: *The use of the linear reservoir concept to quantify the impact of changes in land use on the hydrology of catchments in the Andes*, Hydrology and Earth System Sciences, 8, 108-114, 2004.

Carpentier, S., Konz, M., Fischer, R., Anagnostopoulos, G., Meusburger, K., and Schoeck, K.: *Geophysical imaging of shallow subsurface topography and its implication for shallow landslide susceptibility in the Urseren Valley, Switzerland*, Journal of Applied Geophysics, 83, 46-56, 10.1016/j.jappgeo.2012.05.001, 2012.

Clark, I. D., and Fritz, P.: *Environmental Isotopes in Hydrogeology*, CRC Press/Lewis Publishers, New York, 352 pp., 1997.

Cooper, A. B.: *Nitrate depletion in the riparian zone and stream channel of a small headwater catchment*, Hydrobiologia, 202, 13-26, 10.1007/bf00027089, 1990.

Coppola, A., Dragonetti, G., Comegna, A., Lamaddalena, N., Caushi, B., Haikal, M. A., and Basile, A.: *Measuring and modeling water content in stony soils*, Soil & Tillage Research, 128, 9-22, 10.1016/j.still.2012.10.006, 2013.

Craig, H.: *Isotopic variations in meteoric waters*, Science, 133, 1702-1703, 10.1126/science.133.3465.1702, 1961.

Creed, I. F., Band, L. E., Foster, N. W., Morrison, I. K., Nicolson, J. A., Semkin, R. S., and Jeffries, D. S.: *Regulation of nitrate-N release from temperate forests: A test of the N flushing hypothesis*, Water Resources Research, 32, 3337-3354, 10.1029/96wr02399, 1996.

Dansgaard, W.: *Stable isotopes in precipitation*, Tellus, 16, 436-468, 1964.

Darling, W. G., and Bath, A. H.: *A stable isotope study of recharge processes in the english chalk* Journal of Hydrology, 101, 31-46, 10.1016/0022-1694(88)90026-1, 1988.

Dawson, T. E., and Ehleringer, J. R.: *Streamside trees that do not use stream water*, Nature, 350, 335-337, 10.1038/350335a0, 1991.

Dewalle, D. R., Edwards, P. J., Swistock, B. R., Aravena, R., and Drimmie, R. J.: *Seasonal isotope hydrology of three Appalachian forest catchments*, Hydrological Processes, 11, 1895-1906, 10.1002/(sici)1099-1085(199712)11:15<1895::aid-hyp538>3.3.co;2-r, 1997.

Dietermann, N., and Weiler, M.: *Spatial distribution of stable water isotopes in alpine snow cover*, Hydrology and Earth System Sciences, 17, 2657-2668, 10.5194/hess-17-2657-2013, 2013.

Dobriyal, P., Qureshi, A., Badola, R., and Hussain, S. A.: *A review of the methods available for estimating soil moisture and its implications for water resource management*, Journal of Hydrology, 458, 110-117, 10.1016/j.jhydrol.2012.06.021, 2012.

Dosskey, M. G., and Bertsch, P. M.: *Forest sources and pathways of organic matter transport to a blackwater stream - a hydrologic approach*, Biogeochemistry, 24, 1-19, 1994.

Drever, J. I.: *The geochemistry of natural waters*, Prentice-Hall, USA, 388 pp., 1982.

Drever, J. I., and Zobrist, J.: *Chemical weathering of silicate rocks as a function of elevation in the southern Swiss Alps*, Geochim. Cosmochim. Acta, 56, 3209-3216, 10.1016/0016-7037(92)90298-w, 1992.

Dunne, T.: *Field studies of hillslope flow processes*, in: Hillslope hydrology, edited by: Kirkby, J., Wiley, London, 227-293, 1978.

Dusek, J., Vogel, T., and Sanda, M.: *Hillslope hydrograph analysis using synthetic and natural oxygen-18 signatures*, Journal of Hydrology, 475, 415-427, 10.1016/j.jhydrol.2012.10.025, 2012.

Ehleringer, J. R., and Dawson, T. E.: *Water-uptake by plants - perspectives from stable isotope composition*, Plant Cell and Environment, 15, 1073-1082, 10.1111/j.1365-3040.1992.tb01657.x, 1992.

Eriksson, E.: *Compartment Models and Reservoir Theory*, Annual Review of Ecology and Systematics, 2, 67-84, 10.1146/annurev.es.02.110171.000435, 1971.

Evans, C., and Davies, T. D.: *Causes of concentration/discharge hysteresis and its potential as a tool for analysis of episode hydrochemistry*, Water Resources Research, 34, 129-137, 10.1029/97wr01881, 1998.

Fercher, M.: *Einfluss von Landnutzungsänderungen auf die Hochwassersituation im Urserental: Eine Untersuchung mit dem Model ZEMOKOST*, Masters Thesis, Group of Hydrology, Institute of Geography, University of Bern, Bern, Switzerland, 2013.

Fiebig, D. M., Lock, M. A., and Neal, C.: *Soil-water in the riparian zone as a source of carbon for a headwater stream*, Journal of Hydrology, 116, 217-237, 10.1016/0022-1694(90)90124-g, 1990.

Freeman, M. C., Pringle, C. M., and Jackson, C. R.: *Hydrologic connectivity and the contribution of stream headwaters to ecological integrity at regional scales*, Journal of the American Water Resources Association, 43, 5-14, 10.1111/j.1752-1688.2007.00002.x, 2007.

Freer, J., McDonnell, J. J., Beven, K. J., Peters, N. E., Burns, D. A., Hooper, R. P., Aulenbach, B., and Kendall, C.: *The role of bedrock topography on subsurface storm flow*, Water Resources Research, 38, 10.1029/2001wr000872, 2002.

Frick, U.: *The Grimsel radionuclide migration experiment - a contribution to raising confidence in the validity of solute transport models used in performance assessment*, in: GEOVAL '94 - Validation Through Model Testing, Proceedings of an NEA/SKI Symposium, OECD Nuclear Energy Agency, 245-272, 1994.

Friedman, I., and Smith, G. I.: *Deuterium content of snow cores from sierra nevada area*, Science, 169, 467-470, 10.1126/science.169.3944.467, 1970.

Fry, B.: *Steady state models of stable isotopic distributions*, Isotopes in environmental and health studies, 39, 219-232, 10.1080/1025601031000108651, 2003.

Gabrielli, C. P., McDonnell, J. J., and Jarvis, W. T.: *The role of bedrock groundwater in rainfall-runoff response at hillslope and catchment scales*, Journal of Hydrology, 450, 117-133, 10.1016/j.jhydrol.2012.05.023, 2012.

Garvelmann, J., Külls, C., and Weiler, M.: *A porewater-based stable isotope approach for the investigation of subsurface hydrological processes*, Hydrology and Earth System Sciences, 16, 631-640, 10.5194/hess-16-631-2012, 2012.

Gat, J. R., and Gonfiantini, R.: *Stable isotope hydrology: Deuterium and oxygen-18 in the water cycle*, Technical Reports Series 210, International Atomic Energy Agency, Vienna, 337 pp., 1981.

Gat, J. R.: *Oxygen and hydrogen isotopes in the hydrologic cycle*, Annual Review of Earth and Planetary Sciences, 24, 225-262, 10.1146/annurev.earth.24.1.225, 1996.

Gazis, C., and Feng, X. H.: *A stable isotope study of soil water: evidence for mixing and preferential flow paths*, Geoderma, 119, 97-111, 10.1016/s0016-7061(03)00243-x, 2004.

Gehrels, J. C., Peeters, J. E. M., De Vries, J. J., and Dekkers, M.: *The mechanism of soil water movement as inferred from O-18 stable isotope studies*, Hydrological Sciences Journal-Journal Des Sciences Hydrologiques, 43, 579-594, 10.1080/02626669809492154, 1998.

Genereux, D.: *Quantifying uncertainty in tracer-based hydrograph separations*, Water Resources Research, 34, 915-919, 10.1029/98wr00010, 1998.

Genereux, D. P., and Hooper, R. P.: *Oxygen and hydrogen isotopes in rainfall-runoff studies*, in: Isotope Tracers in Catchment Hydrology, edited by: Kendall, C., and McDonnell, J. J., Elsevier Science, Amsterdam, The Netherlands, 319-346, 1998.

Gibbs, R. J.: *Mechanisms controlling world water chemistry*, Science, 170, 1088-1090, 10.1126/science.170.3962.1088, 1970.

Goldsmith, G. R., Munoz-Villers, L. E., Holwerda, F., McDonnell, J. J., Asbjornsen, H., and Dawson, T. E.: *Stable isotopes reveal linkages among ecohydrological processes in a seasonally dry tropical montane cloud forest*, Ecohydrology, 5, 779-790, 10.1002/eco.268, 2012.

Gonfiantini, R.: *Environmental isotopes in lake studies*, in: Handbook of Environmental Isotope Geochemistry, Vol. 2: The Terrestrial Environment, edited by: Fritz, P., and Fontes, J. C., Elsevier Scientific Publishing Company, Amsterdam, 113-168, 1986.

Grabczak, J., Maloszewski, P., Rozanski, K., and Zuber, A.: *Estimation of the tritium input function with the aid of stable isotopes*, Catena, 11, 105-114, 10.1016/s0341-8162(84)80011-9, 1984.

Grabs, T., Bishop, K., Laudon, H., Lyon, S. W., and Seibert, J.: *Riparian zone hydrology and soil water total organic carbon (TOC): implications for spatial variability and upscaling of lateral riparian TOC exports*, Biogeosciences, 9, 3901-3916, 10.5194/bg-9-3901-2012, 2012.

Granger, R. J., Gray, D. M., and Dyck, G. E.: *Snowmelt infiltration to frozen prairie soils*, Canadian Journal of Earth Sciences, 21, 669-677, 10.1139/e84-073, 1984.

Gurtz, J., Zappa, M., Jasper, K., Lang, H., Verbunt, M., Badoux, A., and Vitvar, T.: *A comparative study in modelling runoff and its components in two mountainous catchments*, Hydrological Processes, 17, 297-311, 10.1002/hyp.1125, 2003.

Gysel, A.: *GIS-gestützte Modellierung der Kohlenstoffkonzentration, der Korngrössen und des Bodentyps mit multipler Regression, Ordinary Kriging und Random Forest in einem alpinen Tal (Urserntal, Schweiz)*, Masters Thesis, Environmental Geosciences, University of Basel, Basel, Switzerland, 144 pp., 2010.

Hagedorn, F., Schleppi, P., Waldner, P., and Flühler, H.: *Export of dissolved organic carbon and nitrogen from Gleysol dominated catchments: The significance of water flow paths*, Biogeochemistry, 50, 137-161, 10.1023/a:1006398105953, 2000.

Hargreaves, G., and Samani, Z.: *Estimating potential Evapotranspiration*, Journal of the Irrigation and Drainage Division, 108, 225–230, 1982.

Heidbuechel, I., Troch, P. A., Lyon, S. W., and Weiler, M.: *The master transit time distribution of variable flow systems*, Water Resources Research, 48, 10.1029/2011wr011293, 2012.

Hendry, M. J., Richman, B., and Wassenaar, L. I.: *Correcting for Methane Interferences on δ2H and δ18O Measurements in Pore Water Using H2O(liquid)–H2O(vapor) Equilibration Laser Spectroscopy*, Analytical Chemistry, 83, 5789-5796, 10.1021/ac201341p, 2011.

Herrmann, A., and Stichler, W.: *Groundwater-runoff relationships*, Catena, 7, 251-263, 10.1016/0341-8162(80)90011-9, 1980.

Hill, A. R.: *Factors affecting export of nitrate-nitrogen from drainage basins in Southern Ontario*, Water Research, 12, 1045-1057, 10.1016/0043-1354(78)90050-7, 1978.

Himmelsbach, T., Hotzl, H., and Maloszewski, P.: *Solute transport processes in a highly permeable fault zone of lindau fractured rock test site (Germany)*, Ground Water, 36, 792-800, 10.1111/j.1745-6584.1998.tb02197.x, 1998.

Hopp, L., and McDonnell, J. J.: *Connectivity at the hillslope scale: Identifying interactions between storm size, bedrock permeability, slope angle and soil depth*, Journal of Hydrology, 376, 378-391, 10.1016/j.jhydrol.2009.07.047, 2009.

Hornberger, G. M., Bencala, K. E., and McKnight, D. M.: *Hydrological controls on dissolved organic-carbon during snowmelt in the snake river near montezuma, colorado*, Biogeochemistry, 25, 147-165, 10.1007/bf00024390, 1994.

Hrachowitz, M., Soulsby, C., Tetzlaff, D., Malcolm, I. A., and Schoups, G.: *Gamma distribution models for transit time estimation in catchments: Physical interpretation of parameters and implications for time-variant transit time assessment*, Water Resources Research, 46, 10.1029/2010wr009148, 2010.

Hrachowitz, M., Soulsby, C., Tetzlaff, D., and Malcolm, I. A.: *Sensitivity of mean transit time estimates to model conditioning and data availabilityle*, Hydrological Processes, 25, 980-990, 10.1002/hyp.7922, 2011.

Hrachowitz, M., Savenije, H., Bogaard, T. A., Tetzlaff, D., and Soulsby, C.: *What can flux tracking teach us about water age distribution patterns and their temporal dynamics?*, Hydrology and Earth System Sciences, 17, 533-564, 10.5194/hess-17-533-2013, 2013.

Inamdar, S. P., Christopher, S. F., and Mitchell, M. J.: *Export mechanisms for dissolved organic carbon and nitrate during summer storm events in a glaciated forested catchment in New York, USA*, Hydrological Processes, 18, 2651-2661, 10.1002/hyp.5572, 2004.

Ingraham, N. L., and Shadel, C.: *A comparison of the toluene distillation and vacuum/heat methods for extracting soil water for stable isotopic analysis*, Journal of Hydrology, 140, 371-387, 10.1016/0022-1694(92)90249-u, 1992.

Ingraham, N. L.: *Isotopic variations in precipitation*, in: Isotope Tracers in Catchment Hydrology, edited by: Kendall, C., and McDonnell, J. J., Elsevier Science, Amsterdam, 87–118, 1998.

IPCC: *Climate Change 2007 - The Physical Science Basis: Working Group I - Contribution to the Fourth Assessment Report of the IPCC*, edited by: Solomon, S., Qin, D., Manning, M., Chen, Z., Marquis, M., Averyt, K. B., Tignor, M., and Miller, H. L., Cambridge University Press, 2007.

IUSS Working Group WRB: *World reference base for soil resources: a framework for international classification, correlation and communication*, 2nd ed., Food and Agriculture Organization of the United Nations, Rome, 128 pp., 2006.

Jadoon, K. Z., Weihermueller, L., Scharnagl, B., Kowalsky, M. B., Bechtold, M., Hubbard, S. S., Vereecken, H., and Lambot, S.: *Estimation of Soil Hydraulic Parameters in the Field by Integrated Hydrogeophysical Inversion of Time-Lapse Ground-Penetrating Radar Data*, Vadose Zone Journal, 11, 10.2136/vzj2011.0177, 2012.

Jarvis, N. J.: *A review of non-equilibrium water flow and solute transport in soil macropores: principles, controlling factors and consequences for water quality*, European Journal of Soil Science, 58, 523-546, 10.1111/j.1365-2389.2007.00915.x, 2007.

Jinhua, C., Hongjiang, Z., Wei, W., Youyan, Z., Ran, W., and Wenxing, L.: *Effects of land use on preferential flow paths distributions in southwestern China*, 2010 Second IITA International Conference on Geoscience and Remote Sensing (IITA-GRS 2010), 13-16, 10.1109/iita-grs.2010.5603182, 2010.

Jonas, T., Marty, C., and Magnusson, J.: *Estimating the snow water equivalent from snow depth measurements in the Swiss Alps*, Journal of Hydrology, 378, 161-167, 10.1016/j.jhydrol.2009.09.021, 2009.

Kägi, H. U.: *Die traditionelle Kulturlandschaft im Urserental; Beitrag zur alpinen Kulturgeographie*, PhD Thesis, University of Zürich, Zürich, Switzerland, 211 pp., 1973.

Kalbitz, K., Solinger, S., Park, J. H., Michalzik, B., and Matzner, E.: *Controls on the dynamics of dissolved organic matter in soils: A review*, Soil Science, 165, 277-304, 10.1097/00010694-200004000-00001, 2000.

Kawasaki, M., Ohte, N., Kabeya, N., and Katsuyama, M.: *Hydrological control of dissolved organic carbon dynamics in a forested headwater catchment, Kiryu Experimental Watershed, Japan*, Hydrological Processes, 22, 429-442, 10.1002/hyp.6615, 2008.

Kendall, K. A., Shanley, J. B., and McDonnell, J. J.: *A hydrometric and geochemical approach to test the transmissivity feedback hypothesis during snowmelt*, Journal of Hydrology, 219, 188-205, 10.1016/s0022-1694(99)00059-1, 1999.

Kirchner, J. W., Feng, X. H., and Neal, C.: *Fractal stream chemistry and its implications for contaminant transport in catchments*, Nature, 403, 524-527, 10.1038/35000537, 2000.

Klaus, J., Zehe, E., Elsner, M., Kuells, C., and McDonnell, J. J.: *Macropore flow of old water revisited: experimental insights from a tile-drained hillslope*, Hydrology and Earth System Sciences, 17, 103-118, 10.5194/hess-17-103-2013, 2013.

Klute, A., and Dirksen, C.: *Hydraulic Conductivity and Diffusivity: Laboratory Methods*, in: Methods of Soil Analysis: Part 1 - Physical and Mineralogical Methods, edited by: Klute, A., American Society of Agronomy, Madison, Wisconsin, 687-734, 1986.

Knowles, R.: *Denitrification*, Microbiological Reviews, 46, 43-70, 1982.

König, N.: *Handbuch forstliche Analytik: Eine lose Blattsammlung der Analysemethoden im Forstbereich*, 1, Bundesministerium für Verbraucherschutz, Ernährung und Landwirtschaft., 568 pp., 2009.

Konz, N., Baenninger, D., Konz, M., Nearing, M., and Alewell, C.: *Process identification of soil erosion in steep mountain regions*, Hydrology and Earth System Sciences, 14, 675-686, 2010.

Körner, C., Wieser, G., and Cernusca, A.: *Der Wasserhaushalt waldfreier Gebiete in den österreichischen Alpen zwischen 600 und 2600 m Höhe*, in: Struktur und Funktion von Graslandökosystemen im Nationalpark Hohe Tauern, edited by: Cernusca, A., Veröffentlichung Oesterreichisches MaB-Programm 13, Wagner, Innsbruck, Austria, 119-153, 1989.

Küttel, M.: *Der subalpine Schutzwald im Urserental - ein inelastisches Oekosystem*, Botanica Helvetica, 100/2, 1990.

Labhart, T. P.: *Aarmassiv und Gotthardmassiv*, Sammlung Geologischer Führer, Volume 63, edited by: Gwinner, M. P., Borntraeger, Berlin, 1977.

Lagger, S.: *Auswirkungen der Landnutzungsänderung auf den Wasserhaushalt im Urserntal*, Masters Thesis, Group of Hydrology, Institute of Geography, University of Bern, Bern, Switzerland, Publikation Gewässerkunde Nr. 521, 2012.

Lambin, E. F., and Geist, H.: *Land-Use and Land-Cover Change: Local Processes and Global Impacts*, Springer, 240 pp., 2008.

Leaney, F. W., Smettem, K. R. J., and Chittleborough, D. J.: *Estimating the contribution of preferential flow to subsurface runoff from a hillslope using deuterium and chloride*, Journal of Hydrology, 147, 83-103, 10.1016/0022-1694(93)90076-l, 1993.

Lindenmaier, F., Zehe, E., Dittfurth, A., and Ihringer, J.: *Process identification at a slow-moving landslide in the Vorarlberg Alps*, Hydrological Processes, 19, 1635-1651, 10.1002/hyp.5592, 2005.

Linsley, K.: *A simple procedure for the day-to-day forecasting of runoff from snow-melt*, Transactions-American Geophysical Union, 24, 62-67, 1943.

Litaor, M. I., Williams, M., and Seastedt, T. R.: *Topographic controls on snow distribution, soil moisture, and species diversity of herbaceous alpine vegetation, Niwot Ridge, Colorado*, Journal of Geophysical Research-Biogeosciences, 113, 10.1029/2007jg000419, 2008.

Lundin, L. C., and Johnsson, H.: *Ion dynamics of a freezing soil monitored in-situ by time-domain reflectometry*, Water Resources Research, 30, 3471-3478, 10.1029/94wr02231, 1994.

Lunt, I. A., Hubbard, S. S., and Rubin, Y.: *Soil moisture content estimation using ground-penetrating radar reflection data*, Journal of Hydrology, 307, 254-269, 10.1016/j.hydrol.2004.10.014, 2005.

Lv, M., Hao, Z., Liu, Z., and Yu, Z.: *Conditions for lateral downslope unsaturated flow and effects of slope angle on soil moisture movement*, Journal of Hydrology, 486, 321-333, 10.1016/j.jhydrol.2013.02.013, 2013.

Majoube, M.: *Fractionement en oxygen-18 et en deuterium entre l'eau et sa vapeur*, J. Chim. Phys.-Chim. Biol., 68, 1423-1436, 1971.

Maloszewski, P., and Zuber, A.: *Determining the turnover time of groundwater systems with the aid of environmental tracers.1. models and their applicability*, Journal of Hydrology, 57, 207-231, 1982.

Maloszewski, P., Rauert, W., Trimborn, P., Herrmann, A., and Rau, R.: *Isotope hydrological study of mean transit times in an alpine basin (Wimbachtal, Germany)*, Journal of Hydrology, 140, 343-360, 10.1016/0022-1694(92)90247-s, 1992.

Maloszewski, P., Stichler, W., Zuber, A., and Rank, D.: *Identifying the flow systems in a karstic-fissured-porous aquifer, the Schneealpe, Austria, by modelling of environmental O-18 and H-3 isotopes*, Journal of Hydrology, 256, 48-59, 10.1016/s0022-1694(01)00526-1, 2002.

Maloszewski, P., and Zuber, A.: *Manual on lumped-parameter models used for the interpretation of environmental tracer data in groundwaters*, in: Use of Isotopes for Analyses of Flow and Transport Dynamics in Groundwater Systems, edited by: Yurtsever, Y., Vienna, 1–50, 2002.

McConville, C., Kalin, R. M., Johnston, H., and McNeill, G. W.: *Evaluation of recharge in a small temperate catchment using natural and applied delta O-18 profiles in the unsaturated zone*, Ground Water, 39, 616-623, 10.1111/j.1745-6584.2001.tb02349.x, 2001.

McDonnell, J. J., Bonell, M., Stewart, M. K., and Pearce, A. J.: *Deuterium Variations in Storm Rainfall: Implications for Stream Hydrograph Separation*, Water Resources Research, 26, 455-458, 10.1029/89wr03000, 1990.

McDonnell, J. J., Stewart, M. K., and Owens, I. F.: *Effect of catchment-scale subsurface mixing on stream isotopic response*, Water Resources Research, 27, 3065-3073, 10.1029/91wr02025, 1991.

McDonnell, J. J., McGuire, K., Aggarwal, P., Beven, K. J., Biondi, D., Destouni, G., Dunn, S., James, A., Kirchner, J., Kraft, P., Lyon, S., Maloszewski, P., Newman, B., Pfister, L., Rinaldo, A., Rodhe, A., Sayama, T., Seibert, J., Solomon, K., Soulsby, C., Stewart, M., Tetzlaff, D., Tobin, C., Troch, P., Weiler, M., Western, A., Wörman, A., and Wrede, S.: *How old is streamwater? Open questions in catchment transit time conceptualization, modelling and analysis*, Hydrological Processes, 24, 1745-1754, 10.1002/hyp.7796, 2010.

McGlynn, B., McDonnell, J., Stewart, M., and Seibert, J.: *On the relationships between catchment scale and streamwater mean residence time*, Hydrological Processes, 17, 175-181, 10.1002/hyp.5085, 2003.

McGlynn, B. L., McDonnell, J. J., Shanley, J. B., and Kendall, C.: *Riparian zone flowpath dynamics during snowmelt in a small headwater catchment*, Journal of Hydrology, 222, 75-92, 10.1016/s0022-1694(99)00102-x, 1999.

McGlynn, B. L., and McDonnell, J. J.: *Role of discrete landscape units in controlling catchment dissolved organic carbon dynamics*, Water Resources Research, 39, 10.1029/2002wr001525, 2003.

McGuire, K. J., McDonnell, J. J., Weiler, M., Kendall, C., McGlynn, B. L., Welker, J. M., and Seibert, J.: *The role of topography on catchment-scale water residence time*, Water Resources Research, 41, W05002, 10.1029/2004wr003657, 2005.

McGuire, K. J., and McDonnell, J. J.: *A review and evaluation of catchment transit time modeling*, Journal of Hydrology, 330, 543-563, 10.1016/j.jhydrol.2006.04.020, 2006.

McGuire, K. J., Weiler, M., and McDonnell, J. J.: *Integrating tracer experiments with modeling to assess runoff processes and water transit times*, Advances in Water Resources, 30, 824-837, 10.1016/j.advwatres.2006.07.004, 2007.

Menzel, L.: *Modellierung der Evapotranspiration im System Boden-Pflanze-Atmosphäre*, PhD Thesis, Züricher Geographische Schriften No. 67, ETH Zürich, Zürich, Switzerland, 128 pp., 1997.

MeteoSwiss: *IDAweb The data portal of MeteoSwiss for research and teaching*: available at: meteoschweiz.admin.ch/web/en/services/data_portal/idaweb.html, access: 1 July 2013, 2013.

Meusburger, K., and Alewell, C.: *Impacts of anthropogenic and environmental factors on the occurrence of shallow landslides in an alpine catchment (Urseren Valley, Switzerland)*, Natural Hazards and Earth System Sciences, 8, 509-520, 2008.

Mitchell, J. S., and Ruess, R. W.: *N2 fixing alder (Alnus viridis spp. fruticosa) effects on soil properties across a secondary successional chronosequence in interior Alaska*, Biogeochemistry, 95, 215-229, 10.1007/s10533-009-9332-x, 2009.

Mitchell, M. J., Piatek, K. B., Christopher, S., Mayer, B., Kendall, C., and McHale, P.: *Solute sources in stream water during consecutive fall storms in a northern hardwood forest watershed: a combined hydrological, chemical and isotopic approach*, Biogeochemistry, 78, 217-246, 10.1007/s10533-005-4277-1, 2006.

Monteith, S. S., Buttle, J. M., Hazlett, P. W., Beall, F. D., Semkin, R. G., and Jeffries, D. S.: *Paired-basin comparison of hydrologic response in harvested and undisturbed hardwood*

forests during snowmelt in central Ontario: II. Streamflow sources and groundwater residence times, Hydrological Processes, 20, 1117-1136, 10.1002/hyp.6073, 2006.

Moore, I. D., Grayson, R. B., and Ladson, A. R.: *Digital terrain modelling: A review of hydrological, geomorphological, and biological applications*, Hydrological Processes, 5, 3-30, 10.1002/hyp.3360050103, 1991.

Moran, T. A., Marshall, S. J., Evans, E. C., and Sinclair, K. E.: *Altitudinal Gradients of Stable Isotopes in Lee-Slope Precipitation in the Canadian Rocky Mountains*, Arctic, Antarctic, and Alpine Research, 39, 455-467, 10.1657/1523-0430(06-022)[moran]2.0.co;2, 2007.

Moriasi, D. N., Arnold, J. G., Van Liew, M. W., Bingner, R. L., Harmel, R. D., and Veith, T. L.: *Model evaluation guidelines for systematic quantification of accuracy in watershed simulations*, Transactions of the Asabe, 50, 885-900, 2007.

Moser, H., and Stichler, W.: *Deuterium and oxygen-18 contents as an index of the properties of snow blankets*, in: Snow Mechanics: Proceedings of the Grindelwald Symposium April 1974, Publication number 114, International Association of Hydrological Sciences, Grindelwald, Switzerland, 122-135, 1975.

Mualem, Y.: *New model for predicting hydraulic conductivity of unsaturated porous-media*, Water Resources Research, 12, 513-522, 10.1029/WR012i003p00513, 1976.

Mueller, M. H., Weingartner, R., and Alewell, C.: *Importance of vegetation, topography and flow paths for water transit times of base flow in alpine headwater catchments*, Hydrology and Earth System Sciences, 17, 1661-1679, 10.5194/hess-17-1661-2013, 2013.

Mullis, J.: *Entstehung alpiner Zerrklüfte und Kluftminerale im Gotthard-Basistunnel, Abschnitt Amsteg-Sedrun und im Zugangs- und Kabelstollen von Amsteg*, in: NEAT-Mineralien - Kristallschätze tief im Berg, edited by: Amacher, P., and Schüpbach, T., GEO-Uri GmbH, Amsteg, Switzerland, 2011.

Munoz-Villers, L. E., and McDonnell, J. J.: *Runoff generation in a steep, tropical montane cloud forest catchment on permeable volcanic substrateRunoff generation in a steep, tropical montane cloud forest catchment on permeable volcanic substrate*, Water Resources Research, 48, 10.1029/2011wr011316, 2012.

Nash, J. E., and Sutcliffe, J. V.: *River flow forecasting through conceptual models part I — A discussion of principles*, Journal of Hydrology, 10, 282-290, dx.doi.org/10.1016/0022-1694(70)90255-6, 1970.

Neff, K. J., Schwartz, J. S., Moore, S. E., and Kulp, M. A.: *Influence of basin characteristics on baseflow and stormflow chemistry in the Great Smoky Mountains National Park, USA*, Hydrological Processes, 10.1002/hyp.9366, 2012.

Nimmo, J. R.: *Preferential flow occurs in unsaturated conditions*, Hydrological Processes, 26, 786-789, 10.1002/hyp.8380, 2012.

Ofterdinger, U. S.: *Ground Water Flow Systems in the Rotondo Granite, Central Alps (Switzerland)*, PhD Thesis, University of Zürich, Switzerland, 2001.

Ofterdinger, U. S., Balderer, W., Loew, S., and Renard, P.: *Environmental isotopes as indicators for ground water recharge to fractured granite*, Ground Water, 42, 868-879, 2004.

Pachepsky, Y. A., Smettem, K. R. J., Vanderborght, J., Herbst, M., Vereecken, H., and Wosten, J. H. M.: *Reality and fiction of models and data in soil hydrology*, in: Unsaturated-Zone Modeling: Progress, Challenges and Applications, edited by: Feddes, R. A., DeRooij, G. H., and VanDam, J. C., 231-260, 2004.

Pacific, V. J., Jencso, K. G., and McGlynn, B. L.: *Variable flushing mechanisms and landscape structure control stream DOC export during snowmelt in a set of nested catchments*, Biogeochemistry, 99, 193-211, 10.1007/s10533-009-9401-1, 2010.

Parriaux, A., Dubois, J. D., and Dray, M.: *Chemical composition of snow cover on the western Swiss Alps*, in: Hydrology in Mountainous Regions 1. Hydrological Measurements. The Water Cycle, edited by: Lang, H., and Musy, A., International Association of Hydrological Sciences, IAHS, Lausanne, 1990, 501-509, 1990.

Pawlowski, K., and Newton, W. E.: *Nitrogen-fixing actinorhizal symbioses*, Springer, Netherlands, 324 pp., 2008.

Penna, D., Borga, M., Norbiato, D., and Fontana, G. D.: *Hillslope scale soil moisture variability in a steep alpine terrain*, Journal of Hydrology, 364, 311-327, 10.1016/j.jhydrol.2008.11.009, 2009.

Perrin, J., Jeannin, P.-Y., and Zwahlen, F.: *Epikarst storage in a karst aquifer: a conceptual model based on isotopic data, Milandre test site, Switzerland*, Journal of Hydrology, 279, 106-124, 10.1016/s0022-1694(03)00171-9, 2003.

Renger, M., Bohne, K., Facklam, M., Harrach, T., Riek, W., Schäfer, W., Wessolek, G., Zacharias, S., Bachmann, J., Dehner, U., Duijnisveld, W., Eckelmann, W., Hartge, K.-H., Hennings, V., Knoblauch, S., Müller, L., Müller, U., Plagge, R., Schindler, U., Schwärzel, K., Sponagel, H., and Vorderbrügge, T.: *Ergebnisse und Vorschläge der DBG-Arbeitsgruppe „Kennwerte des Bodengefüges“ zur Schätzung bodenphysikalischer Kennwerte*, in: Bodenökologie und Bodengenese: Bodenphysikalische Kennwerte und Berechnungsverfahren für die Praxis, edited by: Wessolek, G., Kaupenjohann, M., and Renger, M., Technische Universität Berlin, Berlin, Germany, 51, 2009.

Rhoades, C., Oskarsson, H., Binkley, D., and Stottlemyer, B.: *Alder (Alnus crispa) effects on soils in ecosystems of the Agashashok River valley, northwest Alaska*, Ecoscience, 8, 89-95, 2001.

Richard, T., Mercury, L., Massault, M., and Michelot, J.-L.: *Experimental study of D/H isotopic fractionation factor of water adsorbed on porous silica tubes*, Geochim. Cosmochim. Acta, 71, 1159-1169, 10.1016/j.gca.2006.11.028, 2007.

Richards, L. A.: *Capillary conduction of liquids through porous mediums*, Physics - a Journal of General and Applied Physics, 1, 318-333, 10.1063/1.1745010, 1931.

Roa-Garcia, M. C.: *Wetlands and water dynamics in small headwater catchments of the Andes*, PhD Thesis, Institute for Resources, Environment and Sustainability, University of British Columbia, Vancouver, Canada, 153 pp., 2009.

Roa-Garcia, M. C., and Weiler, M.: *Integrated response and transit time distributions of watersheds by combining hydrograph separation and long-term transit time modeling*, Hydrology and Earth System Sciences, 14, 1537-1549, 10.5194/hess-14-1537-2010, 2010.

Rodgers, P., Soulsby, C., and Waldron, S.: *Stable isotope tracers as diagnostic tools in upscaling flow path understanding and residence time estimates in a mountainous mesoscale catchment*, Hydrological Processes, 19, 2291-2307, 10.1002/hyp.5677, 2005.

Rodhe, A., Nyberg, L., and Bishop, K.: *Transit times for water in a small till catchment from a step shift in the oxygen 18 content of the water input*, Water Resources Research, 32, 3497-3511, 10.1029/95wr01806, 1996.

Rodhe, A.: *Snowmelt-dominated systems*, in: Isotope Tracers in Catchment Hydrology, edited by: Kendall, C., and McDonnell, J. J., Elsevier Science, Amsterdam, The Netherlands, 391-433, 1998.

Rogora, M., Mosello, R., Arisci, S., Brizzio, M., Barbieri, A., Balestrini, R., Waldner, P., Schmitt, M., Stahli, M., Thimonier, A., Kalina, M., Puxbaum, H., Nickus, U., Ulrich, E., and Probst, A.: *An overview of atmospheric deposition chemistry over the Alps: Present status and long-term trends*, Hydrobiologia, 562, 17-40, 10.1007/s10750-005-1803-z, 2006.

Rusjan, S., Brilly, M., and Mikos, M.: *Flushing of nitrate from a forested watershed: An insight into hydrological nitrate mobilization mechanisms through seasonal high-frequency stream nitrate dynamics*, Journal of Hydrology, 354, 187-202, 10.1016/j.jhydrol.2008.03.009, 2008.

Saxena, R. K., and Dressie, Z.: *Estimation of groundwater recharge and moisture movement in sandy formations by tracing natural oxygen-18 and injected tritium profiles in the unsaturated zone*, in: Isotope Hydrology, Isotope Hydrology in Water Resources Development 1983, Vienna, 1983, pp. 139-150, 1984.

Saxena, R. K.: *Estimation of canopy reservoir capacity and O-18 fractionation in throughfall in a pine*, Nordic Hydrology, 17, 251-260, 1986.

Saxton, K. E., Rawls, W. J., Romberger, J. S., and Papendick, R. I.: *Estimating generalized soil-water characteristics from texture*, Soil Science Society of America Journal, 50, 1031-1036, 1986.

Sayama, T., McDonnell, J. J., Dhakal, A., and Sullivan, K.: *How much water can a watershed store?*, Hydrological Processes, 25, 3899-3908, 10.1002/hyp.8288, 2011.

Schaub, M., Seth, B., and Alewell, C.: *Determination of delta O-18 in soils: measuring conditions and a potential application*, Rapid Communications in Mass Spectrometry, 23, 313-318, 10.1002/rcm.3871, 2009.

Scherrer, S.: *Abflussbildung bei Starkniederschlägen. Identifikation bei Abflussprozessen mittels künstlicher Niederschläge*, PhD, ETH Zürich, Zürich, Switzerland, 178 pp., 1996.

Schmidt, P.: *Auswirkungen der Landnutzungsänderung auf die Hydrologie im Urserental*, Masters Thesis, Group of Hydrology, Institute of Geography, University of Bern, Bern, Switzerland, Publikation Gewässerkunde Nr. 520, 2012.

Schmocker-Fackel, P.: *A method to delineate runoff processes in a catchment and its implications for runoff simulations*, PhD Thesis, ETH Zürich, ETH Zürich, Zürich, Switzerland, 197 pp., 2004.

Schroeder, L.: *Der Beitrag kleinflächiger Feuchtgebiete (Hangmoore) auf die Abflussdynamik im Quellgebiet - am Beispiel des subalpinen Nordhangs (Urserental)*, Masters Thesis, Environmental Geosciences, University of Basel, Basel, Switzerland, 2012.

Schulla, J., and Jasper, K.: *Model Description WaSiM-ETH*, Institute of Geography, ETH Zürich, Zürich, Switzerland, Technical Report, 181, 2007.

Sebestyen, S. D., Boyer, E. W., Shanley, J. B., Kendall, C., Doctor, D. H., Aiken, G. R., and Ohte, N.: *Sources, transformations, and hydrological processes that control stream nitrate and dissolved organic matter concentrations during snowmelt in an upland forest*, Water Resources Research, 44, 10.1029/2008wr006983, 2008.

Seibert, J., and McGlynn, B. L.: *A new triangular multiple flow direction algorithm for computing upslope areas from gridded digital elevation models*, Water Resources Research, 43, 10.1029/2006wr005128, 2007.

Shaftel, R. S., King, R. S., and Back, J. A.: *Alder cover drives nitrogen availability in Kenai lowland headwater streams, Alaska*, Biogeochemistry, 107, 135-148, 10.1007/s10533-010-9541-3, 2012.

Sheppard, S. M. F., and Gilg, H. A.: *Stable isotope geochemistry of clay minerals*, Clay Minerals, 31, 1-24, 10.1180/claymin.1996.031.1.01, 1996.

Shurbaji, A. R. M., and Phillips, F. M.: *A numerical model for the movement of H2O, H2(18)O, and (2)HHO in the unsaturated zone*, Journal of Hydrology, 171, 125-142, 10.1016/0022-1694(94)02604-a, 1995.

Sidle, R. C., Tsuboyama, Y., Noguchi, S., Hosoda, I., Fujieda, M., and Shimizu, T.: *Stormflow generation in steep forested headwaters: a linked hydrogeomorphic paradigm*, Hydrological Processes, 14, 369-385, 10.1002/(sici)1099-1085(20000228)14:3<369::aid-hyp943>3.0.co;2-p, 2000.

Siegenthaler, U., and Oeschger, H.: *Correlation of O-18 in precipitation with temperature and altitude*, Nature, 285, 314-317, 10.1038/285314a0, 1980.

Simunek, J., Jarvis, N. J., van Genuchten, M. T., and Gardenas, A.: *Review and comparison of models for describing non-equilibrium and preferential flow and transport in the vadose zone*, Journal of Hydrology, 272, 14-35, 2003.

Sklash, M. G., and Farvolden, R. N.: *Role of groundwater in storm runoff*, Journal of Hydrology, 43, 45-65, 10.1016/0022-1694(79)90164-1, 1979.

Soderberg, K., Good, S. P., Wang, L., and Caylor, K.: *Stable Isotopes of Water Vapor in the Vadose Zone: A Review of Measurement and Modeling Techniques*, Vadose Zone Journal, 11, 10.2136/vzj2011.0165, 2012.

Soil Survey Division Staff: *Soil survey manual*, Soil Conservation Service. U.S. Department of Agriculture, Handbook 18, Washington, USA, 315 pp., 1993.

Soulsby, C., and Tetzlaff, D.: *Towards simple approaches for mean residence time estimation in ungauged basins using tracers and soil distributions*, Journal of Hydrology, 363, 60-74, 10.1016/j.jhydrol.2008.10.001, 2008.

Soulsby, C., Tetzlaff, D., and Hrachowitz, M.: *Are transit times useful process-based tools for flow prediction and classification in ungauged basins in montane regions?*, Hydrological Processes, 24, 1685-1696, 10.1002/hyp.7578, 2010.

Sponagel, H., Grottenthaler, W., Hartmann, K.-J., Hartwich, R., Janetzko, P., Joisten, H., Kühn, D., Sabel, K.-J., and Traidl, R.: *Bodenkundliche Kartieranleitung*, edited by: Bundesanstalt für Geowissenschaften und Rohstoffe, E. Schweizerbart'sche Verlagsbuchhandlung, Hannover, Germany, 438 pp., 2005.

Stähli, M., Jansson, P. E., and Lundin, L. C.: *Preferential water flow in a frozen soil - A two-domain model approach*, Hydrological Processes, 10, 1305-1316, 10.1002/(sici)1099-1085(199610)10:10<1305::aid-hyp462>3.0.co;2-f, 1996.

Steelman, C. M., and Endres, A. L.: *Assessing vertical soil moisture dynamics using multi-frequency GPR common-midpoint soundings*, Journal of Hydrology, 436, 51-66, 10.1016/j.jhydrol.2012.02.041, 2012.

Stewart, G. L.: *Clay-water interaction, behavior of H-3 and H-2 in adsorbed water, and isotope-effect*, Soil Science Society of America Proceedings, 36, 421-426, 1972.

Stewart, M. K., and McDonnell, J. J.: *Modeling base-flow soil-water residence times from deuterium concentrations*, Water Resources Research, 27, 2681-2693, 10.1029/91wr01569, 1991.

Stumm, W., and Morgan, J. J.: *Aquatic chemistry: chemical equilibria and rates in natural waters*, Wiley, New York, 1996.

Stumpp, C., Maloszewski, P., Stichler, W., and Fank, J.: *Environmental isotope (δ18O) and hydrological data to assess water flow in unsaturated soils planted with different crops: Case study lysimeter station "Wagna" (Austria)*, Journal of Hydrology, 369, 198-208, 10.1016/j.jhydrol.2009.02.047, 2009a.

Stumpp, C., Stichler, W., and Maloszewski, P.: *Application of the environmental isotope δ18O to study water flow in unsaturated soils planted with different crops: Case study of a weighable lysimeter from the research field in Neuherberg, Germany*, Journal of Hydrology, 368, 68-78, 10.1016/j.jhydrol.2009.01.027, 2009b.

Stumpp, C., and Maloszewski, P.: *Quantification of preferential flow and flow heterogeneities in an unsaturated soil planted with different crops using the environmental isotope δ18O*, Journal of Hydrology, 394, 407-415, 10.1016/j.jhydrol.2010.09.014, 2010.

Stumpp, C., and Hendry, M. J.: *Spatial and temporal dynamics of water flow and solute transport in a heterogeneous glacial till: The application of high-resolution profiles of delta O-18 and delta H-2 in pore waters*, Journal of Hydrology, 438, 203-214, 10.1016/j.jhydrol.2012.03.024, 2012.

Stumpp, C., Stichler, W., Kandolf, M., and Simunek, J.: *Effects of Land Cover and Fertilization Method on Water Flow and Solute Transport in Five Lysimeters: A Long-Term Study Using Stable Water Isotopes*, Vadose Zone Journal, 11, vzj2011.0075, 10.2136/vzj2011.0075, 2012.

Tardy, Y.: *Characterization of principal weathering types by geochemistry of waters from some european and african crystalline massifs*, Chemical Geology, 7, 253-271, 1971.

Tasser, E., Tappeiner, U., and Cernusca, A.: *Ecological effects of land use changes in the European Alps* in: Global Change and Mountain Regions - A State of Knowledge Overview, edited by: Huber, U. M., Bugmann, H. K. M., and Reasoner, M. A., Springer, Dordrecht, The Netherlands, 413-425, 2005.

Taylor, S., Feng, X. H., Kirchner, J. W., Osterhuber, R., Klaue, B., and Renshaw, C. E.: *Isotopic evolution of a seasonal snowpack and its melt*, Water Resources Research, 37, 759-769, 10.1029/2000wr900341, 2001.

Tetzlaff, D., Seibert, J., McGuire, K. J., Laudon, H., Burns, D. A., Dunn, S. M., and Soulsby, C.: *How does landscape structure influence catchment transit time across different geomorphic provinces?*, Hydrological Processes, 23, 945-953, 10.1002/hyp.7240, 2009.

Tetzlaff, D., Soulsby, C., Hrachowitz, M., and Speed, M.: *Relative influence of upland and lowland headwaters on the isotope hydrology and transit times of larger catchments*, Journal of Hydrology, 400, 438-447, 10.1016/j.jhydrol.2011.01.053, 2011.

Turner, J. V., Bradd, J. M., and Waite, T. D.: *Conjunctive use of isotopic techniques to elucidate solute concentration and flow processes in dryland salinized catchments*, in: Isotope Techniques in Water Resources Development 1991, Proceedings of a Symposium, Vienna, 11-15 March 1991, edited by: IAEA, Vienna, 1991.

Turner, J. V., and Barnes, C. J.: *Modeling of isotopes and hydrogeochemical responses in catchment hydrology*, in: Isotope Tracers in Catchment Hydrology, edited by: Kendall, C., and McDonnell, J. J., Elsevier Science, Amsterdam, 723-760, 1998.

Uchida, T., Kosugi, K., and Mizuyama, T.: *Effects of pipeflow on hydrological process and its relation to landslide: a review of pipeflow studies in forested headwater catchments*, Hydrological Processes, 15, 2151-2174, 10.1002/hyp.281, 2001.

Uhlenbrook, S., Frey, M., Leibundgut, C., and Maloszewski, P.: *Hydrograph separations in a mesoscale mountainous basin at event and seasonal timescales*, Water Resources Research, 38, 10.1029/2001wr000938, 2002.

UNESCO-IHE: *Mid-term Research Agenda (2011-2015) of the chair group Hydrology and Water Resources (HWR core)*: unesco-ihe.org/sites/default/files/hwr_researchstrategy_18november2011.pdf, access: 31 May 2014, 2011.

ValUrsern: *Final report of the ValUrsern project: "The ecological and socio-economic consequences of land transformation in alpine regions: an interdisciplinary assessment and valuation of current changes in the Ursern Valley, key region in the Swiss central Alps."*, Swiss National Science Foundation, Switzerland, 51, 2012.

van den Bergh, T., Hiltbrunner, E., and Körner, C.: *A landcover map and land cover statistics for the Urserntal, Central Alps, Switzerland*, Institute of Botany, Section Plant Ecology, University of Basel, Technical report, unpublished, 10 pp., 2011.

van der Heijden, G., Legout, A., Pollier, B., Brechet, C., Ranger, J., and Dambrine, E.: *Tracing and modeling preferential flow in a forest soil - Potential impact on nutrient leaching*, Geoderma, 195, 12-22, 10.1016/j.geoderma.2012.11.004, 2013.

van Genuchten, M. T.: *A closed form equation for predicting the hydraulic conductivity of unsaturated soils*, Soil Science Society of America Journal, 44, 892-898, 1980.

van Genuchten, M. T., and Wierenga, P. J.: *Solute dispersion coefficients and retardation factors*, in: Methods of Soil Analysis: Part 1 - Physical and Mineralogical Methods, edited by: Klute, A., American Society of Agronomy, Madison, Wisconsin, 1025-1054, 1986.

van Genuchten, M. T., and Simunek, J.: *Integrated modeling of vadose zone flow and transport processes*, in: Unsaturated Zone Modelling: Progress, Challenges and Applications, edited by: Feddes, R. A., de Rooij, G. H., and van Dam, J. C., Wageningen UR Frontis Series, Volume 2, Kluwer Academic Publishers, Dordrecht, The Netherlands, 37-69, 2004.

Vanderborght, J., and Vereecken, H.: *Review of dispersivities for transport modeling in soils*, Vadose Zone Journal, 6, 29-52, 10.2136/vzj2006.0096, 2007.

Vereecken, H., Huisman, J. A., Bogena, H., Vanderborght, J., Vrugt, J. A., and Hopmans, J. W.: *On the value of soil moisture measurements in vadose zone hydrology: A review*, Water Resources Research, 44, 10.1029/2008wr006829, 2008.

Viville, D., Ladouche, B., and Bariac, T.: *Isotope hydrological study of mean transit time in the granitic Strengbach catchment (Vosges massif, France): application of the FlowPC model with modified input function*, Hydrological Processes, 20, 1737-1751, 10.1002/hyp.5950, 2006.

Viviroli, D., Weingartner, R., and Messerli, B.: *Assessing the hydrological significance of the world's mountains*, Mountain Research and Development, 23, 32-40, 10.1659/0276-4741(2003)023[0032:athsot]2.0.co;2, 2003.

Viviroli, D., Archer, D. R., Buytaert, W., Fowler, H. J., Greenwood, G. B., Hamlet, A. F., Huang, Y., Koboltschnig, G., Litaor, M. I., Lopez-Moreno, J. I., Lorentz, S., Schaedler, B., Schreier, H., Schwaiger, K., Vuille, M., and Woods, R.: *Climate change and mountain water resources: overview and recommendations for research, management and policy*, Hydrology and Earth System Sciences, 15, 471-504, 10.5194/hess-15-471-2011, 2011.

Wassenaar, L. I., Hendry, M. J., Chostner, V. L., and Lis, G. P.: *High Resolution Pore Water delta H-2 and delta O-18 Measurements by H2O(liquid)-H2O(vapor) Equilibration Laser Spectroscopy*, Environmental Science & Technology, 42, 9262-9267, 10.1021/es802065s, 2008.

Weiler, M., and McDonnell, J. R. J.: *Testing nutrient flushing hypotheses at the hillslope scale: A virtual experiment approach*, Journal of Hydrology, 319, 339-356, 10.1016/j.jhydrol.2005.06.040, 2006.

Weingartner, R., Viviroli, D., and Schaedler, B.: *Water resources in mountain regions: a methodological approach to assess the water balance in a highland-lowland-system*, Hydrological Processes, 21, 578-585, 10.1002/hyp.6268, 2007.

Wenjie, L., Wenyao, L., Hongjian, L., Wenping, D., and Hongmei, L.: *Runoff generation in small catchments under a native rain forest and a rubber plantation in Xishuangbanna,*

southwestern China, Water and Environment Journal, 25, 138-147, 10.1111/j.1747-6593.2009.00211.x, 2011.

West, A. G., Goldsmith, G. R., Brooks, P. D., and Dawson, T. E.: *Discrepancies between isotope ratio infrared spectroscopy and isotope ratio mass spectrometry for the stable isotope analysis of plant and soil waters*, Rapid Communications in Mass Spectrometry, 24, 1948-1954, 10.1002/rcm.4597, 2010.

Wettstein, S.: *Grünerlengebüsche in den Schweizer Alpen: Ein Simulationsmodell aufgrund abiotischer Faktoren und Untersuchungen über morphologische und strukturelle Variabilität*, Masters Thesis, University of Bern, Bern, Switzerland, 62 pp., 1999.

Williams, C. J., McNamara, J. P., and Chandler, D. G.: *Controls on the temporal and spatial variability of soil moisture in a mountainous landscape: the signature of snow and complex terrain*, Hydrology and Earth System Sciences, 13, 1325-1336, 2009.

Williams, M., Kattelmann, R., and Melack, J.: *Groundwater contribution to the hydrochemistry of an alpine basin*, in: Proceedings of two Lausanne Symposia, August 1990, Hydrology in Mountainous Regions I - Hydrological Measurements, The Water Cycle, Lausanne, Switzerland, 1990, 810 pages, 1990.

Winterhalter, R. U.: *Zur Petrographie und Geologie des östlichen Gotthardmassivs*, PhD Thesis, A.G. Gebr. Leemann, Zürich, 1930.

Wittenberg, H.: *Baseflow recession and recharge as nonlinear storage processes*, Hydrological Processes, 13, 715-726, 10.1002/(sici)1099-1085(19990415)13:5<715::aid-hyp775>3.0.co;2-n, 1999.

Worrall, F., Gibson, H. S., and Burt, T. P.: *Production vs. solubility in controlling runoff of DOC from peat soils - The use of an event analysis*, Journal of Hydrology, 358, 84-95, 10.1016/j.jhydrol.2008.05.037, 2008.

Zehe, E., Graeff, T., Morgner, M., Bauer, A., and Bronstert, A.: *Plot and field scale soil moisture dynamics and subsurface wetness control on runoff generation in a headwater in the Ore Mountains*, Hydrology and Earth System Sciences, 14, 873-889, 10.5194/hess-14-873-2010, 2010.

Zimmermann, U., Ehhalt, D., and Munnich, K. O.: *Soil-water movement and evapotranspiration: Changes in the isotopic composition of the water*, in: Isotopes in Hydrology, edited by: IAEA, International Atomic Energy Agency, Vienna, 567-584, 1967.

Zuber, A.: *Review of existing mathematical models for interpretation of tracer data in hydrology, Report 1270/AP of the Institute of Nuclear Physics, Cracow*, in: Mathematical models for the interpretation of tracer data in groundwater hydrology, edited by: IAEA, 69-116, 1986.

6 Appendix 1: Deuterium data of hillslope soil water

6.1 Introduction and Objectives

The Stable isotope analysis of the soil water with the Wavelength-Scanned Cavity Ring Down Spectroscopy (WS-CRDS, Picarro, USA) also gave δ^2H values, which were not presented in the thesis so far. δ^2H values and the results and difficulties of the calibration methods will shortly be presented. δ^2H data of the south-facing hillslope will also be given in this chapter.

6.2 Results, Discussion and Conclusions

δ^2H values of soil water from the year 2010 were systematically shifted below the local meteoric water line (LMWL, $\delta^2H = 7.9 \bullet \delta^{18}O + 10.1$). These values were calculated via the equilibrium fractionation factors between water vapor and liquid water of Majoube (1971). The regression line of the samples from the north-facing hillslope (year 2010) had a slope similar to the LMWL but an implausibly high d-excess ($\delta^2H = 7.3 \bullet \delta^{18}O - 49.9$).

In order to check the reliability of our calculation method (year 2010) of the soil water stable isotopes via the fractionation factors, we used spiked "calibration samples" (year 2011). These spiked "calibration samples" in 2011 were produced by adding water with a known stable isotope value to dried soil samples. The spiked samples were used as calibration standards in the year 2011. For these spiked samples, we also calculated the stable isotope values of soil water using the equilibrium fractionation factors between water vapor and liquid water. $\delta^{18}O$ values of the known added water have been reproduced by using the equilibrium fractionation factor between liquid water and water vapor. But δ^2H values of the added water could not be reproduced. They were systematically shifted below the LMWL on a $\delta^{18}O$ vs. δ^2H plot. This underpins that the calculation of soil water $\underline{\delta^{18}O}$ values via the equilibrium fractionation factors proved to be reliable. We therefore suggest that our presented $\delta^{18}O$ values of our study of both hillslopes are correct, but δ^2H values were prone to high uncertainty.

The reasons for the shifts of the δ^2H values might be manifold. Here, we present some possible explanations, which have not been investigated so far and need further, systematic analysis in further, new studies:

1. The strong deviation of the samples from the north-facing hillslope might be due to the used equilibrium fractionation factors between H_2O_{liquid} and H_2O_{vapor} from Majoube (1971), which refer to free water without being mixed with soil particles. Equilibrium fractionation factors can differ, when different substrates, e.g. clays (Stewart, 1972) or porous silica tubes (Richard et al., 2007), are involved (see also Sheppard and Gilg (1996) and Soderberg et al. (2012) for further reading). Soderberg et al. (2012) states that "the indication is that α(liquid-vapor)" for ^2H between water and clay "can have a wide range but with values below the isotopic fractionation factor for free water at a

given temperature". To our knowledge, there are no systematic studies on the influence of soil texture (i.e. mixed grain sizes) on stable isotope equilibrium fractionation factors between water vapor and liquid water related to the presented method. Therefore no unique equilibrium fractionation factor can be chosen from literature in this case.

2. Also, organic compounds could have influenced δ^2H data of samples from both hillslopes. West et al. (2010) showed in a study, where extracted plant and soil water was directly injected to laser spectroscopic instruments, that stable isotope values can be biased by organic compounds. Similar effects were found for soil core analysis and interferences with methane by Hendry et al. (2011). Spectral interferences of natural soil gas production during isotope measurements using the soil core method is currently investigated by Gralher and Stumpp (unpublished data). Detection of such compounds was not implemented in the applied instrument at the time of measurements.

3. Finally, we noted a smell of hydrogen sulfide during field sampling of the north-facing hillslope (year 2010). Usually, formation of H_2S would shift the stable isotope value of the remaining water above the meteoric water line (not below as in our case) due to the large enrichment factor between H_2S and H_2O (Clark and Fritz, 1997). However, complete re-oxidation of the formed H_2S might then lead to soil water, which is depleted in the heavier isotope ^2H. Of course, this depends on the total amount of available H_2S in the system.

A complex interplay of these hypothetical explanations might be responsible for the uncertainty of δ^2H values. We suggest that they need further investigations, but are considered of minor importance for our presented $\delta^{18}O$ data, as explained above.

Soil water stable isotope signals were within the range of precipitation signals and soil water therefore represented a mixture of spring, summer, autumn and winter precipitation (Figure 6.1). In general, scattering of soil water samples from the south-facing hillslope was high (Figure 6.1). Despite the high scatter, the samples from the upper 0 to 0.25 m of the soil profiles at the south-facing hillslope deviate systematically from the LMWL (Figure 6.1). This can indicate substantial evaporation in these upper soil layers. However, the regression line of these samples (not shown) has a slope of only 2.7, which is considered too low for the given climatic conditions in the Urseren Valley (e.g. Gat and Gonfiantini, 1981). As explained above, volatile organic compounds, which interfere during laser measurements, might also have introduced measurement artifacts. But this hypothesis has not been tested with samples from our sites so far. Detection of volatile organic compounds was not implemented in the applied instrument at the time of measurements.

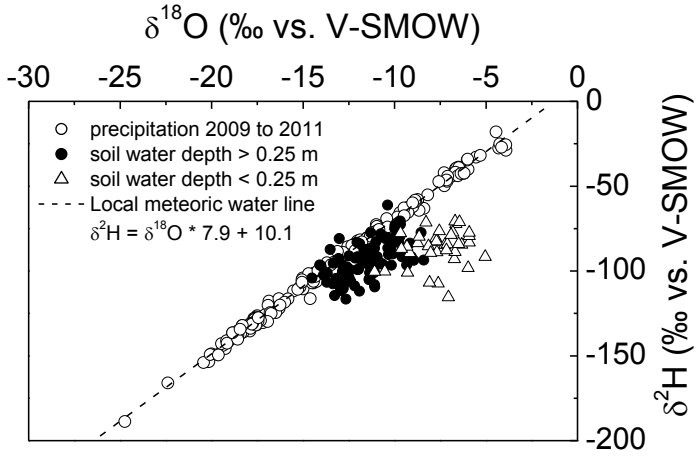

Figure 6.1: $\delta^{18}O$ vs. $\delta^{2}H$ plot for precipitation and soil water samples from the south-facing hillslope.

The y-axes of the $\delta^{2}H$ data in Figure 6.2 are scaled via the equation of the LMWL to allow direct comparison with the respective $\delta^{18}O$ data. Since $\delta^{18}O$ and $\delta^{2}H$ values of precipitation are linearly correlated (LMWL, Figure 6.1), the $\delta^{18}O$ and $\delta^{2}H$ values of soil water profiles should match if no substantial evaporation occurred. However, the $\delta^{18}O$ vs. $\delta^{2}H$ data in Figure 6.1 scatter around the LMWL and we therefore did not expect a perfect match of $\delta^{18}O$ and $\delta^{2}H$ depth profiles. Nevertheless, a general pattern between the $\delta^{18}O$ and $\delta^{2}H$ values can be observed: There is an increase of the spread between the two curves from the bottom to the top of each profile (e.g. profiles 1, 5, 6, 8 and 11; Figure 6.2). As mentioned above, this might suggest evaporative processes in the upper soil horizons at the south-facing hillslope, but measurement artifacts in $\delta^{2}H$ data of the upper soil layers cannot be excluded. In the deeper soil layers, the $\delta^{2}H$ profiles are similar to the patterns of the $\delta^{18}O$ profiles, at least in the profiles 1, 5, 6, 8, and 11. In the profiles 7, 9, 10 and 12 the pattern of the $\delta^{2}H$ profiles roughly corresponds to the patterns of the $\delta^{18}O$ profiles.

Also, the simulated $\delta^{2}H$ profiles matched the measured $\delta^{2}H$ profiles and were able to reproduce roughly the patterns, at least in the deeper soil layers (e.g. profiles 3, 5, 7, 8, 9, 10, and 11; Figure 6.3). This underpins that the modified calibration method in 2011 also worked well for $\delta^{2}H$ data from the deeper soil layers, since measured $\delta^{2}H$ values of precipitation were used as the model input. As for the $\delta^{18}O$ profiles, the model therefore also served as an independent estimate for the plausibility of measured $\delta^{2}H$ values. In conclusion, the measured and simulated $\delta^{2}H$ profiles support the implications for water flow patterns (vertical *versus* lateral), which were discussed using the $\delta^{18}O$ profiles (see section 3.4).

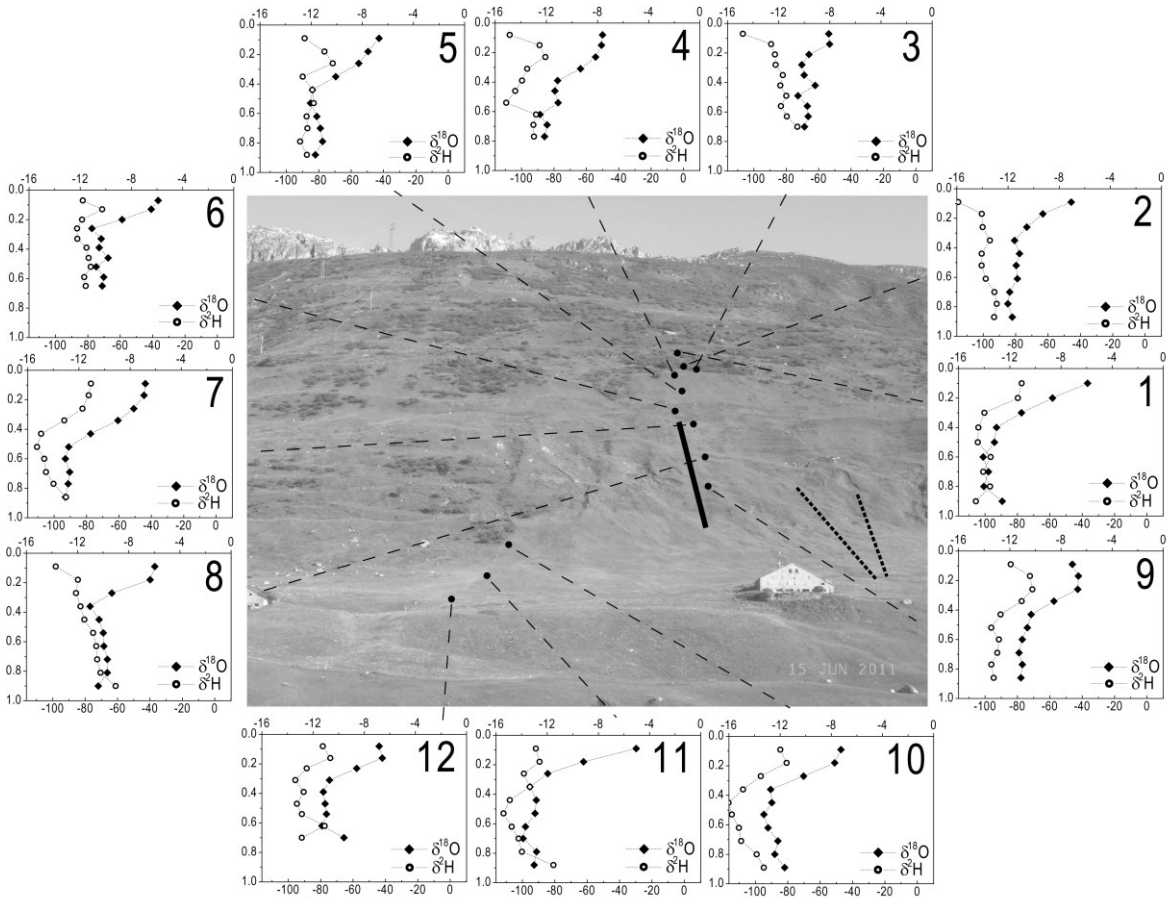

Figure 6.2: Measured soil water stable isotope profiles ($\delta^{18}O$ and $\delta^{2}H$) at the south-facing hillslope. Top x-axes show $\delta^{18}O$ (♦) of soil water from -16 to 0 ‰ and bottom x-axes show $\delta^{2}H$ (○) from -116.3 to 10.1 ‰ (scaled to allow comparison with $\delta^{18}O$). Y-axes show depth from 0 to 1 m. Axes are the same for each plot. Locations of the ERT profile (▬) and selected GPR profiles (▪▪▪▪▪▪▪) from the study of Carpentier et al. (2012) are also given.

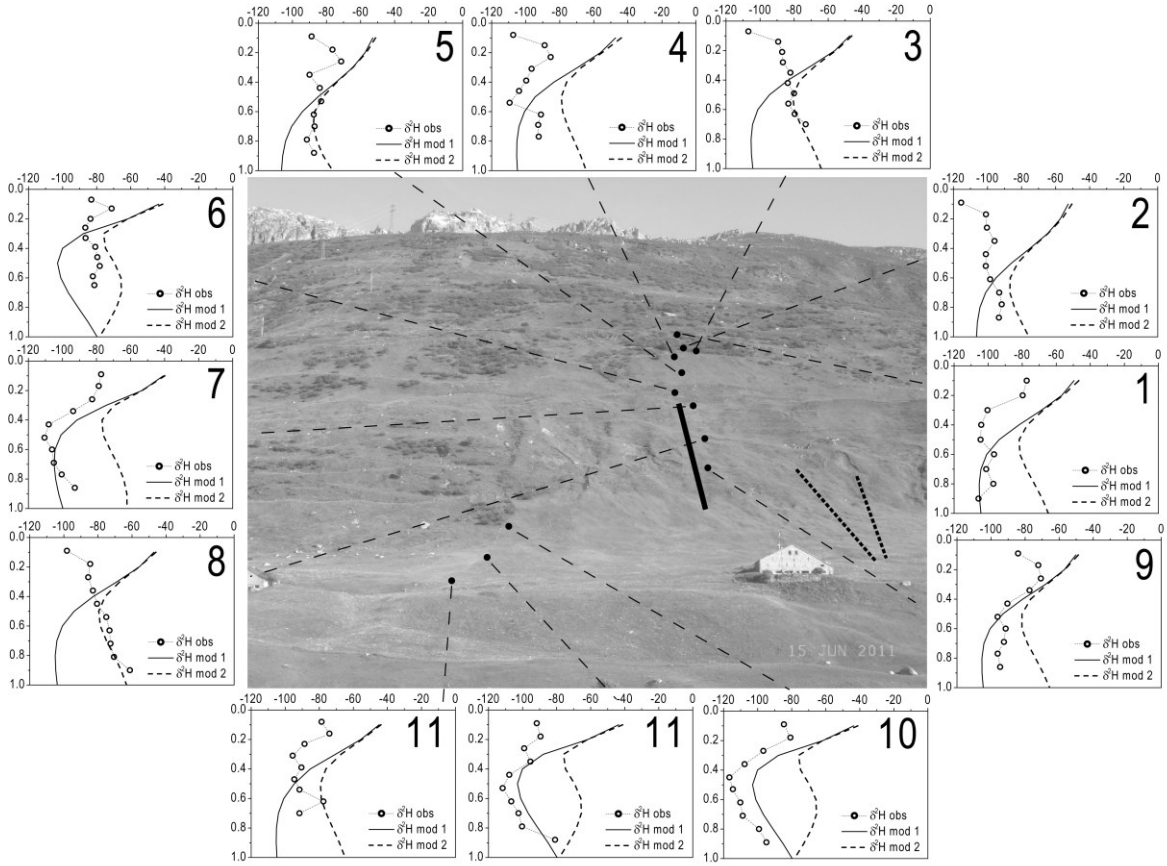

Figure 6.3: Measured ("obs") and modeled ("mod") δ^2H values of soil water stable isotope profiles at the south-facing hillslope. X-axes show δ^2H of soil water from -120 to 0 ‰ and y-axes show depth from 0 to 1 m. Axes are the same for each plot. "mod1" refers to the model which includes snowmelt; "mod2" refers to the model which excludes snowmelt (see section 3.3.2.3). Locations of the ERT profile (▬▬) and selected GPR profiles (┅┅┅) from the study of Carpentier et al. (2012) are also given.

7 Appendix 2: Supplementary data to the study in chapter 3

Photo 7.1: Animal burrows at the soil surface of a south-facing slope, which have been observed after snowmelt.

Photo 7.2: Surface runoff during a snowmelt period.

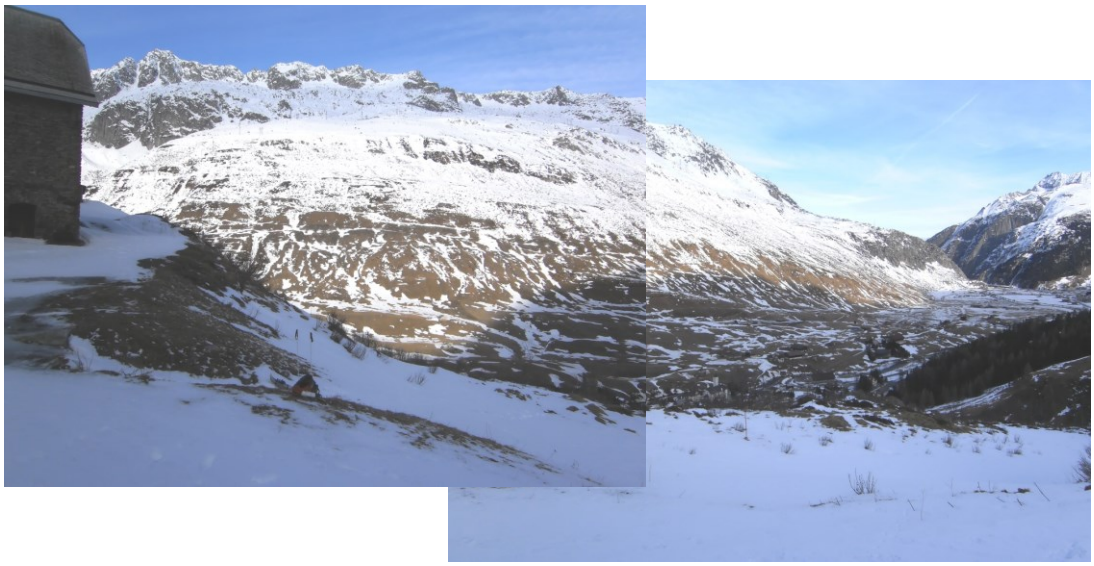

Photo 7.3: Spatially heterogeneous snow cover at the south-facing hillslope in the Urseren Valley.

8 Appendix 3: Additional physical and hydrological soil data

8.1 Introduction

During the study, we also measured surface runoff and volumetric soil water content at grassland and green alder sites in order to describe water pathways at the plot scale. Soil temperature was measured, since it provides useful additional information, especially during snowmelt periods. Sediment transport (sheet erosion) due to surface runoff was also investigated at these sites.

8.2 Material and Methods

Most of the surface runoff plots in the lower Urseren Valley were associated with the four micro catchments, but instead of the Laubgädem micro catchment, we chose the site "March" near Andermatt because it was not possible to find an appropriate slope at the Laubgädem micro catchment (Table 8.1). In summer 2011, we installed the equipment at grassland sites at the Furka Pass (2450 m a.s.l.) (Table 8.1).

Table 8.1: Coordinates of plot sites (Swiss coordinate system CH 1903/LV03).

Site	X coordinates	Y coordinates
Chämleten green alder	686329	163027
Wallenboden grassland	685390	163184
Wallenboden green alder	685421	163207
Bonegg grassland	681682	160932
Bonegg green alder	681758	160938
March grassland	687733	164484
March green alder	687759	164430
Furka Pass south "left"	675236	158919
Furka Pass south "middle"	675241	158924
Furka Pass south "right"	675284	159011
Furka Pass west "high"	674833	157690
Furka Pass west "middle"	674797	157684
Furka Pass west "low"	674783	157693

Surface runoff was measured with a tipping bucket (UP GmbH, Germany) installed at the lower end of a v-shaped steel plate of 2 m width. The plate was inserted at about 0 to 0.03 m depth into the soil at the hillslopes to concentrate surface runoff. Additionally, the steel plate was equipped with a geotextile in order to collect eroded sediment, which was collected monthly. The EC-5 sensors for volumetric soil water content were calibrated in the laboratory against gravimetric measurements (Figure 8.1). This was done by continuous measurements of volumetric soil water content in a container with a known soil volume (sieved soil particles < 2 mm). Gravimetric measurements were taken regularly and volumetric soil water content was then calculated.

Precipitation in the field was measured with ECRN-50 rain gage tipping buckets (Decagon Devices, USA). Soil temperature was measured using high-resolution Thermochron iButton devices of the type DS1921Z (Maxim Integrated, USA).

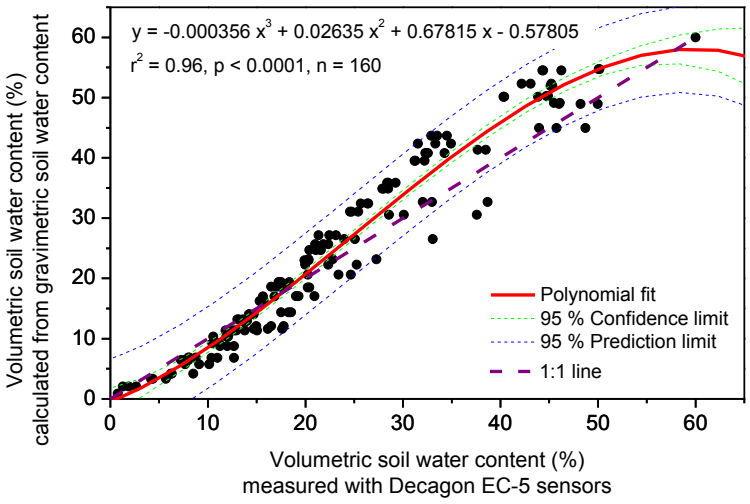

Figure 8.1: Calibration of EC-5 sensors.

8.3 Results and Discussion

8.3.1 Soil water content and surface runoff

Volumetric soil water content, precipitation and surface runoff on green alder and grassland sites suggest that infiltration and percolation of precipitation was fast and nearly complete at six stations and only small fractions of precipitation led to detectable surface runoff in the lower parts of the Urseren Valley (Figure 8.2 to Figure 8.6). Volumetric soil water content quickly reacted with the onset of precipitation events. Surface runoff in the green alder sites was mostly lower than in the grassland sites. At the Wallenboden grassland site, the steel plate was installed at a slightly concave site, where runoff was presumably concentrated at the (sub)surface from 0 to 0.05 m below surface. We measured very high rates of surface runoff and high levels of soil water contents in 0.10 and 0.50 m depth at this site (Figure 8.5). The data indicate that surface runoff is collected in small depressions (which are not only restricted to the north-facing slopes of the valley). Surface runoff even continued for 2 days after precipitation has ceased and the decline of soil water content also lasted about 2 days after a precipitation event.

At higher elevations in the Urseren Valley (Furka Pass), surface runoff was in general higher than at the lower elevations in Chämleten, Bonegg, March, and Wallenboden (green alder) (Figure 8.6 and Figure 8.7, only data from two sites are presented). This can be explained by the hydrophobic organic layer which was often observed on the grassland plots of the Furka Pass region. However, surface runoff rates are still low compared to rainfall, which indicates high infiltration capacity of the soils.

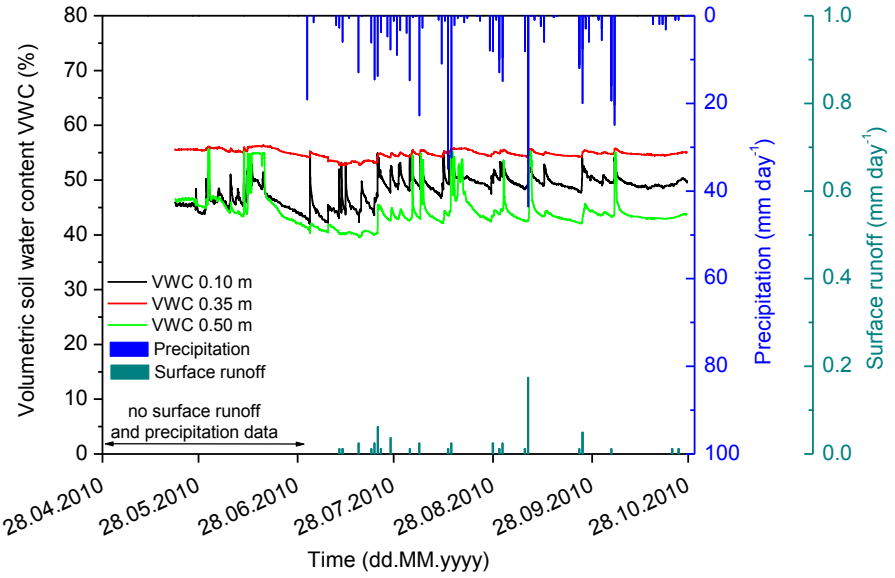

Figure 8.2: Volumetric soil water content, surface runoff and precipitation at the green alder site in Chämleten.

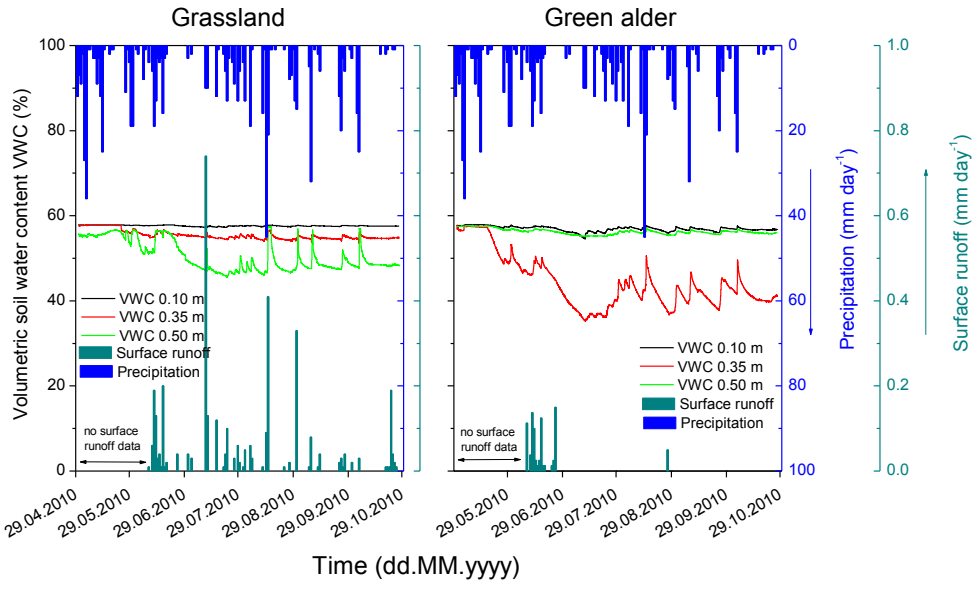

Figure 8.3: Volumetric soil water content, surface runoff and precipitation at the grassland and green alder site in Bonegg.

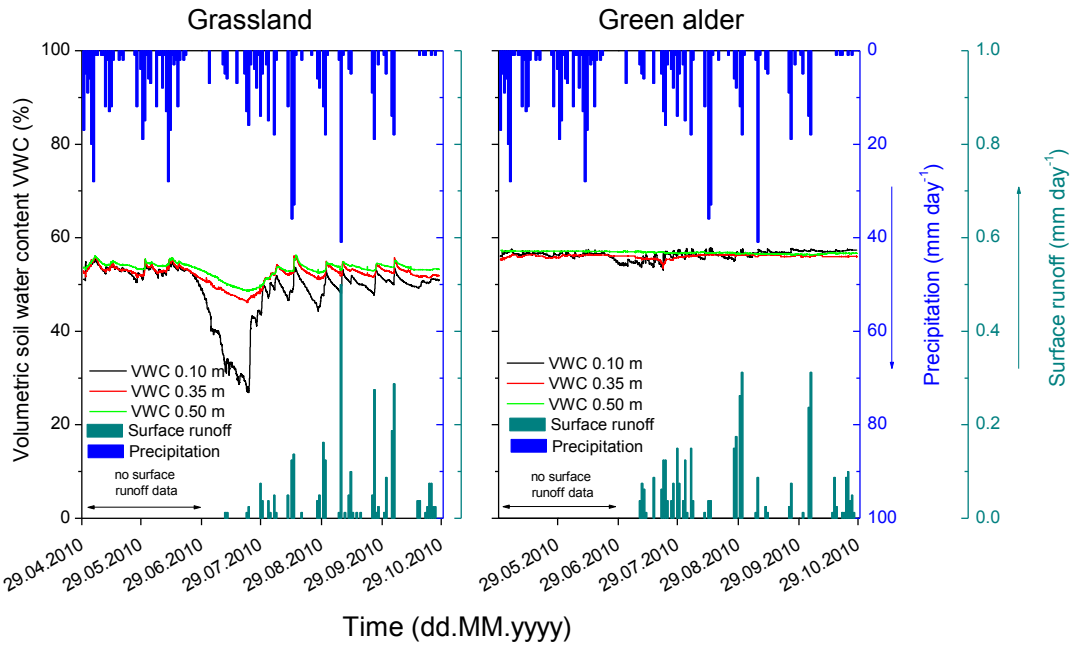

Figure 8.4: Volumetric soil water content, surface runoff and precipitation at the grassland and green alder site in March.

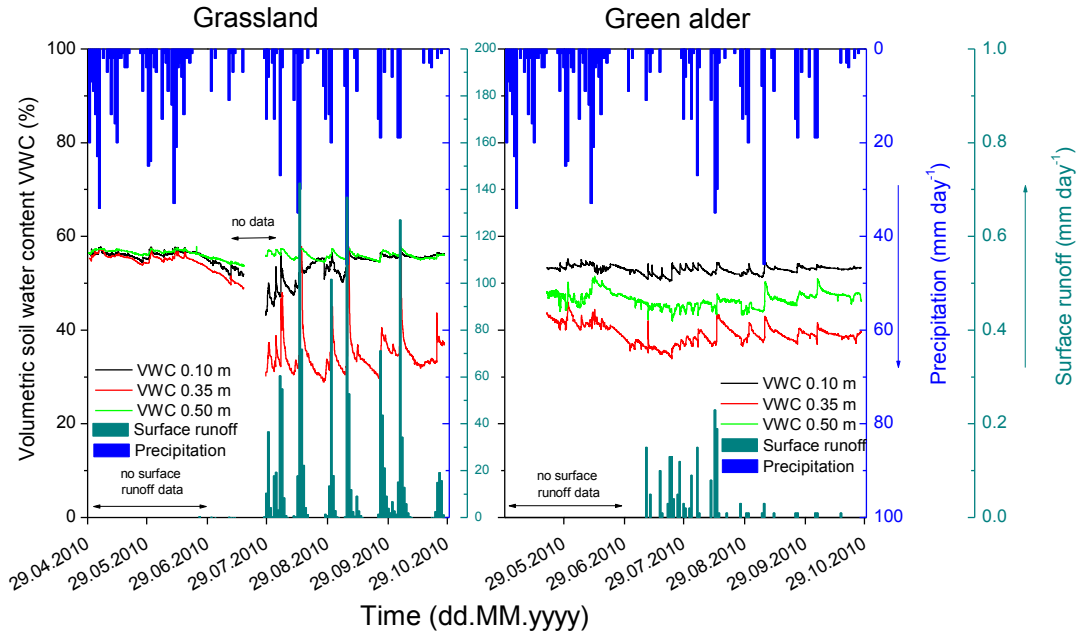

Figure 8.5: Volumetric soil water content, surface runoff and precipitation at the grassland and green alder site in Wallenboden. Please note the different scale for surface runoff in the grassland site.

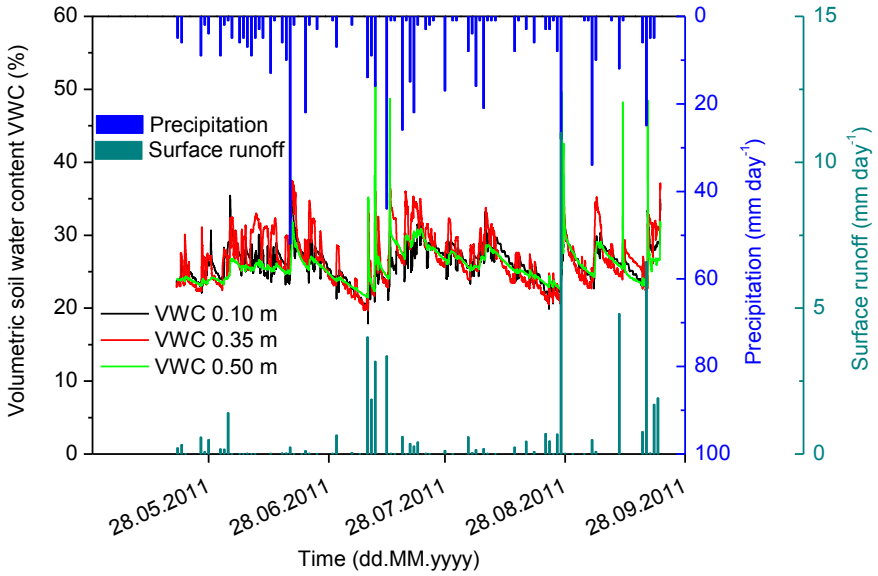

Figure 8.6: Volumetric soil water content, surface runoff and precipitation at the grassland site "Furka Pass south left".

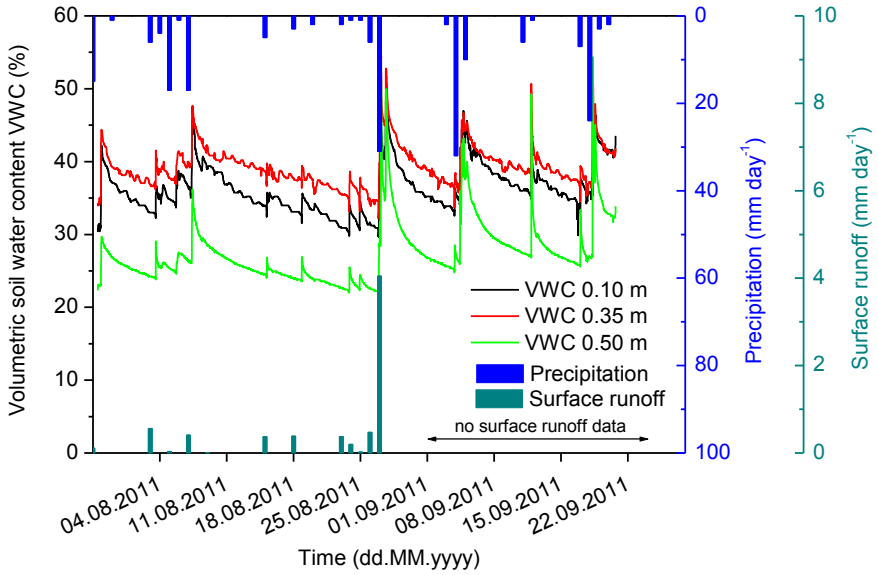

Figure 8.7: Volumetric soil water content, surface runoff and precipitation at the grassland site "Furka Pass west middle".

8.3.2 Soil texture and saturated hydraulic conductivity

Judging merely from soil texture (Figure 8.8), hydraulic conductivity of soils in the Urseren Valley can be denoted as moderate to rapid (Saxton et al., 1986).

Measured saturated hydraulic conductivity (K_{sat}) ranges from 2.3 x 10^{-6} to 2.4 x 10^{-4} m s^{-1} (Figure 8.9) with a mean of 4.2 x 10^{-5} m s^{-1} (n = 24) over both depth intervals in soils from the north-facing hillslope near the rain simulation experiments (see chapter 3). K_{sat} can be classified as moderately high to high according to the Soil Survey Division Staff (1993) and precipitation can therefore quickly pass the upper soil layers and percolate towards deeper soil zones.

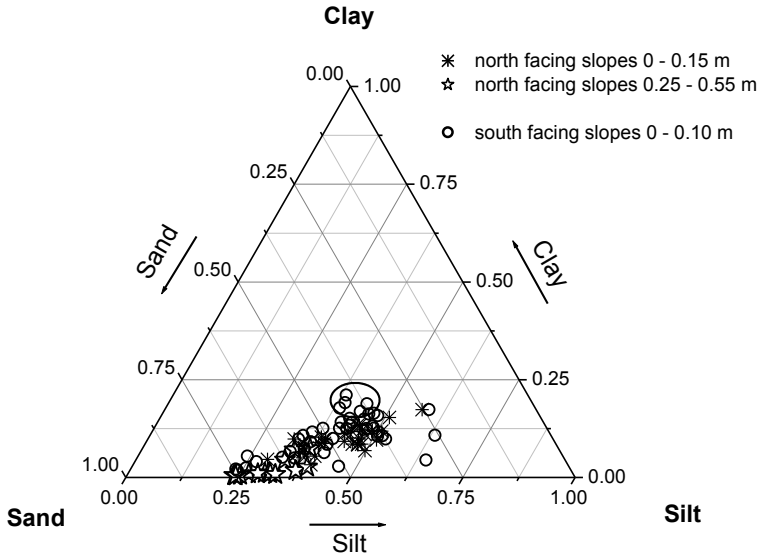

Figure 8.8: Grain size analyses of the soils along the Urseren Valley (particles < 2 mm). The big circle marks samples from sites at the south-facing hillslopes, which are partially influenced by the Mesozoic and Permocarbonic sediments and tend to have a slightly higher clay content. Additional data points are taken from Gysel (2010).

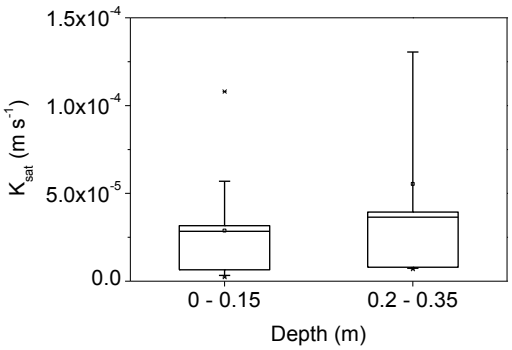

Figure 8.9: Saturated hydraulic conductivity in two depths at grassland sites at the north-facing hillslope (n = 12 per depth).

8.3.3 Sheet erosion

The amount of eroded sediment was in general lower at grassland sites compared to green alder sites (Figure 8.10). Initially, it was expected that the green alder shrubs protect the soil surface against falling precipitation and therefore reduce soil erosion (e.g. splash erosion). Visual field observations revealed that the soils under green alder shrubs are more loose and less protected through fine roots as under grassland. Therefore, soils in green alder sites might be more susceptible to soil erosion. Higher biological activity (e.g. mice) led to a constant soil transport to the steel plate in the green alder sites. In general, the erosion rates are comparable to sites from the south-facing slopes in the Urseren Valley (Konz et al., 2010). Because of the low surface runoff rates, combined with higher soil erosion rates in green alder sites, it can be hypothesized that soil erosion in these sites is not necessarily coupled to erosion processes by water.

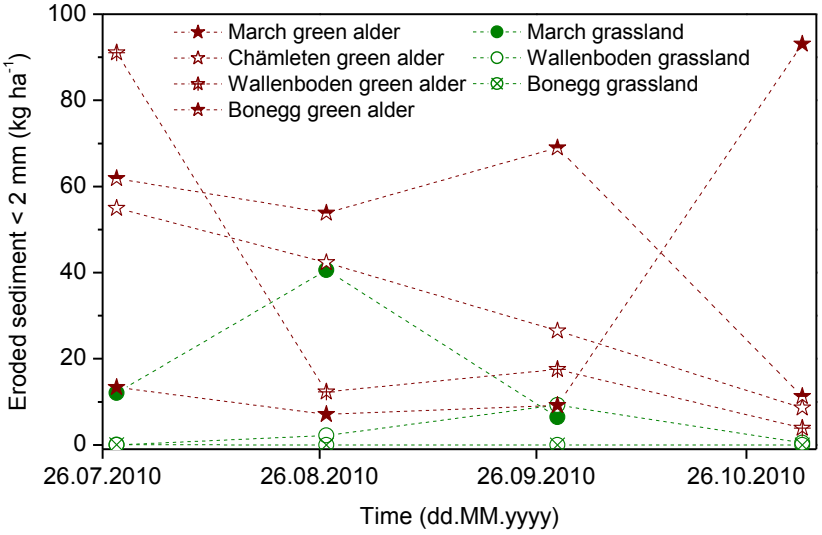

Figure 8.10: Eroded sediment at the grassland and green alder sites.

8.3.4 Soil temperature

Soil temperature ranged from -3 °C to about +17 °C and there was a clear seasonal pattern with lower temperatures in the dormant season and higher temperatures in the growing season (Figure 8.11). Soil temperature usually was higher in grasslands than in green alder sites during the growing season, which can be attributed to the cooling effect of green alder shrubs. Daily amplitudes during the growing season were also more dampened in green alder sites than in grasslands. In spring, the increase of soil temperature started earlier in the grassland sites than in the green alder sites in Wallenboden and Bonegg. This can be due to the snow cover, which lasted longer between the branches of the green alder shrubs than on open grassland sites. The lag time was about two weeks.

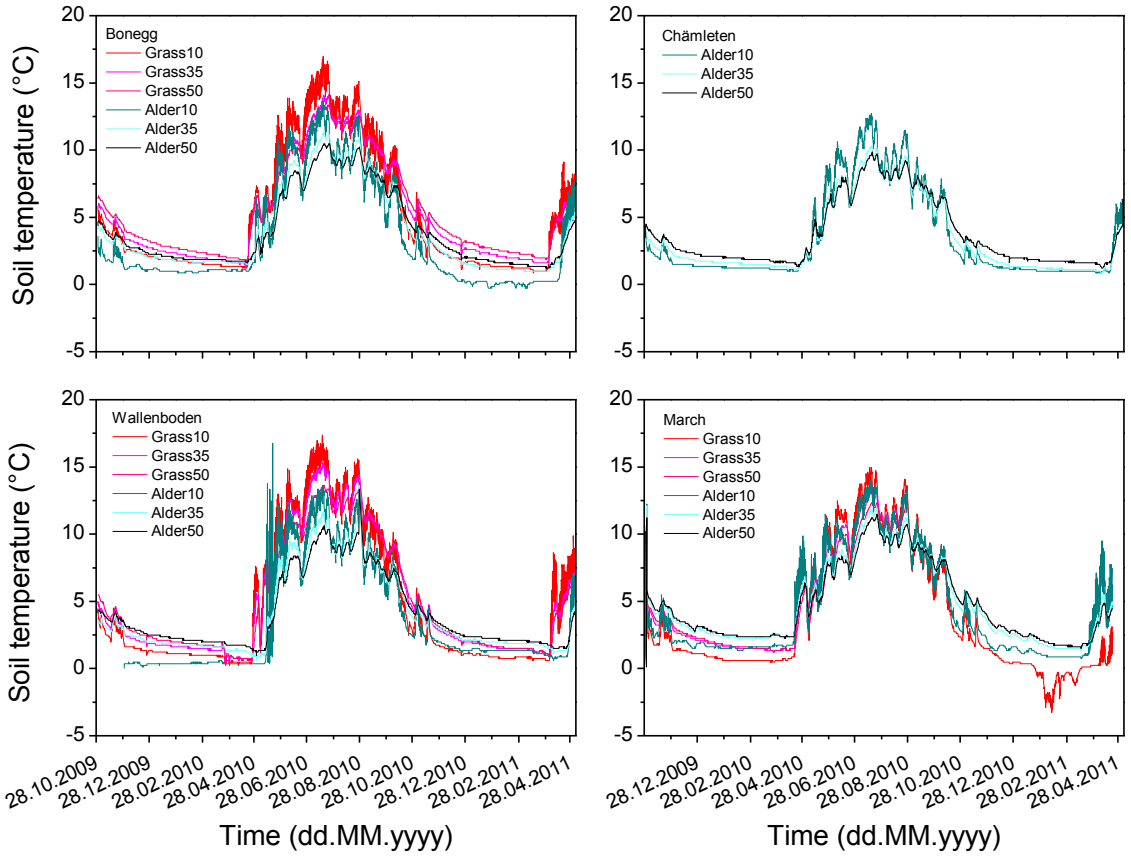

Figure 8.11: Soil temperature at the grassland and green alder sites at Bonegg, Chämleten, Wallenboden and March. "Grass/Alder 10, 35, 50" = soil temperature at grassland and green alder sites in 0.10, 0.35 and 0.5 m depth.

8.4 Conclusions

In general, there was a substantial influence of green alder shrubs on soil physical and hydrological phenomena. For example, soil temperature in spring, which was related to the timing of snowmelt, indicated that green alder shrubs might slow down snowmelt rates. This in turn influences e.g. soil hydrology and the start of plant growth in spring. Surface runoff rates were in general lower in green alder sites than in grassland sites, which can be attributed to a change of soil structure by encroaching green alder shrubs (Alaoui et al., 2013). Further encroachment of green alder shrubs in the valley might therefore affect various soil hydrological processes, at least at the plot scale.

9 Appendix 4: Stream water turbidity

Turbidity sensors were installed in the streams of the four micro catchments, as a first investigation on transport of suspended sediments in these headwater catchments. Turbidity was measured continuously during the growing season with an optical back scatter (OBS) probe (Campbell Scientific, OBS-3+). Turbidity data (measured as nephelometric turbidity units, NTU) were not calibrated to the amount of suspended sediment within this project. However, the turbidity data can be qualitatively used as an indicator for suspended sediment.

Turbidity during base flow conditions was low, indicating low amounts of suspended sediments (Figure 9.1). It clearly increased during rainfall events. High values were very often detected in Laubgädem (Figure 9.1 and Table 9.1). Data have not been further analyzed within this study.

Table 9.1: Means and standard errors of turbidity measurements.

	Chämleten	Wallenboden	Bonegg	Laubgädem
Mean (NTU)	6.1	7.7	3.1	21.6
Standard error (NTU)	0.1	0.1	0.1	0.3

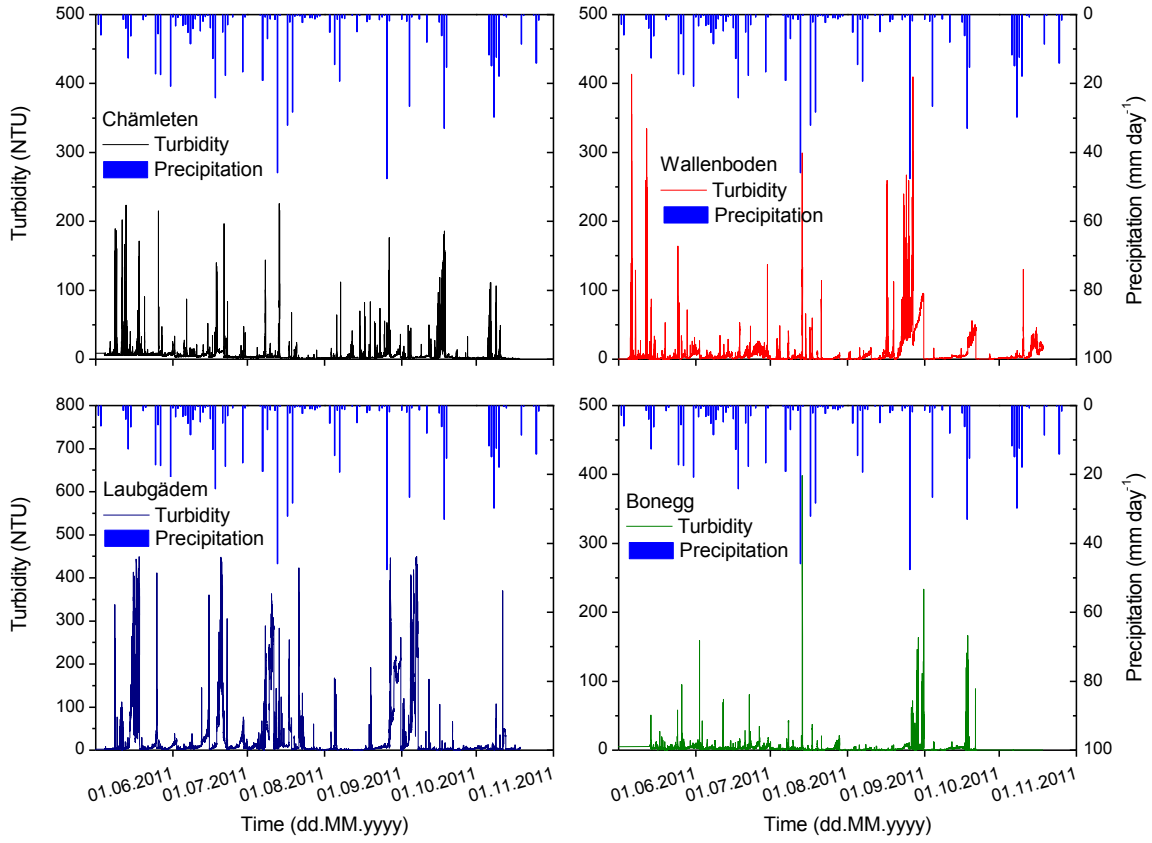

Figure 9.1:Turbidity data of the four micro catchments. Precipitation data from the MetwoSwiss station in Andermatt (MeteoSwiss, 2013).

Matthias Heidulf Müller

Professional experience

04/2014 – present	**Post-Doc** at the Group of **Applied and Environmental Geology**, University of Basel, Switzerland.
05/2009 – 10/2009	**Research Assistant** at the Chair of **Hydrology**, Albert-Ludwigs-University of Freiburg, Germany.
10/2008 – 03/2009	Leonardo da Vinci – Mobility Scholarship for a **Trainee** position at the hydrological company **Ecohidráulica**, Madrid, Spain.
03/2006	**Internship** at the Stable Isotope Laboratory of the **Paul-Scherrer-Institute**, Villigen, Switzerland.
09/2005 – 04/2008	Student **assistant** in the Group of **Applied and Environmental Geology**, University of Basel, Switzerland.
05/2003 – 07/2003	Student **assistant** in the Group of **Mineralogy and Geochemistry**, Albert-Ludwigs-University of Freiburg.

University Education

10/2009 – 02/2014	**PhD student** at the Group of Environmental Geosciences, University of Basel, Switzerland.
09/2006 – 06/2008	**M. Sc. in Environmental Geosciences**, University of Basel, Switzerland.
09/2004 – 08/2006	**B. Sc. in Geosciences**. Major in Environmental Geosciences, University of Basel, Switzerland.
03/2004 – 08/2004	Studies of **Geology**, University of Granada, Spain (Erasmus-Exchange Scholarship).
10/2003 – 02/2004	Studies of **Environmental Sciences**, University of Almería, Spain (Erasmus-Exchange Scholarship).
10/2001 – 09/2003	Studies of **Mineralogy** („Vordiplom“), Albert-Ludwigs-University of Freiburg, Germany.

School education

27/06/2000	University-entrance diploma, Theodor-Heuss-Gymnasium, Freiburg, Germany.

Additional experiences

01/2010 – 07/2010	Advanced training in **Environmental and Outdoor Education** at Zwerger & Raab GmbH, Freiburg, Germany.
2011 – 2013	Organization and Supervision of **Environmental and Outdoor Camps** at the WWF, Switzerland.